New Fluorescent Optical pH Sensors with Minimal Effects of Ionic Strength

Dissertation zur Erlangung des Doktorgrades der Naturwissenschaften

(Dr. rer. nat.)

der Naturwissenschaftlichen Fakultät IV – Chemie und Pharmazie

der Universität Regensburg

vorgelegt von

Bernhard M. Weidgans

aus Passau

September 2004

Diese Doktorarbeit entstand in der Zeit von Juni 2001 bis September 2004 am Institut für Analytische Chemie, Chemo- und Biosensorik an der Universität Regensburg.

Die Arbeit wurde angeleitet von Prof. Dr. Otto S. Wolfbeis.

Promotionsgesuch eingereicht am 25.8.2004

Kolloquiumstermin: 24.9.2004

Prüfungsausschuß:	Vorsitzender:	Prof. Dr. H.-H. Kohler
	Erstgutachter:	Prof. Dr. O. S. Wolfbeis
	Zweitgutachter:	Prof. Dr. I. Klimant
	Drittprüfer:	Prof. Dr. W. Kunz

Danksagung

Diese Doktorarbeit entstand in der Zeit zwischen Juni 2001 und Juni 2004 am Institut für Analytische Chemie, Chemo- und Biosensorik der Universität Regensburg.

Mein erster Dank gilt **Prof. Dr. Otto S. Wolfbeis** für die Bereitstellung der interessanten Themen, für sein Interesse am Fortgang dieser Arbeit, sowie für die ausgezeichneten Arbeitsbedingungen am Lehrstuhl. Für die Möglichkeit, zahlreiche nationale und internationale Konferenzen zu besuchen, möchte ich mich auch bedanken.

Ein großes Dankschön möchte ich auch **Prof. Ingo Klimant (TU Graz)** aussprechen. Trotz seiner knapp bemessenen Zeit in Regensburg nahm er sich wöchentlich meiner angehäuften Schwierigkeiten an. Seine wissenschaftlichen Anleitungen und die ausgiebigen Diskussionen halfen unüberwindbare Probleme am Ende einfach erscheinen zu lassen.

Ein herzliches *Vergelt's Gott* geht an **Dr. Christian Krause (PreSens Precision GmbH).** Gerade am Anfang der Arbeit war er ein unverzichtbarer Lehrer, der mir unermüdlich die Grundlagen optischer pH-Sensorik beibrachte. Danke auch für die Bereitstellung von Chemikalien und die zahlreichen Diskussionen fernab der Chemie und Sensorik.

Des Weiteren möchte ich mich bei **Dr. Tobias Werner** und den ehemaligen Mitgliedern unserer Arbeitsgruppe **Dr. Torsten Mayr**, **Michael Meier**, **Paweł Choijnacki und Hannelore Brunner** für die ausgezeichnete Arbeitsatmosphäre während des ersten Jahres der Doktorarbeit bedanken.

Weiterhin bedanke ich mich bei:
Athanas Apostolidis, Sarina Arain, Claudia Schröder, Dr. Gregor Liebsch, Stephan Nagl, Bianca Wetzl und Dr. Axel Dürkop für lustige Kaffee- und Teepausen und eine sehr, sehr schöne Zeit der Zusammenarbeit in unserer Arbeitsgruppe.
- meinen Kollegen aus dem Reich der Mitte, **Dr. Meng Wu** und **Dr. Zhihong Lin**, dass sie mir eine fernöstliche Sicht des bayrischen Alltags beibrachten.

Table of Contents

6.   Dual Lifetime Referenced (DLR) Optical Sensor Membranes for the Determination of pH

Chapter 1

Introduction

Preliminary remark

According to the Cambridge definition, a chemical sensor can be defined as a portable analytical device that can deliver real-time on-line information in the presence of specific compounds or ions in complex samples[1]. In this work, the term "optical pH sensor" relates throughout only to the optical sensitive element consisting of a pH-indicator, a polymeric matrix and a support material.

1.1. Motivation

The determination of pH (latin: *pondus hydrogenii*) is one of the most important analytical methods in chemical laboratories and industry. Firstly, pH is used as a quality parameter, e.g. in clinical analysis of blood (blood gas analysis)[2] and body fluids (gastric pH)[3-9], for the control of freshness of food (e.g. milk[10-15], meat[16], drinking water[17, 18]), to guarantee the neutrality of treated industrial waste waters and to control the acidity of rain ("*environmental monitoring*")[19, 20]. Secondly, pH is used as a process control parameter to find the optimum reaction conditions, e.g. in process control in bioreactors[21, 22], during fermentation of microorganisms[23, 24], precipitation of heavy metal ions in industrial waste waters and for the adaptation of pH of detoxification reactions of industrial waste waters (e.g. for cyanides at pH 12, for nitrites at pH 4, for chromates at pH 2)[25, 26].

Although the determination of pH with electrochemical sensors is a well-established method, there is a certain number of applications where the employment of glass electrodes is impossible or causes severe problems, e.g. electromagnetic fields disturb the measurement signal of potentiometric sensors; aggressive analytes (alkaline solutions or the presence of F^--ions) cause errors and/or destroy rapidly the glass surface irreversibly and make the sensor useless. In some cases of permanent online-monitoring, the sensor has to be renewed every day.

Optical pH sensors offer a promising alternative. Most of the optical pH sensors consist of a pH-sensitive indicator which is immobilized in a suitable, proton-permeable polymer matrix. The physical, mechanical, chemical and optical properties of the sensor can be governed by the combination of indicator and polymer[27, 28]. The indicator changes its

spectral properties reversible with varying pH. The optical parameters that can be exploited are absorbance[29, 30], reflectance[31, 32], or fluorescence. The latter includes information about fluorescence intensity[33-37], fluorescence intensity ratios[38-43], fluorescence decay time[44-46] and polarization[47] and is one of the most promising analytical techniques in the field of chemistry, biology and medicine since the late 20th century. In an increasing cost-consuming and cost-conscious world, optical pH sensors benefit most from the fact that they are easy and inexpensive to fabricate. Also advantageous is the higher versatility of optical sensors in contrast to electrodes. There are three prevalent formats of optical pH sensing (Fig. 1.1.):

1.) fiber optical sensors, wherein the pH-sensitive polymer-indicator mixture is fixed on the tip of an optical fiber, providing a highly spatial resolution (in case of pH-microsensors the spatial resolution is around 20-30 µm),

2.) coated microtiter plates for high-throughput screening (HTS) where the sensor is placed in planar form on the bottom of each well.

3.) planar sensor membranes for the visualization of pH gradients via imaging in two dimensions over large surfaces with highly local resolution.

Fig. 1.1. Fiber-optic pH-microsensor based on a coated fiber (diameter 140 µm) and a steel needle housing as protecting device (left). Polystyrene-based 96 well microtiter plate with immobilized planar pH sensors on the bottom (middle). Planar sensor foil for areal visualization of pH gradients (right). Printed with permission from PreSens GmbH.

1.2. Presentation of the Problem and Aim of the Work

There is still a lack of commercial applications of pH sensors due to the decisive disadvantage that the signal is depending on the ionic strength of the sample. pH is defined as the negative logarithm of the *activity* of protons in aqueous solution, while the optical parameter (e.g. change of absorption or fluorescence) correlates with the *concentration* of

the pH-sensitive dye[48, 49]. A detailed discussion of this problem is given in Chapter 2. The cross-sensitivity of the calibration curve towards ionic strength can cause pH errors of up to 1.5 pH[50] units and depends on the charge of the indicator substance and its environment, e.g. the immobilization matrix or the electrolyte concentration of the sample. Since the electrolyte concentration, respectively the ionic strength, is not constant in most real samples, optical pH sensors have not often been applied in these systems. In systems with constant ionic strength (e.g. blood[51-54], sea water[55-59]) pH was successfully determined via optical sensors.

Therefore, there is a need for optical sensors displaying a comparably negligible effect of ionic strength on the measured signal. This work describes the fabrication, characterization, optimization and application of novel, fluorescent pH sensors. Special attention is given to the investigation of methods and ways to minimize of the effect of ionic strength on the sensor.

1.3. References

1. The "Cambridge Definition" of Chemical Sensors by K. Camman, G. Guilbault, E. Hall, R. Kellner, M.-L. Schmidt, and O. S. Wolfbeis (**1996**).

2. Y. Badonnel, J. P. Crance, J. M. Bertrand, E. Panek, **Determination of pH, carbon dioxide tension, and oxygen tension by micromethods,** Pharmacien Biologiste (Paris), **1969**, 6(61), 149-154.

3. R. M. Durham, J. A. Weigelt, **Monitoring gastric pH levels,** Surgery, gynecology & obstetrics, **1989**, 169(1), 14-16.

4. M. Kristensen, **Continuous intragastric pH determination. I. pH of the gastric juice determined in situ and following aspiration**, Den. Acta Medica Scand., **1965**, 177(4), 415-425.

5. L. N. Davydov, **Hydrogen electrodes for the determination of pH and potentio-metric titration,** Laboratornoe Delo, **1960**, 6(4), 54-57.

6. C.-Y. Lin, **A simple glass-electrode system for the determination of pH of blood and other biological fluids with temperature control,** Journal of Scientific Instruments, **1944**, 21-32.

7. S. A. Grant, K. Bettencourt, P. Krulevitch, J. Hamilton, R. Glass, **In vitro and in vivo measurements of fiber optic and electrochemical sensors to monitor brain tissue pH,** Sens. Actuat. B, **2001**, B72(2), 174-179.

8.   H. E. Posch, M. J. P. Leiner, O. S. Wolfbeis, **Towards a gastric pH-sensor: an optrode for the pH 0-7 range,** Fresen. J. Anal. Chem., **1989**, 334(2), 162-165.

9.   M. Ganter, A. Zollinger, **Continuous intravascular blood gas monitoring: development, current techniques, and clinical use of a commercial device,** Brit. J. Anaesth, **2003**, 91(3), 397-407.

10. J. H. Labuschagne, **Determination of pH in dairy products,** S. Afr. J. Dairy Technology, **1976**, 8(2), 87-91.

11. A, Canuti, P. Bertola, **The application of instrumental analyses to the rapid analysis of milk. I. Potentiometric determination of pH applied to the analysis of milk,** Latte, **1965**, 39(10), 747-750.

12. E. Duvernoy, **Determination of pH in milk and cheese production,** Milchwissenschaftliche Berichte, **1957**, 7, 380-386.

13. L. Seekles, **The determination of pH in milk and whey by means of color indicator paper,** J. Dairy Res., 1940, 11, 79-83.

14. R. Aschaffenburg, **The colorimetric determination of pH in milk and whey by means of the Wulff pH tester,** J. Dairy Res., **1938**, 9, 335-338.

15. G. T. John, D. Goelling, I. Klimant, H. Schneider, E. Heinzle, **pH-Sensing 96-well microtitre plates for the characterization of acid production by dairy starter cultures,** J. Dairy Res., **2003**, 70(3), 327-333.

16. O. A. Young, R. D. Thomson, V. G. Merhtens, M. P. F. Loeffen, **Industrial application to cattle of a method for the early determination of meat ultimate pH,** Meat Sci., **2004**, 67(1), 107-112.

17. F. Canete, A. Rios, M. D. Luque de Castro, M. Valcarcel, **Determination of analytical parameters in drinking water by flow injection analysis. Part 1. Simultaneous determination of pH, alkalinity, and total ionic concentration.** Analyst, **1987**, 112(3), 263-266.

18. A. Dybko, W. Wroblewski, J. Maciejewski, R. Romaniuk, Z. Brzozka, **Fiber optic probe for monitoring of drinking water,** Proc. SPIE, **1997**, 3105, 361-366.

19. G. Marinenko, W. F. Koch, **A critical review of measurement practices for the determination of pH and acidity of atmospheric precipitation,** Environment Int., **1984**, 10(4), 315-319.

20. C. J. Brennan, M. E. Peden, **Theory and practice in the electrometric determination of pH in precipitation,** Atmos. Environ., **1987**, 21(4), 901ff.

21. A. S. Jeevarajan, S. Vani, T. D. Taylor, M. M. Anderson, **Continuous pH monitoring in a perfused bioreactor system using an optical pH sensor.** Biotechnol. Bioeng., **2002**, 78(4), 467-472.

22. B. H. Weigl, A. Holobar, W. Trettnak, I. Klimant, H. Kraus, P. O'Leary, O. S. Wolfbeis, **Optical triple sensor for measuring pH, oxygen and carbon dioxide,** J. Biotechnol., **1994**, 32(2), 127-138.

23. P. Harms, Y. Kostov, G. Rao, **Bioprocess monitoring,** Curr. Opin. Biotech., **2002**, 13(2), 124-127.

24. V. Agayn, D. R. Walt, **Fiber-optic sensor for continuous monitoring of fermentation pH,** Bio/Technology, **1993**, 11(6), 726-729.

25. J. Bourilkov, M. Belz, W. Boyle, K. Grattan, **Electrical pH control in aqueous solutions,** Proc. SPIE, **1999**, 3538, 268-277.

26. K. Xiong, G. L. Horacek, R. L. Wetegrove, R. H. Banks, **Pseudo-fouling detector and use thereof to control an industrial water process,** U.S. Pat. Appl. Publ. 2002108911, **2002.**

27. O. S. Wolfbeis, **Fiber Optic Chemical Sensors and Biosensors**, Vol. I, CRC Press, Boca Raton, **1991**.

28. J. Lin, **Recent development and applications of optical and fiber-optic pH sensors,** TrAC, **2000**, 19(9), 541-552.

29. Y. Kostov, S. Tzonkov, L. Yotova, M. Krysteva, **Membranes for optical pH sensors,** Anal. Chim. Acta, **1993**, 280(1), 15-19.

30. Z. Zhang, Z. Shakhsher, W. R. Seitz, **Aminated polystyrene membranes for a fiber optic pH sensor based on reflectance changes accompanying polymer swelling.** Mikrochim. Acta (1995), 121(1-4), 41-50.

31. W.R. Seitz, M.T.V. Rooney, E.W. Miele, H. Wang, N. Kaval, L. Zhang, S. Doherty, S. Milde, J. Lenda, **Derivatized, swellable polymer microspheres for chemical transduction,** Anal. Chim. Acta, **1999**, 400(1-3), 55-64.

32. E. J. Netto, J. I. Peterson, M. McShane, V. Hampshire, **A fiber-optic broad-range pH sensor system for gastric measurements,** Sens. Actuat. B, **1995**, B29(1-3), 157-163.

33. M. Cajlakovic, A. Lobnik, T. Werner, **Stability of new optical pH sensing material based on cross-linked poly(vinyl alcohol) copolymer,** Anal. Chim. Acta, **2002**, 455(2), 207-213.

34. D. R. Fry, D. R. Bobbitt, **Investigation of dynamically modified optical-fiber sensors for pH sensing at the extremes of the pH scale,** Microchem. J., **2001**, 69(2), 123-131.

35. A. Lobnik, I. Oehme, I. Murkovic, O. S. Wolfbeis, **pH optical sensors based on sol-gels. Chemical doping versus covalent immobilization,** Anal. Chim. Acta, **1998**, 367(1-3), 159-165.

36. D. A. Nivens, Y. Zhang, S. M. Angel, **A fiber-optic pH sensor prepared using a base-catalyzed organo-silica sol-gel,** Anal. Chim. Acta, **1998**, 376(2), 235-245.

37. P. Boutin, J. Mugnier, B. Valeur, **A fast-responding optical pH sensor based on the fluorescence of eosin trapped in a TiO_2 Sol-Gel thin film,** J. Fluoresc., **1997**, 7(1), 215S-218S.

38. H. R. Kermis, Y. Kostov, G. Rao, **Rapid method for the preparation of a robust optical pH sensor,** Analyst, **2003**, 128(9), 1181-1186.

39. D. A. Nivens, M. V. Schiza, S.M. Angel, **Multilayer sol-gel membranes for optical sensing applications: single layer pH and dual layer CO_2 and NH_3 sensors,** Talanta, **2002**, 58(3), 543-550.

40. S. Brasselet, W. E. Moerner, **Fluorescence behavior of single-molecule pH-sensors,** Single Mol., **2000**, 1(1), 17-23.

41. K. L. Michael, L. C. Taylor, D. R. Walt, **A Far-Field-Viewing Sensor for Making Analytical Measurements in Remote Locations,** Anal. Chem., **1999**, 71(14), 2766-2773.

42. J. Ji, Z. Rosenzweig, **Fiber optic pH/Ca^{2+} fluorescence microsensor based on spectral processing of sensing signals,** Anal. Chim. Acta, **1999**, 397(1-3), 93-102.

43. J. A. Ferguson, B. G. Healey, K. S. Bronk, S. M. Barnard, D. R. Walt, **Simultaneous monitoring of pH, CO_2 and O_2 using an optical imaging fiber,** Anal. Chim. Acta, **1997**, 340(1-3), 123-131.

44. S. A. Grant, R. S. Glass, **A sol-gel based fiber optic sensor for local blood pH measurements,** Sens. Actuat. B, **1997**, B45(1), 35-42.

45. U. Kosch, I. Klimant, T. Werner, O.S. Wolfbeis, **Strategies To Design pH Optodes with Luminescence Decay Times in the Microsecond Time Regime,** Anal. Chem., **1998**, 70(18), 3892-3897.

46. S. B. Bambot, J. Sipior, J. R. Lakowicz, G. Rao, **Lifetime-based optical sensing of pH using resonance energy transfer in sol-gel films.** Sens. Actuat. B, **1994**, B22(3), 181-188.

47. J. R. Lakowicz, I. Gryczynski, Z. Gryczynski, J. D. Dattelbaum, **Anisotropy-Based Sensing with Reference Fluorophores,** Anal. Biochem., **1999**, 267(2), 397-405.

48. J. Janata, **Do optical sensors really measure pH,** Anal. Chem., **1987**, 59(9), 1351-1356.

49. J. Janata, **Ion optodes,** Anal. Chem., **1992**, 64(19), 921A-927A.

50. T. E. Edmonds, N. J. Flatters, C. F. Jones, J. N. Miller, **Determination of pH with acid-base indicators: implications for optical fiber probes,** Talanta, **1988**, 35(2), 103-107.

51. I. Klimant, M. J. P. Leiner, **Optical sensors and sensor arrays comprising indicators and reference substances,** WO Patent 2002056023, **2002.**

52. C. K. Mahutte, **Online arterial blood gas analysis with optodes: current status.** Clin. Biochem., **1998**, 31(3), 119-130.

53. S. Ohkawa, K. Kogo, **Research trends of blood pH and gas sensors,** Medicina Philosophica, **1986**, 5(8), 601-606.

54. J. A. Schweitzer, K.J. Proctor, **Sensor for monitoring blood pH, blood gases, and/or other chemical parameters of the blood,** U.S. Patent 5047208, **1991.**

55. S. Hulth, R. C. Aller, P. Engstrom, E. Selander, **A pH plate fluorosensor (optode) for early diagenetic studies of marine sediments,** Limnol. Oceanogr., **2002**, 47(1), 212-220.

56. R. G. J. Bellerby, A. Olsen, T. Johannessen, P. Croot, **A high precision spectrophotometric method for on-line shipboard seawater pH measurements: the automated marine pH sensor (AMpS),** Talanta, **2002**, 56(1), 61-69.

57. Z. Zhuang, W. Li, X. Chen, D. Sun, X. Wang, **Study on the fiber optic chemical sensors and biosensors applied to monitoring of environmental contaminants in seawater,** Ziran Kexueban, (2001), 40(2), 477-485.

58. C. Huber, T. Werner, O. S. Wolfbeis, T. E. Bell, C. H. Young, T. Susannah, **Optical-chemical sensor for chloride determination composed of luminescent indicator and polymer carrier,** WO Patent 2000042438, **2000.**

59. A. G. Mignani, M. Brenci, A. Mencaglia, **Fiber optic sensors for environmental monitoring. An overview of technologies and materials,** NATO ASI Series, Series E: Applied Sciences, **1995**, 285, 691-708.

Chapter 2

Physico-chemical Background

2.1. Determination of pH

2.1.1. Definition of pH

Søren Peter Lauritz Sørensen, a Danish biochemist, was the first who established the modern concept of pH, defining it as pH = -log [H^+]. He did not discover the autoprotolysis of water or the existence of protons, but hydrogen ion concentration played a key role in enzymatic reactions and he devised a simple way of expressing it[1]. By taking the negative logarithm of Friedenthal's definition of hydrogen ion concentration, a convenient scale with manageable numbers can be established; this is the well-known pH value. Numerical values based on this unit give an indication of the acidity of solutions. He also developed buffer solutions to maintain constant pH of solutions (Sørensen buffers)[2-4].

Historical Background for pH

In 1887 Svante Arrhenius proposed that the characteristic properties of acids might be explained in terms of dissociation[5]. He defined acids as substances that deliver hydrogen ions to the solution. He also pointed out that the law of mass action could be applied to ionic reactions, such as an acid dissociating into hydrogen ion and a negatively charged anion. This idea was followed up by Wilhelm Ostwald, who calculated the acidity constants (the modern symbol is K_a) of many weak acids[6]. Ostwald also showed that the value of the constant is a measure of an acid's strength. By 1894, the dissociation constant of water (today called K_w) was measured to the actual value of 1×10^{-14}. In 1904, H. Friedenthal recommended that the hydrogen ion concentration could be used to characterize solutions[7]. He also pointed out that alkaline solutions could also be characterized this way since the hydroxyl ion concentration was always 1×10^{-14} / hydrogen ion concentration. Many consider this to be the real introduction of the pH scale.

The context for the introduction of pH was the slow changeover from the old color-change tests for indicating the degree of acidity or basicity to electrical methods. In the latter, the current generated in an electrochemical cell by ions migrating to oppositely charged electrodes was measured, using a highly sensitive (and delicate) galvanometer.

Until Sørensen developed the pH scale, there was no widely accepted way of expressing hydrogen ion concentrations. His scale removed the awkward negative power for hydrogen ion concentrations that range over many orders of magnitude: from about ~12 M at the high end to ~10^{-15} M at the low end. Instead Sørensen suggested that the power could be represented by a pH scale in which 7 is neutral, and 1 and 14 are the extremes of acidity and alkalinity, respectively[8]. The letters pH are an abbreviate for "*pondus hydrogenii*" (translated as potential of hydrogen) meaning hydrogen power as acidity is caused by a predominance of hydrogen ions (H^+). In Sørensen's original paper, pH is written as P_H. Sørensen does not explain his notation any further, nor does he account for his choice of the letter "P". Others, though, have claimed that it is derived from the german word *Potenz*, meaning power or concentration[9]. According to the Compact Oxford English Dictionary, the modern notation "pH" was first adopted in 1920 by W. M. Clark (inventor of the Clark oxygen electrode) for typographical convenience. "p-Functions" have also been adopted for other concentrations and concentration-related numbers. For example, "pCa = 5.0" means a concentration of calcium ions equal to 10^{-5} M, and $pK_a = 4.0$ means an acid dissociation constant equal to 10^{-4} M.

The Theoretical Definition that Uses the Hydrogen Ion Activity

The modern formulation of the equation defining pH is $pH = -\log a_{H+}$ where a_{H+} is the hydrogen ion activity. This builds on Lowry's recognition[10] of the activity of the hydronium ion rather than of the hydrogen ion as the key to pH. The activity is an effective concentration of hydrogen ions, rather than the true concentration; it accounts for the fact that other ions surrounding the hydrogen ions will shield them and affect their ability to participate in chemical reactions. These other ions effectively change the hydrogen ion concentration in any process that involves H^+. In practice, Sørensen's original definition can still be used, because the instrument used to make the measurement can be calibrated with solutions of known $[H^+]$, in which the concentration of background ions are carefully controlled.

The Experimental Definition

IUPAC has endorsed two pH scales based on comparison with a standard buffer of known pH using electrochemical measurements:

a) the British Standard Institution (BSI) scale has one fixed point, which is the reference buffer. The pH of a potassium hydrogen phthalate solution with b = 0.05 mol/kg was set to be $4.000 + (T-15)^2 \cdot 10^{-4}$, where T is the temperature. Any other standard solutions are derived by measure with a reference electrode and a hydrogen electrode. The signal includes a residual, non-eliminable diffusion potential. This scale is predominently used in Great Britain and Japan[11].

b) the National Bureau of Standards (NBS) scale uses several fixed points[12]. The fixed points are set by so-called primary pH standard solutions. The signal is determined with chains without electrochemical transport and is therefore free of non-eliminable diffusion potential. This scale is adopted by most national standards, e.g. Germany's DIN 19266.

2.1.2. Principle of Optical Sensing

Color changes of solutions in the presence of acids or bases rank among the eldest observations in chemistry[13]. The first pH scale was done by Friedenthal, who listed pH-sensitive indicators and their properties[7].

Indicators are weak acids or bases, wherein in most cases the pH-sensitivity is based on a color or intensity change. The color is based on a change in the electronic π-system of the chromophore caused by the acceptance or separation of protons. One of the best-known pH-sensitive fluorescent indicators is fluorescein[14-28]. The fluorescence intensity change is based on a transition from a non-phenolic form into a phenolic form. Fig 2.1. shows the pH-dependent structures of fluorescein with the non-phenolic form for pHs < 4.0 and the phenolic form for pH > 8.0.
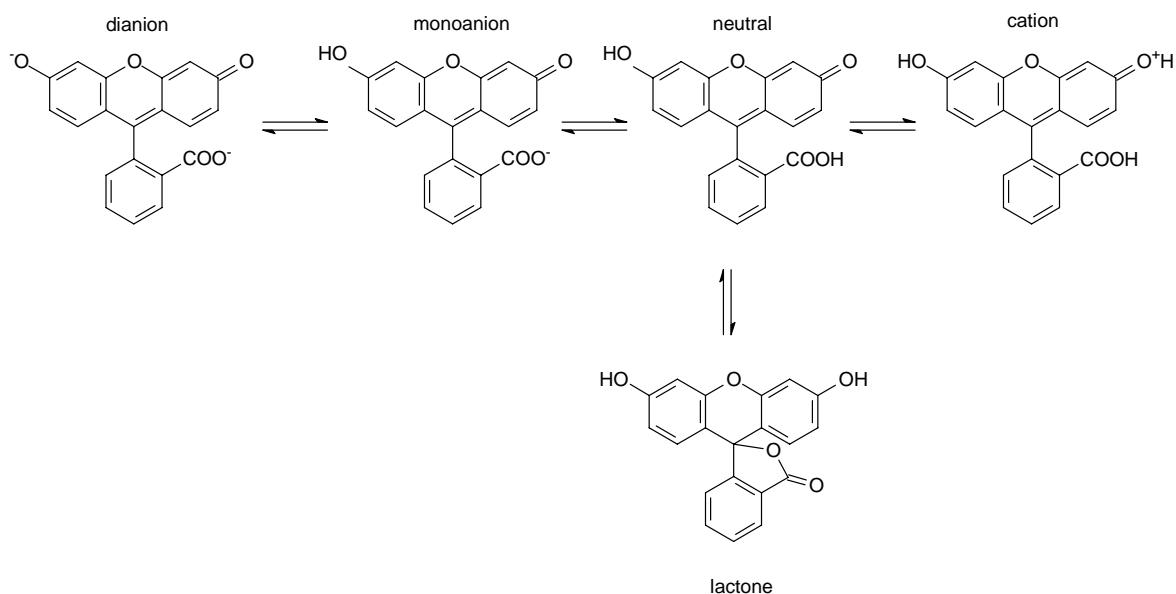
Fig 2.1. The pH-dependent structures of fluorescein. Only monoanion and dianion are fluorescent.

According to the type of indicator the dissociation reaction can be described as:

a) $\quad HA \rightleftharpoons H^+ + A^-$ $\qquad$ for neutral indicators

b) $\quad HA^+ \rightleftharpoons H^+ + A$ $\qquad$ for cationic indicators

c) $\quad HA^- \rightleftharpoons H^+ + A^{2-}$ $\qquad$ for anionic indicators

For a) the mass action law yields

$$K_c = \frac{[A^-][H^+]}{[HA]} \qquad (2\text{-}1)$$

where K_c is the concentration constant of the indicator, and [HA], [A$^-$] and [H$^+$] are the *concentrations* of the indicator, its conjugate base and protons respectively. The concentration constant is related to the thermodynamic constant K_a by the activity coefficients f_x on the individual components (Eq. 2-2)

$$K_a = K_c \cdot \frac{f_{A-} \cdot f_{H+}}{f_{HA}} \qquad (2\text{-}2)$$

When expressed in logarithmic form, the activity based Henderson-Hasselbalch equation is obtained as Eq. 2-3.

$$pH = pK_a + \log\frac{[A^-]}{[HA]} + \log\frac{f_{A-}}{f_{HA}} \qquad (2\text{-}3)$$

where pK_a is $-lg\ K_a$.

Electrochemical pH determinations are based on a measurement of the electromotive force of a cell having a reversible electrode whose potential is linearly dependent on activity of hydrogen ions, and hence on pH. Optical measurements are a linear function of the dye concentration ($[A^-]$ or $[HA]$), but not the activity. As the pH varies, the relative fractions of the acid and basic forms are changed and changes can be detected by means of absorption or fluorescence intensity or lifetime measurements. Therefore, the Henderson-Hasselbalch equation based on the concentration constant K_c is commonly used and the activities are ignored (Eq. 2-4).

$$pH = pK_c + \frac{\left[A^-\right]}{\left[HA\right]} \qquad (2\text{-}4)$$

The concentration of indicator should always be kept very low in comparison to the buffer capacity of the analyte to avoid the so-called indicator error. Otherwise, the indicator can have a noticeable effect on the pH of low buffered waters.

2.1.3. Ionic Strength, Activity Coefficients and the Debye-Hückel Theory

Why is it advisable to use calibration buffers of constant ionic strength? As mentioned in Chapter 1.2. ionic strength is influencing activity coefficients. According to Randall and Lewis[29], ionic strength IS is defined as

$$IS = \tfrac{1}{2}\sum z_i^2 c_i , \qquad (2\text{-}5)$$

where z_i is the valency of each single ion and c_i its concentration. IS is a quantitative measure of how "ionic" a solution is. It is noticeable that the definition of IS is a mathematical one that is independent of the ion nature (except of valency). Aqueous solutions of Na_2SO_4 and K_2SO_4 ($c_i = 0.1$ M) have the same ionic strength (0.3 M), while the IS for 0.1 M NaCl is 0.1 M.

As mentioned above, pH is defined as negative logarithm of the activity of protons. For solutions with total ion concentrations of higher than 1 mM, one must use activities rather than concentrations because ions show interionic interactions that cause local electric fields. Therefore, the mobility of ions is hindered and causes deviations from the ideal behavior, so that the "active" concentration is always smaller than the real concentration. The mathematical correction is expressed by a factor f_i (see Eq. 2-2), the activity coefficient. Debye and Hückel[30] developed a theory in 1923 that allows calculating interionic interactions, or activity coefficients, respectively. One result of their theory is the

limiting-Debye-Hückel law (Eq. 2-6) that is based on a few assumptions (complete dissociation of ions; only electrostatic interactions are regarded; ions consist of point-shaped charges; and solution and solvent have the same dieletric constant) and is valid for ISs up to 1 mM:

$$\lg f_i = -z^2 A (IS)^{1/2} \qquad (2\text{-}6)$$

The extended-Debye-Hückel-Law is working in the range from ISs of 10 mM to 100 mM and can be amended by the constant C to give the Davies equation which is valid for ISs higher than 100 mM (Eq. 2-7)

$$\lg f_i = \frac{A \cdot z_i \cdot (IS)^{1/2}}{1 + B \cdot d \cdot (IS)^{1/2}} + C \cdot IS \qquad (2\text{-}7)$$

where z_i is the charge of species, d is the mean ionic diameter, A and B are temperature-dependent constants (0.509 and 0.328 for 25 °C) and C is an empirical parameter ($\sim$ 0.2). An example how IS can affect the pH of a solution is given in Table 2.1 for an HCl solution of c = 10^{-5} mol/L at 25 °C. IS was varied from zero, meaning no background electrolytes, to 1 M. Robinson and Stokes[31] found that the activity coefficient affects the concentration only marginal in the region of validity (100 mM – 1 M), but in the region of low ionic strength, the activity coefficients change significantly and thus concentration and pH.

Table 2.1. Effect of increasing ionic strength on pH.

Ionic Strength [M]	0.000	0.002	0.01	0.02	0.05	0.1	0.2	0.3	0.4	0.5	1
Activity Coefficient f	1.00	0.952	0.905	0.876	0.830	0.796	0.767	0.756	0.755	0.757	0.809
pH value	5.00	5.02	5.04	5.06	5.08	5.10	5.12	5.12	5.12	5.12	5.09

The results in Table 2.1 show that different ionic strength can cause pH changes that can not be neglected. In terms of pH indicators, one must remind that in Eq. 4 the activity coefficients (and therefore IS) are disregarded. This is only allowed in very dilute solution (c < 1 mM), where the activity coefficients are close to unity. Otherwise, changes in ionic strength will alter the activitiy coefficients and alterate the calibration of a sensor. This can be explained by comparision of Eq. 2-4 with Eq. 2-3 which results in Eq. 2-8,

$$pK_c = pK_a + \log \frac{f_{A^-}}{f_{HA}} \qquad (2\text{-}8)$$

While pK_a is the true value of the acidity constant and only dependent on temperature, the concentration constant pK_c is only valid for a given ionic strength and should be

considered as an "apparent" constant that is dependent on factors that are able to modify activity coefficients, like specific interactions depending on the chemical nature of the indicator and the surrounding media (microenvironment), structural changes of the medium (e.g. the vicinity of interfaces of micelles or sensor membranes), temperature and ionic strength of the system. Therefore, the last two parameters should be kept constant during calibration. At least one form of the indicator is an ion and takes an active part in making up the total IS of the sample. When IS in the system is varying, K_c and pK_c are changed due to the changes of the activities of the indicator f_{A^-} and f_{HA} and the calibration plot is shifted. The pH error caused by ionic strength effects can be expressed by equation 2-9.

$$\Delta pH = \log\frac{f_{A^-}^c}{f_{HA}^c} - \log\frac{f_{A^-}^s}{f_{HA}^s} \qquad (2\text{-}9)$$

where subscript c denotes the calibration solution and s the sample solution. Comparing the measured pH of electrodes and optical sensors, the difference in pH can be expressed by Eq. 2-10:

$$pH_{El} = pH_{Opt} \cdot \log\frac{f_{A^-}}{f_{HA}} \qquad (2\text{-}10)$$

In general, the effect of IS on the apparent pK_a of an indicator is called *cross-sensitivity* towards IS. Kilpatrick[32] studied the apparent pK_a shifts of Bromothymol Blue in presence of different concentrations of background electrolytes. A detailed discussion about fluorescent pH indicators and their cross-sensitivity to IS is given in Chapter 3.

Table 2.2. gives information about fields of application for optical pH measurement under conditions of varying IS.

Table 2.2. Ionic strengths, pHs and main electrolytes of waters and physiological fluids

Sample	Ionic Strength/mM	pH range	Predominant Ions
Freshwater	<6	~7.8 - 8.8	Na^+, Ca^{2+}, HCO_3^-
River Water	2	6.0 - 8.5	Na^+, Ca^{2+}, HCO_3^-
Mineral Sparkling Water	~30	6.0 - 7.0	Na^+, Ca^{2+}, HCO_3^-
Brackish Water	50-100	6.0 - 8.0	Na^+, Cl^-
Blood Serum, Culture Media	135-170	7.0 - 7.5	Na^+, proteins, NH_3^+, organic acids, Cl^-
Sea Water	500-700	7.4 - 8.3	Na^+, Cl^-

2.1.4. Optical Sensors vs. Electrodes

Electrochemical and optical sensors form the two most important groups of sensors. The glass electrode is the best known electrochemical sensor, wherein an electrochemical interaction between analyte and electrode is converted into a potential difference. Major advantages of electrochemical sensors include[33]

a) high sensitivity and wide dynamic range (for pH electrodes linear from pH 1 to 13)

b) small power requirements

c) good performance in electrolyte sensing

and as the most important benefit

d) activities rather than concentrations are measured

On the other hand, electrodes suffer from the following disadvantages

a) poor performance at extreme pHs

b) difficulties in remote sensing

c) the need for a reference electrode

d) sensitivity to electrical fields

e) miniaturization involves several steps

f) sometimes lack in specificity.

The signal of optical sensors generally is derived from intrinsic or extrinsic optical signals. In the first, the spectral properties of the analyte are used for its determination. The color of blood can be taken as measure for the oxygen saturation. The fluorescence of chlorophyll gives information about the photosynthesis activity (Kautsky effect[34]). If the analyte does not display changes of optical properties, an indicator or label is used to transduce the analyte concentration into an useful optical signal (e.g. pH and oxygen sensors). The advantages of optical sensors are:

a) they no requirements for an additional reference element as do electrodes.

b) not subject to electrical interferences.

c) insensitive towards magnetic fields and high pressure.

d) ease of miniaturization.

e) their dynamic range is smaller, but resolution that is better than that of electrodes

f) optical sensors do not consume the analyte (e.g. oxygen consumption of Clark electrodes)

g) the optical signals can transmit more information than electrical signals

h) using arrays of ion- or gas-sensitive sensors enable simultaneous multianalyte analysis

i) they are non-invasive

j) can be used as disposable sensors.

Otherwise optical sensors have the drawbacks that

a) ambient light can interfere

b) narrow dynamic range compared to electrochemical sensors

c) limited long-term stability due to photobleaching or leaching of the immobilized indicator

d) the fact that concentrations rather than activities are measured

e) surface potentials caused by charged sensor surfaces affect the sensor signal with varying IS.[39, 40]

The last two facts are less important for optical sensors if electrically neutral species are detected (e.g. O_2, CO_2, etc.). In those sensors the effects of activity and surface potentials are much less critical than in ionic sensors (e.g. pH, alkali ions, halides).

2.1.5. State of the Art in Optical pH Sensing

Basically, optical pH sensors can be separated into fiber optic and non-fiber optic pH sensors. The development of fiber optical sensors in general is closely connected to the proceedings in optical telecommunication. Fibers, detection systems, LEDs and other optoelectronic parts are an outgrowth of communication industry and paved the way for cheaper detection systems for fiber optical chemical sensors (FOCS), fiber optical biosensors (FOBS) and optical sensors. This progress can be seen in the number of publications (>770) concerning optical pH sensors since the early 80's as shown in Fig 2.2.
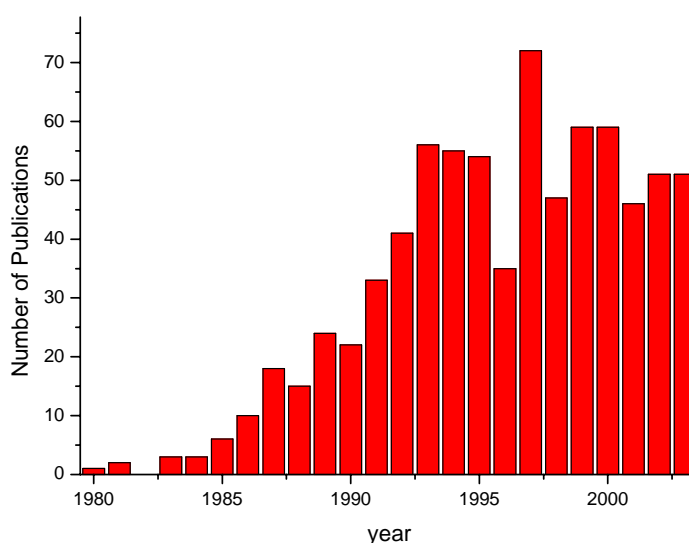
Fig. 2.2. Increasing number of publications concerning optical pH sensors. (Enquiry was done with SciFinder Scholar using the Caplus Database. Status April 2004).

Due to this enormous number of papers, this chapter can only deliver insight into a few exemplary papers. Special attention is given to papers reporting on methods to minimize the cross-sensitivity of IS in optical pH sensors.

The first sensors for continuous use where those for pH and for oxygen. It has been known for decades that cellulosic paper can be soaked with pH indicator dyes to give pH indicator strips which, however, leached and thus were of the "single-use" type. The respective research and development is not easily traced back since it is not well documented in the public literature. However, in the 1970s, indicator strips became available where they pH indicator dye was covalently linked to the cellulose matrix. These "non-bleeding" test strips allowed a distinctly improved and continuous pH measurement, initially by visual inspection. In the late 1980's instruments were made available that enabled the color (more precisely the reflectance) of such sensor strips to be quantified and related to pH.[35]

The first fiber optic pH sensor was reported by Peterson et al.[36] in 1980. A mixture of light-scattering polystyrene microspheres was mixed with phenol red-dyed polyacrylamide microspheres and packed into a cellulosic dialysis tubing as pH probe at the end of a fiber. One fiber of the sensor was used to conduct light toward the probe tip and the other fiber to conduct light to the sensor. The sensor was successfully used for in-vivo and in-vitro blood evaluation. The effect of ionic strength was studied and showed a shift of 0.01 pH by a change in IS from 0.05 to 0.3 M. Saari and Seitz[28] developed the first fluorescent pH

sensor. They used fluoresceinamin immobilized on controlled pore glass. They did not investigate the cross-sensitivity towards IS. In 1983, a technique was reported[37] that works in aqueous solutions, wherein two differently charged indicators were used to determine both pH and ionic strength. Later, two sensor schemes were described[38] based on one indicator with different surface chemistries. In a first sensor, the indicator is embedded in an uncharged micro-environment. This sensor is highly sensitive to changes in ionic strength. In a second sensor, the indicator is placed in a highly charged environment. This sensor is less sensitive towards changes in ionic strength. The optical pH determination using two sensors or indicators which respond to different degrees of a measurement solution requires complex equipment and additional calculations. A methodology for determination of ionic strength of solutions, based on these effects, has been proposed. The articles by Janata[39, 40] about optical ion sensors and especially optical pH sensors critically appraise the state of the art in optical sensing from a thermodynamic point of view and include advices of data interpretation.

Papers discussing methods to compensate or minimize the effect of ionic strength are very rare. In 1997, Barnard et al.[41, 42] reported an optical sensor system for pH determination independently of ionic strength. They have found that selection of very particular polyurethane compositions in combination with a fluorescein dye allows the production of an optical sensor which permits optical pH measurement of high accuracy in the physiological range independently of ionic strength, making a second measurement and a calculation step for eliminating the effect of ionic strength dispensable. Unfortunately, there is no detailed information about the performance and cross-sensitivity of the sensor given in the patent. The system described in this paper represents the current trend in optical pH sensor development: The characteristics of the sensor are governed by a suitable combination of polymer and indicator. Complicated evaluation methods, circumstantial fabrication and difficult experimental set-up are avoided.

A noteworthy sensor that is not based on a pH-indicator is the work done by Raimundo et al[43]. The color-change of PANI-porous Vycor glass nanocomposites was used to determine pH. The negligible cross-sensitivity to IS and varying ions in the range from 150 mM to 500 mM are remarkable.

2.2. Luminescence

The word luminescence is an umbrella term for all phenomena associated with emission of light (e.g. electroluminescence, thermoluminescence, bio- and chemiluminescence etc.). In general, only photoluminescence is of interest for optical chemical sensors. Fluorescence and phosphorescence are particular cases of photoluminescence and shall be further discussed in the following paragraph.

2.2.1. Fluorescence Intensity

Once a molecule (organic or inorganic) is excited by absorption of a photon in the UV or VIS area, it can return to the ground state by several pathways (e.g. electron transfer, energy transfer, proton transfer, conformational change, photochemical transformation, intersystem crossing $\rightarrow$ phosphorescence, fluorescence emission). Luminescence is the emission of light and occurs from electronically excited states.
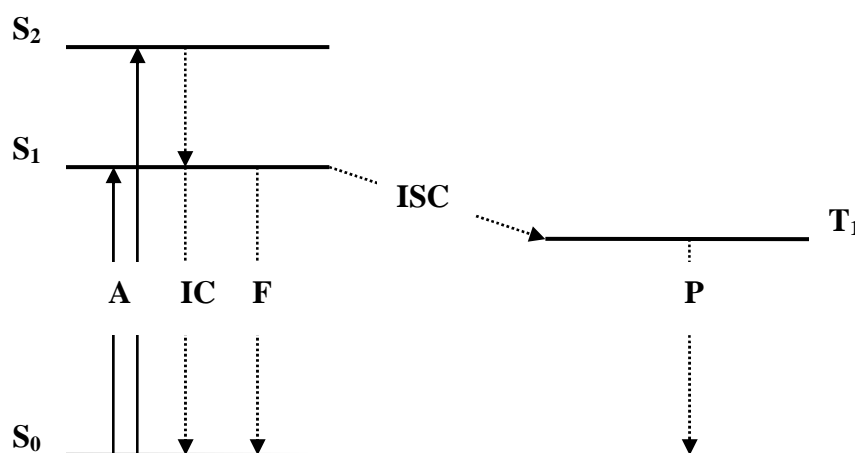
Fig. 2.3. Simplified Jablonski diagram. The following abbreviations are used: S_0, S_1, S_2 = singlet states, T_1 = triplet state, A = absorbance (10^{-15}s), F = fluorescence (10^{-9}-10^{-7}s), P = phosphorescence (10^{-7}-10^{-2}s), IC = internal conversion, ISC = intersystem crossing.

In case of organic molecules, absorbed light energy can cause luminescence that is shifted longwave in comparison to the absorption wavelength, because energy was lost via IR-vibrations of the chemical bonds. Depending on the nature of the excited state, luminescence can be divided into fluorescence and phosphorescence. Fluorescence occurs when a molecule in the first excited singlet state (S_1) returns to the ground state (S_0). This

E

excited state

2

1

0

2

1

0

ground state

nuclear
configuration
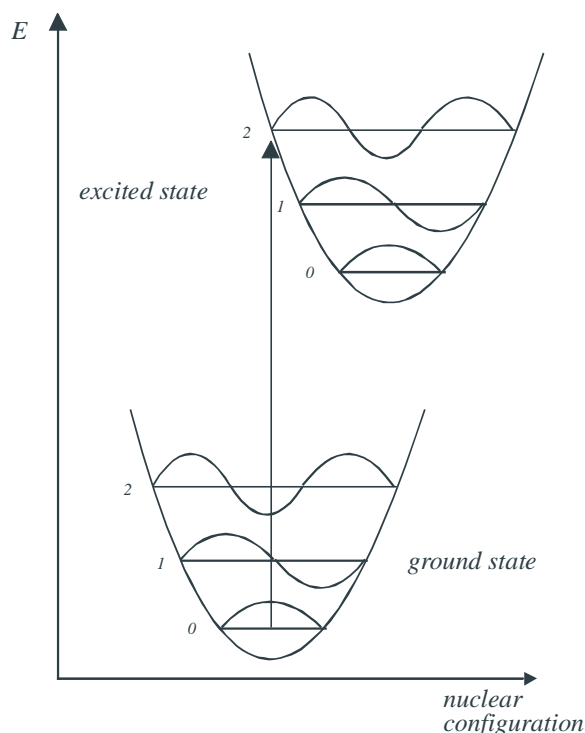
Fig. 2.4. Potential energy diagrams with
vertical transitions (Franck-Condon-Principle)

transition is spin-allowed. The emission rates of fluorescence are typically 10^{-8} s^{-1} and a typical fluorescence lifetime is near 10 ns. Phosphorescence is emission of light that results from transitions from triplet excited states to the ground state. Because these transitions are spin-forbidden, the emission rates are slow and lifetimes are typically in the range of milliseconds to seconds. The processes which occur between absorption and emission are usually illustrated by a Jablonski diagram (Fig. 2.3.). The singlet ground, first and second electronic states are depicted by S_0, S_1 and S_2. Fluorophores can exist in several vibrational energy levels (0, 1, 2,...) at each of these electronic levels. The transitions are depicted as vertical lines, according to the Franck-Condon principle (Fig 2.4.), which says that the transitions between the various states occurs so fast (in about 10^{-15} s) that there is no time for molecular motion during the transition processes. At room temperature, most molecules are present in the vibrational ground state. This is the reason why absorption typically occurs from the lowest vibrational energy.

There are several processes that can occur after light absorption. The fluorophore is excited to some higher vibrational level of S_1 or S_2. With a few rare exceptions, molecules relax in 10^{-12} s or less to the lowest vibrational level of SI (= internal conversion). The return to the ground state (= fluorescence) typically occurs to a higher excited vibrational ground state level, which then quickly reaches vibrational ground state. The absorption spectrum reflects the vibrational levels of the electronically excited states, and the emission spectrum reflects the vibrational levels of the electronic ground state. Generally, electronic excitation does not greatly alter the spacing of the vibrational energy levels and therefore the vibrational structures seen in the absorption and the emission spectra are similar. Molecules in the S_1 state can also undergo a spin conversion to T_1 (= intersystem crossing) and relax to the ground state by *phosphorescence*. Rate constants for

triplet emission are several orders of magnitude smaller than those for fluorescence, because phosphorescence is spin-forbidden.

2.2.1.1. *Referencing via Ratiometric Measurements*

In contrast to single-intensity based measurements, ratiometric or dual-wavelength measurements are preferable because the ratio of the fluorescence intensities at two wavelengths is in fact independent of the total concentration of the dye, photobleaching, fluctuations of the light source intensity, sensitivity of the instrument, etc[44]. On the other hand, this method requires two separate optical channels thus complicating the optical setup. For example, the drift in the sensitivity of both channels can be different, as can be the intensities at two excitation wavelengths. Light scatter and signal loss caused by fiber bending (e.g. in fiber optic sensors or certain sensortiterplate readers) further contribute to effects not compensated by two-wavelength referencing.

Fluorescent pH indicators allowing ratiometric measurements are e.g. HPTS, fluorescein, FAM, BCECF, SNAFL and SNARF dyes, CNF and the novel, lipophilic fluorescein derivatives in Chapter 5.

Ratiometric measurements can follow three different methods:

a) *one emission and two excitation wavelengths*: this ratio method is possible for most indicators and is used in conventional fluorescence microscopy.

b) *one excitation and two emission wavelengths*: this ratio method is applicable only to indicators exhibiting dual emission. This method is preferred for flow cytometry and confocal microscopy and allows emission ratio imaging.

c) *two excitation and two emission wavelengths:* this method is also possible for indicators exhibiting dual emission.

The principle of method a) was used for the sensors described in Chapter 5 and is shown in Fig. 2.5.
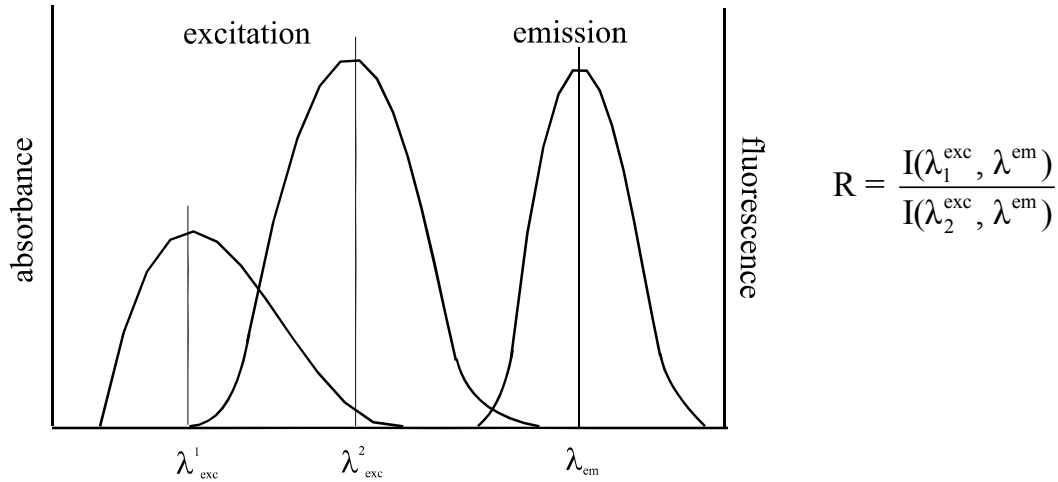
Fig. 2.5. Principle of ratiometric measurement for double-excitation measurements.

2.2.1.2. *Referencing via Dual Lifetime Referencing (DLR)*

Dual Lifetime Referencing (DLR) is a new principle to reference fluorescence intensities via fluorescence decay times[45]. Most fluorescent pH indicators have decay times in the nanosecond range (e.g. ~5 ns for fluoresceins). Common ratiometric methods use two excitation or two emission wavelengths to reference the sensor signal, whereas the DLR method uses two different luminophores having different decay times: A pH-sensitive, short-lived indicator and a pH-insensitive reference dye with a decay time in the µs or ms range. Both luminophores must have overlapping excitation and emission spectra. Excitation can be performed at the same wavelength and emission can be measured with one photodetector. The indicator is excited sinusoidal and therefore its fluorescence emission is also modulated sinusoidal, showing a shift of the phase angle.

Equation 2-11 depicts the relation between the phase angle Φ measured at a single modulation frequency f_{mod} and the luminescence decay time τ:

$$\tau = \frac{\tan \Phi}{2\pi f_{mod}} \tag{2-11}$$

Here, the phase shift of the overall signal is only dependent on the ratio of the two luminophores (Fig. 2.7.)
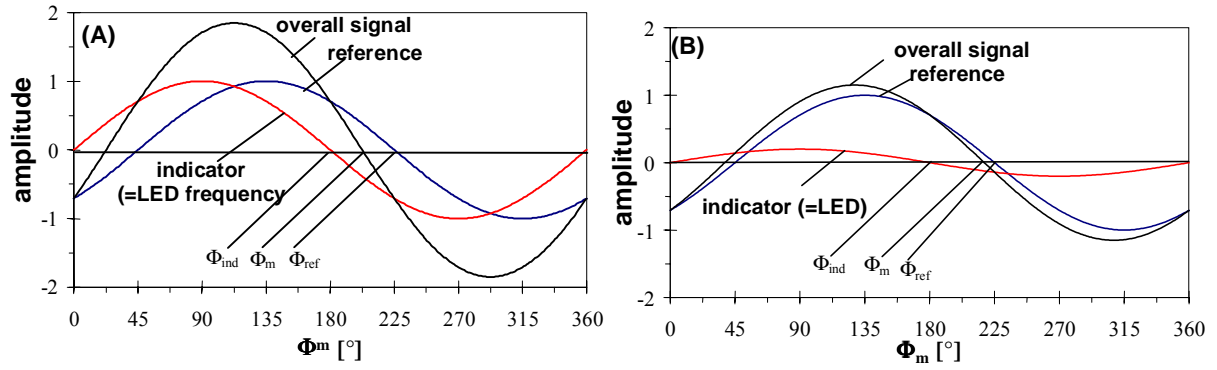
Fig. 2.7. Phase shift of the overall luminescence Φ_m, the reference Φ_{ref} and the indicator Φ_{ind}. Fluorescence of the indicator in (**A**) absence and (**B**) presence of the analyte.

Equations 2-12 and 2-13 show the superposition of the phase signals of the reference dye with constant decay time and luminescent intensity, and the indicator with pH-dependent decay time and intensity:

$$A_m \cdot \cos \Phi_m = A_{ref} \cdot \cos \Phi_{ref} + A_{ind} \cdot \cos \Phi_{ind} \qquad (2\text{-}12)$$

$$A_m \cdot \sin \Phi_m = A_{ref} \cdot \sin \Phi_{ref} + A_{ind} \cdot \sin \Phi_{ind} \qquad (2\text{-}13)$$

where A is the amplitude (intensity) of the overall signal (m), the reference (ref), or the indicator (ind). Φ_{ind} can be assumed to be equal to zero, because the reference luminophore has a decay time that is orders of magnitude longer than that of the indicator. Therefore, equations 2-12 and 2-13 can be simplified to give

$$A_m \cdot \cos \Phi_m = A_{ref} \cdot \cos \Phi_{ref} + A_{ind} \qquad (2\text{-}14)$$

$$A_m \cdot \sin \Phi_m = A_{ref} \cdot \sin \Phi_{ref} \qquad (2\text{-}15)$$

Dividing equation 2-14 by 2-15 results in a correlation of the phase angle and the intensity ratio of the indicator (A_{ind}) and reference luminophore (A_{ref}):

$$\cot \Phi_m = \frac{A_{ref} \cdot \cos \Phi_{ref} + A_{ind}}{A_{ref} \cdot \sin \Phi_{ref}} = \cot \Phi_{ref} + \frac{1}{\sin \Phi_{ref}} \cdot \frac{A_{ind}}{A_{ref}} \qquad (2\text{-}16)$$

Equation 2-16 results in a linear relation between phase angle Φ_m and the ratio of A_{ind}/A_{ref}, because the phase angle of the reference luminophore Φ_{ref} was assumed to be constant. Therefore, the phase angle of the overall signal can be taken as a referenced measure for the pH-dependent amplitude of the indicator.

The DLR-scheme has been applied to reference the signals of several optical sensors for different analytes[46-49], including a pH sensor using the t-DLR scheme (*time-domain – DLR*), which is explained elsewhere[50].

2.2.2. Fluorescence Decay Time

The luminescence decay time τ of a substance is defined as the average time the molecule remains in the excited state prior to its return to the ground state[51, 52]. Since this is a statistical consideration, it can, in the case of single exponential decay τ, also be described as the time after which 1/e of the initial excited molecules are not deactivated yet (Fig. 2.6.).
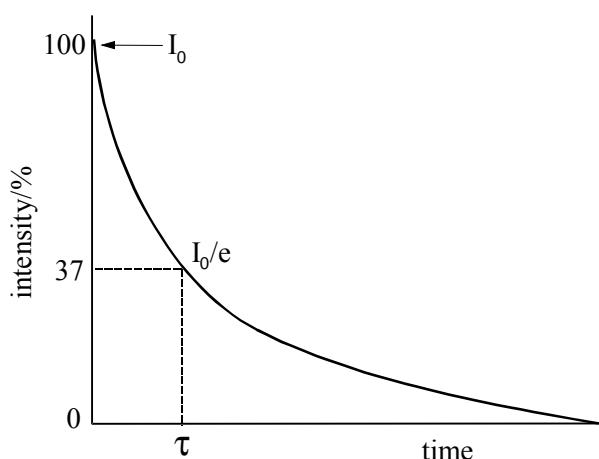
Fig. 2.6. Schematic of the single exponential decay. τ is the average decay time of the excited state.

The general relation between the fluorescence intensity I(t) and the decay time τ is given by equation 2-17:

$$\frac{I(t)}{I_0} = e^{-t/t_0} \qquad (2\text{-}17)$$

where I(t) is the fluorescence intensity at time t, I_0 is the maximum fluorescence intensity during excitation, t is the time after the excitation has ceased, and τ is the average decay time of the excited state. The decay time can be influenced by excited state reactions, energy transfer and collisional quenching (dynamic quenching)[53].

A collision between fluorophore in its excited state and the quencher results in radiationless deactivation and is called collisional or dynamic quenching. One of the best known collisional quenchers is molecular oxygen, which quenches almost all known fluorophores. Complex formation (static quenching) can be observed beneath collisional quenching. Both complex formation and collisional quenching require molecular contact between fluorophore and quencher. In case of static quenching a complex is formed between the fluorophore and the quencher, and this ground state complex is nonfluorescent. Static quenching causes no change of the fluorescence decay time of the fluorophore, because the process takes place in the ground state.

Two methods are widely used for the measurement of the fluorescence decay time, namely the pulse method (time domain measurement)[54] and the harmonic or phase modulation method (frequency domain measurement)[55].

In the time domain method or pulse method, the sample is excited with short pulses of light and the time-dependent decay of luminescence intensity is measured. The pulse method has the advantage that disturbing fluorophores or autofluorescence of the sample with short lifetimes can be easily separated, but the instrumentation is very sophisitcated.

In the frequency domain or phase modulation method, the sample is excited by sinusoidal light. The lifetime of the fluorophore causes a time lag between the absorbance and emission, expressed by the phase angle Φ and a decreased intensity relative to the incident light, called demodulation.

For example, SNARF-6 is a pH-sensitive indicator with different lifetimes for the acidic and the basic form. Apparently, the decay time of the base form is less than that of the acid form. Szmacinski and Lakowicz determined the decay times at pH 4.9 and 9.3 to be 4.51 and 0.95 ns, respectively[56]. Such a difference in decay times allows discrimination of basic and acidic form and makes *ratiometric lifetime measurement* possible.

2.3. References

1.   S. P. L. Sorensen, **Enzyme Studies. II. The Measurement and Importance of the Hydrogen Ion Concentration in Enzyme Reactions,** Biochemische Zeitschrift, **1909**, 21, 131-304.

2.   F. Kober, **Soerensen and pH,** Praxis der Naturwissenschaften, Chemie, **1991**, 40(2), 43-45.

3.   F. Szabadvary, **Geschichte der Analytischen Chemie (History of Analytical Chemistry),** Vieweg & Sohn-Verlag, **1966**.

4.   http://www.geocities.com/bioelectrochemistry/sorensen.htm

5.   S. Arrhenius, **Über die Dissoziation der im Wasser gelösten Stoffe**, Z. Phys. Chem., **1887**, 1, 631-648.

6.   W. Ostwald, **Grundlagen der Analytischen Chemie**, Theodor Steinkopf, Dresden und Leipzig, **1894**.

7.   H. Friedenthal, **Die Bestimmung der Reaktion einer Flüssigkeit mit Hilfe von Indikatoren**, Z. Elektrochem., **1904**, 10, 113-119.

8. H. Galster, **pH Measurement: Fundamentals, Methods, Applications, Instrumentation,** VCH Wiley**, 1991**.

9. J. W. Nicholson, **A brief history of acidity,** Education in Chemistry, **2004**, 41(1), 18-20.

10. P. Atkins, J. de Paula, **Physical Chemistry**, 7th edition, Oxford, **2002**.

11. G. Mattock, G. R. Taylor, **pH Measurements and Titration**, Heywodd & Comp. Ltd., London, **1961**.

12. A. K. Covington, R. G. Bates, R. A. Durst, **Definition of pH Scales, Standard Reference Values, Measurement of pH and Related Terminology**, Pure Appl. Chem., **1985**, 531-542.

13. G. Bugge, **Der Alchemist – Die Geschichte Leonhard Thurneyssers, des Goldmachers von Berlin**, Wilhelm-Limpert-Verlag, Berlin, **1943**.

14. M. Cajlakovic, A. Lobnik, T. Werner, **Stability of new optical pH sensing material based on cross-linked poly(vinyl alcohol) copolymer,** Anal. Chim. Acta, **2002**, 455(2), 207-213.

15. S. Weib, E. Heinzle, G. T. John, I. Klimant, **Oxygen transfer and mixing behavior in 96-well microtiter plates,** Bioforum, **2001**, 24(10), 662-664.

16. K. P. McNamara, T. Nguyen, G. Dumitrascu, J. Ji, N. Rosenzweig, Z. Rosenzweig, **Synthesis, characterization, and application of fluorescence sensing lipobeads for intracellular pH measurements,** Anal. Chem., **2001**, 73(14), 3240-3246.

17. J. R. Lakowicz, J. D. Dattelbaum, I. Gryczynski, **Intensity measurements in scattering media,** Sens. Actuat. B, **1999**, B60(1), 1-7.

18. S. C. Furlong, **Simultaneous dual excitation/single emission fluorescent sensing method for pH and pCO$_2$,** U.S. Patent 5672515, **1997**.

19. Y. Yang, P. A. Wallace, M. Campbell, A. S. Holmes-Smith, **Alteration in the response of fluorescein immobilized in sol-gel thin films as an optical fiber sensing mechanism for pH,** Proc. SPIE, **1996**, 2895, 237-242.

20. M. Plaschke, R. Czolk, J. Reichert, H. J. Ache, **Stability improvement of optochemical sol-gel film sensors by immobilization of dye-labeled dextrans,** Thin Solid Films, **1996**, 279(1-2), 233-235.

21. T. F. Liebert, D. R. Walt, **Synthesis of pH-sensitive modified cellulose ether half esters and their use in pH detecting systems based on fiber optics,** J. Control Release, **1995**, 35(2-3), 155-163.

22. G. Boisde, J. J. Perez, **Active chemical sensor using optical fibers,** EP 284513,

1988.

23.   H. E. Posch, M. J. P. Leiner, O. S. Wolfbeis, **Towards a gastric pH-sensor: an optrode for the pH 0-7 range,** Fresen. J. Anal. Chem., **1989**, 334(2), 162-165.

24.   D. R. Walt, S. Luo, C. Munkholm, **Fiber optic chemical sensors using immobilized bioreceptors,** Proc. SPIE, **1988**, 906, 60-64.

25.   T. Hirschfeld, F. Wong, **Preparation and use of a pH-sensitive optrode, especially for invasive monitoring of blood pH,** EP 247261, **1987.**

26.   H. Diehl, N. Horchak-Morris, **Studies on fluorescein V. The absorbance of fluorescein in the ultraviolet, as a function of pH**, Talanta, **1987**, 34, 739.

27.   H. Leonhardt, L. Gordon, R. Livingstone, **Acid-base equlilibra of fluorescein and 2',7'-dichlorofluorescein in their ground and fluorescent state**, J. Phys. Chem., **1971**, 75, 245.

28.   L. Saari, W. R. Seitz, **pH sensor based on immobilized fluoresceinamine**, Anal. Chem., **1982**, 54, 821.

29.   G. N. Lewis, M. Randall, **The activity coefficient of strong electrolytes,** J. Am. Chem. Soc., **1921**, 43, 1112-1154.

30.   P. Debye, E. Hückel, **The theory of electrolytes. I. Lowering of freezing point and related phenomena,** Physik. Z., **1923**, 24, 185-206.

31.   R. H. Stokes, R. A. Robinson, R. A., **Ionic hydration and activity in electrolyte solutions,** J. Am. Chem. Soc., **1948**, 70, 1870-1878.

32.   M. Kilpatrick, **The colorimetric determination of hydrogen-ion concentration in aqueous solution,** Chem. Rev., **1935**, 16, 57-66.

33.   O. S. Wolfbeis, **Fiber Optic Chemical Sensors and Biosensors**, Vol. I, CRC Press, Boca Raton, **1991,** pp. 10.

34.   H. Kautsky, A. Hirsch, **Energy transformations on boundary surfaces. IV. Interaction of excited dyestuff molecules and oxygen,** Ber., **1931**, 64B, 2677-2683.

35.   O. S. Wolfbeis, B. M. Weidgans, **Fiber Optic Chemical Sensors and Biosensors – A View back,** in **"Optical Chemical Sensors",** F. Baldini & J. Homola (eds.), NATO Adv. Study Series, **2004**, Kluwer (Doordrecht), in press.

36.   S. R. Goldstein, J. I. Peterson, R.V. Fitzgerald, **A miniature fiber optic pH sensor for physiological use,** J. Biomech. Eng., **1980**, 102(2), 141-146.

37.   N. Opitz, D. W. Luebbers, **New fluorescence photometrical techniques for simultaneous and continuous measurements of ionic strength and hydrogen ion activities,** Sens. Actuat., **1983**, 4(3), 473-479.

38. O. S. Wolfbeis, H. Offenbacher, **Fluorescence sensor for monitoring ionic strength and physiological pH values,** Sens. Actuat., **1986**, 9(1), 85-91.

39. J. Janata, **Do Optical Sensors Really Measure pH,** Anal. Chem., **1987**, 59, 1351.

40. J. Janata, Anal. Chem., **1992**, 64, 921A-927A.

41. S. M. Barnard, D. Beckelmann, J. Berger, M. Rouilly, A. Waldner, **Optical sensor system for pH determination independently of the ion strength using fluorescein bound to a polymer via a urethane and/or urea group,** WO Patent 9747966, **1997**.

42. S. M. Barnard, D. Beckelmann, J. Berger, M. Rouilly, A. Waldner, **Optical sensor system for the determination of pH values independently of ionic strength.** WO Patent 9715832, **1997**.

43. P. T. Sotomayor, I. M. Raimundo, A. J. G. Zarbin, J. J. R. Rohwedder, G. O. Neto, O. L. Alves, **Construction and evaluation of an optical pH sensor based on polyaniline-porous Vycor glass nanocomposite,** Sens. Actuat. B, **2001**, B74(1-3), 157-162.

44. B. Valeur, **Molecular Fluorescence - Principles and Applications, 1st Edition,** VCH Wiley**,** Weinheim, **2000,** 276-287.

45. I. Klimant, C. Huber, G. Liebsch, G. Neurauter, A. Stangelmayer, O. S. Wolfbeis, **Dual Lifetime Referencing (DLR) - a new scheme for converting fluorescence intensity into a frequency-domain or time-domain information.** In *New Trends in Fluorescence Spectroscopy*, Springer Series on Fluorescence, **2001**, 257-274.

46. T. Mayr, I. Klimant, O. S. Wolfbeis, T. Werner, **Dual lifetime referenced optical sensor membrane for the determination of copper(II) ions,** Anal. Chim. Acta, **2002**, 462(1), 1-10.

47. C. Huber, I. Klimant, C. Krause, T. Werner, O. S. Wolfbeis, **Nitrate-selective optical sensor applying a lipophilic fluorescent potential-sensitive dye,** Anal. Chim. Acta, **2001**, 449(1-2), 81-93.

48. C. Huber, I. Klimant, C. Krause, O. S. Wolfbeis, **Dual Lifetime Referencing as Applied to a Chloride Optical Sensor,** Anal. Chem., **2001**, 73(9), 2097-2103.

49. T. Mayr, C. Igel, G. Liebsch, I. Klimant, O. S. Wolfbeis, C**ross-Reactive Metal Ion Sensor Array in a Micro Titer Plate Format,** Anal. Chem., **2003**, 75(17), 4389-4396.

50. G. Liebsch, I. Klimant, C. Krause, O. S. Wolfbeis, **Fluorescent Imaging of pH with Optical Sensors Using Time Domain Dual Lifetime Referencing**, Anal. Chem., **2001**, 73(17), 4354-4363.

51. E. A. H. Hall, **Photometric assay techniques. In** *Biosensors*, Open University Press, Buckingham, **1990**, 141-219.

52. J. R. Lakowicz, **Introduction to fluorescence. In** *Principles of Fluorescence Spectroscopy*, 2nd edition, Kluwer Academic/Plenum Publishers, New York, **1999**, 1-23.

53. C.A. Parker, **Photoluminescence of Solutions**, Elsevier, Amsterdam, 1968.

54. J. R. Lakowicz, **Time-domain lifetime measurements. In** *Principles of Fluorescence Spectroscopy*, 2nd edition, Kluwer Academic/Plenum Publishers, New York, **1999**, 95-140.

55. J. R. Lakowicz, **Frequency-domain lifetime measurements. In** *Principles of Fluorescence Spectroscopy*, 2nd edition, Kluwer Academic/Plenum Publishers, New York, **1999**, 141-184.

56. H. Szmacinski, J. R. Lakowicz, **Optical measurements of pH using fluorescence lifetime and phase-modulation fluorometry**, Anal. Chem., **1993**, 65, 1668-1674.

Chapter 3

Effects of Ionic Strength on Fluorescent pH Indicators in Aqueous Solutions

In this chapter different, fluorescent pH indicators are compared with respect to the their cross-sensitivity of the signal towards ionic strength. Ionic strength was varied in the range from 50 mM to 400 mM with NaCl as background electrolyte. The method of mixing two differently charged indicators to minimize the effect of ionic strength is evaluated.

3.1. Introduction

In the 16th century, the alchemist Leonhard Thurneysser found the color change of viola sap by acids[1]. This first pH "indicator" was used for a long time for the detection of acids. Based on this observation, Friedenthal created a first pH scale based on the color changes of indicator molecules[2].

pH glass electrodes nowadays are the most popular instruments for pH detection, because of their ease of use, low costs and availability of well characterized buffer solutions for calibration. 30 years ago however, colorimetric methods based on water-soluble pH-indicators were frequently used. These days, optical pH sensors become more and more competitive in comparison to the electrode, but the soluble-indicator based methods are still of interest. Many of them are used for specialized tasks not well suited to pH meters nor optical pH sensors. Chlorophenol red, for instance, is used for biological research to stain certain kinds of cells, as well as to identify alkaline paper[3]. Especially for the determination of freshwater pH (rivers, lakes or ground waters)[4-8], indicator-based measurements are even preferable. Electrodes behave unpredictably in low ionic strength solutions and even under the best conditions, electrode potentials take several minutes to stabilize after the electrode is placed in a low ionic strength (low buffered) solution[9-11].

The classical pH indicators are based on changes of absorbance. The absorption dyes can be classified in triphenylmethane dyes, including phthaleins and sulfophthaleins and

azo dyes. Table 3.1. gives information about a few examples of absorption-based pH indicators.

Tab. 3.1. pH indicators, color change interval and pK_a values.

Indicator	pH range	Color change acid-basic	pK_a
Thymol blue (1st diss.)*	1.2-2.8	red $\rightarrow$ yellow	1.5
Methyl orange*	3.1-4.4	red $\rightarrow$ yellow	4.2
Congo Red	3.0-5.2	blue $\rightarrow$ red	3.7
Bromophenol blue[#,+]	3.0-4.6	yellow $\rightarrow$ blue-violet	4.1
Bromocresol green[+]	3.8-5.4	yellow $\rightarrow$ blue	4.7
Methyl red[+]	4.2-6.3	red $\rightarrow$ yellow	5.1
Litmus	5.0-8.0	red $\rightarrow$ blue	n.d.
Bromothymol blue	6.0-7.7	yellow $\rightarrow$ blue	6.8
Phenol red[*,+]	6.8-8.4	yellow $\rightarrow$ red	7.6
Thymol blue (2nd diss.)[*]	8.0-9.6	yellow $\rightarrow$ blue	8.9
Phenolphthalein[*]	8.2-10.0	colorless $\rightarrow$ red	9.4
Thymolphthalein	9.3-10.5	colorless $\rightarrow$ blue	9.9

Edmonds([+])[12], Bates(*)[13] and Kilpatrick([#])[14] studied the effect of changing salt concentrations (*ionic strength*) on the marked indicators in the range from 10 mM to 3 M, respectively.

Fluorescent pH indicators offer much better sensitivity than the classical dyes listed in Tab. 3.1. based on color change. In contrast to absorptiometry, in fluorometry light does not have to pass the colored solution and can be detected at the same site where the light source is located (remission mode). Therefore, fluorescent pH indicators can be used in colored or turbid solutions and have found widespread application in analytical and bioanalytical chemistry and cellular biology (e.g. for measuring intracellular pH[15-18]). Most of the fluorescent pH indicators are based on the structure of coumarins (e.g. 4-methylumbelliferone), pyranine (HPTS and DHPDS), fluorescein and its derivatives (e.g. FAM, BCECF), or SNARF and SNAFL dyes. Table 3.2. contains a selection of frequently used fluorescent pH indicators.

Tab. 3.2. Fluorescent pH indicators, spectroscopic properties and pK_a.

Fluorophore	Excitation / Emission [nm]	pK_a
Fluorescein	490/520	6.7
Eosin	520/550	3.80
2',7'-Dichlorofluorescein	502/526	5.0
5(6)-Carboxyfluorescein	490/520	6.4

5(6)-Carb-2',7'-Dichlorofluorescein	505/530	5.0-5.3
5(6)-Carboxyeosin	525/560	3.6
SNAFL	550/620	7.8
SNARF	560/625	7.5
HPTS	454/511	7.3

Note: Data taken from www.probes.com

In a search for suitable indicators for the application in optical pH sensors with low cross-sensitivity towards ionic strength we focussed on highly fluorescent pH indicators with pK_a in the physiological range. HPTS, carboxyfluorescein, and fluorescein are often used indicators in fluorescence-based pH sensors. Their spectral properties are similar and the pK_a's are in the range from 6.4 to 7.3. The structures and their charge difference depending on pH are given Figure 3.1. The charge of the indicators differ from –4 (HPTS) to –1 (fluorescein), or 0 for the lactonized form, respectively (see Fig. 2.1).

While electrodes measure the activity of protons in an aqueous solution, the signal of optical sensors is based on the ratio of concentrations of acid and base form of a pH-sensitive dye. Considering the activity of both forms, the Henderson-Hasselbalch equation relates this concentration ratio to pH:

$$pH = pK_a + \log \frac{c(A^-)}{c(HA)} + \log \frac{f_{A^-}}{f_{HA}} - \log a_{H_2O} \qquad (3\text{-}1)$$

While the activity of water a_{H2O} is almost constant and can be neglected, the activity coefficients f are only close to unity in very dilute solutions of low ionic strength. This is not the case in most real samples.

Depending on the ionic strength I of the analyte solution, the activity coefficient may be estimated by the extended Debye-Hueckel equation for aqueous solutions

$$\log f_x (I,B) = \frac{-0.509 \cdot z_i^2 \cdot I^2}{1 + B \cdot I^2} \qquad (3\text{-}2)$$

where z_i is the charge on species i and B is an empirical parameter[19]. In this chapter, negative charged indicators and a novel, partially positive charged carboxyfluorescein derivative (*Fluamin*) were characterized with respect to their sensitivity of ionic strength using phosphate buffers in the range from IS = 50 to 400 mM.

HPTS
$\mathbf{zA^{-}}/A = \mathbf{-4}/-3$
$pK_a = 7.3$

5(-6)-carboxyfluorescein
$\mathbf{zA^{-}}/A = \mathbf{-3}/-2$
$pK_a = 6.4$

Fluorescein
$\mathbf{zA^{-}}/A = \mathbf{-2}/-1$
$pK_a = 6.4$

Fluamin
$\mathbf{zA^{-}}/A = \mathbf{-1}/0$
$pK_a = 6.2$
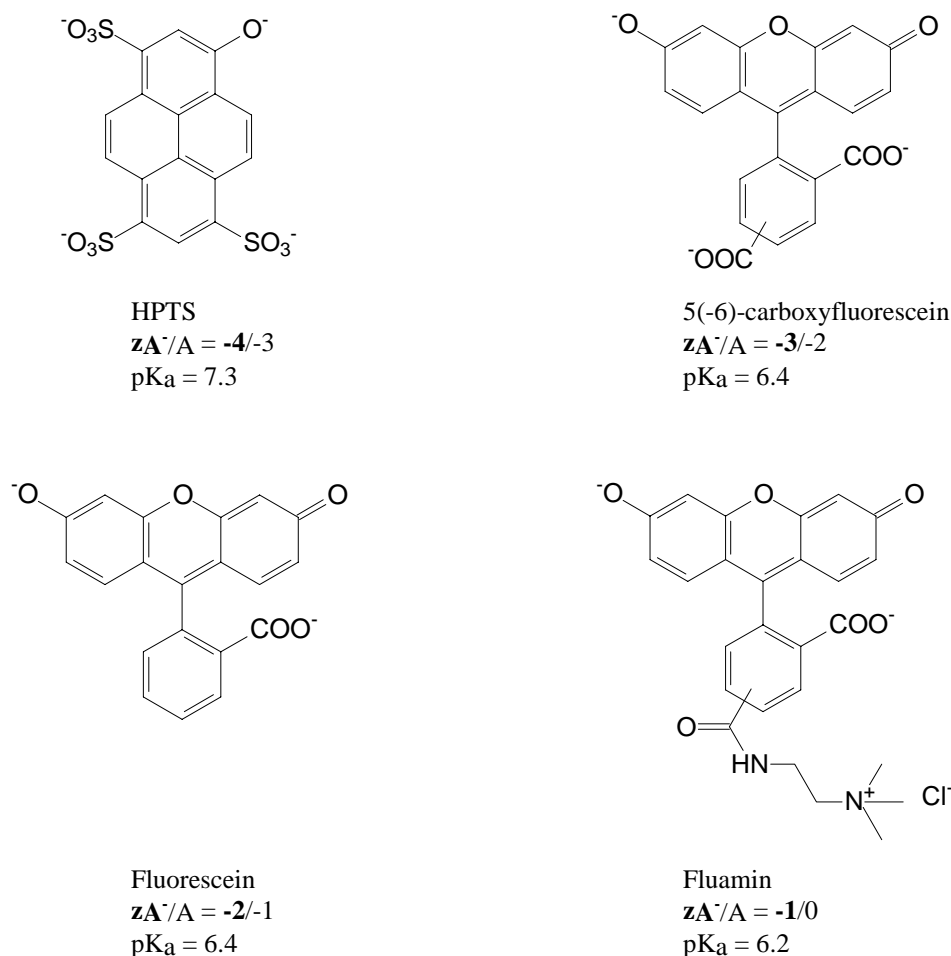
Fig. 3.1. Structures of fluorescent pH indicators, respective charges for basic and acidic form and pK_a. In case of fluoresceins, the resulting charge for the lactonized form is given in parentheses.

3.2.   Materials and Methods

3.2.1.   Chemicals

All chemicals used were of analytical grade and used without further purification, except that 8-hydroxypyrene-1,3,6-trisulfonic acid (HPTS, Otto Krieger, Vienna, Austria) was recrystallized in methanol. (2-Aminoethyl)trimethylammonium chloride hydrochloride (AETA, product no. 06730), dimethylformamide (DMF, product no. 40248), 5(6)-carboxyfluorescein (product no. 21877) and fluorescein (product no. 46955) were purchased from Fluka (Buchs, Switzerland, www.sigmaaldrich.com). Phosphate buffer solutions of defined pH were prepared from respective sodium salts from hydrogen phosphate and dihydrogen phosphate of analytical grade from VWR (Darmstadt, Germany, www.vwr.de). Methanesulfonic acid, resorcin and benzoyl chloride were also from VWR.

Ionic strength of buffer solutions was adjusted with sodium chloride as background electrolyte. Sodium hydroxide (product no. 7098) and hydrochloric acid (product no. 7038) were from J. T. Baker (Phillipsburg, NJ, USA, www.jtbaker.com). Polystyrene microtiterplates (96 wells, product no. 650101) with round bottom were obtained from Greiner (Frickenhausen, Germany, www.greinerbioone.com). Aqueous solutions were prepared from doubly distilled water.

3.2.2. Buffer preparation

Phosphate buffers with a total phosphate concentration of 10 mM and with sodium chloride to adjust ionic strength were used. Buffers were prepared by mixing two stock solutions of defined ionic strength. An acidic stock solution A was prepared by dissolving 1.3799 g of NaH$_2$PO$_4$ x H$_2$O and sodium chloride in 1 L of water. 1.799 g (1.1866 g for IS = 25 mM) of Na$_2$HPO$_4$ x 2 H$_2$O and sodium chloride were dissolved in 1 L of water for a basic stock solution B. Table 3 gives the corresponding amounts of sodium chloride for each stock solution to adjust the desired ionic strength. Ionic strength of the buffers was calculated by means of an Excel sheet according to the equation of Debye and Hückel.

Table 3.3.   Amounts of additional sodium chloride to adjust the total ionic strength of the stock solutions A and B.

Ionic strength [mM]	Amount of NaCl for solution A [g]	Amount of NaCl for solution B [g]
25	0.8766	0.2922
50	2.3376	1.1688
100	5.2596	4.0908
200	11.1036	9.9348
300	16.9476	15.7788
400	22.7916	21.6228
500	28.6356	27.4668

Stock solutions A and B of the same ionic strength were mixed, controlled by a pH meter, to obtain the desired solutions of defined pH. For 2 mM phosphate buffer concentration was set to the respective phosphate concentration without background electrolyte.

3.2.3. pH Meter

The pH values of solutions were checked using a digital pH meter (Schott, Mainz, Germany, www.schott.de) calibrated with standard buffers of pH 7.00 and 4.00 (VWR, Darmstadt, Germany, www.vwr.de) at 20 ± 2 °C.

3.2.4. Fitting function and calibration curves

Calibration curves were fitted with the Boltzmann-function:

$$F = \frac{A_1 - A_2}{1 + e^{(x - x_0)/dx}} + A_2 \qquad (3\text{-}3)$$

A_1, A_2, x_0, dx are empirical parameters describing the initial value (A_1), final value (A_2), center (x_0) and the width of the fitting curve (dx).

Fitting curves were characterized by the point of inflection ($K_{1/2}$) of the Boltzmann fit.

3.2.5. Absorbance Measurements

Absorbance spectra were performed on a UV/VIS spectrophotometer Cary 50 Bio from Varian (Darmstadt, Germany, www.varian.de), shown in Figure 3.2., using a xenon flash lamp as light source. Polystyrene cuvettes (product no.1960, Kartell, Italy, www.kartell.it) with a cell length of 1 cm to measure the spectra of solutions. The baseline was determined against PBS pH 9.0.

Fig. 3.2. Varian Cary 50 Bio UV-VIS photometer.

3.2.6. Fluorescence Measurements

Fluorescence emission spectra were acquired with an Aminco Bowman Series 2 luminescence spectrometer from SLM-Aminco (Rochester, NY 14625, USA) equipped with a continuous wave 150 W xenon lamp as the light source, as shown in Figure 3.3. Measurements were performed at 20 ± 1 °C by means of Haake B3 constant temperature water bath.

Fig. 3.3. SLM-Aminco luminescence spectrometer

3.2.6. Fluorescence Measurements in Microtiterplates

A Fluoreskan Ascent microplate reader from Labsystems (Helsinki, Finland, see Figure 3.4.) was used. Fluorescence was measured from the bottom of the microtiter plates. For the fluoresceins, a 485 nm bandpass filter was used for excitation and a 530 nm bandpass filter for emission. For HPTS, the excitation was changed to a 460 nm bandpass filter. A 30 W quartz halogen lamp was used as light source. By means of an internal incubator temperature was kept constant at 25 ± 1 °C.
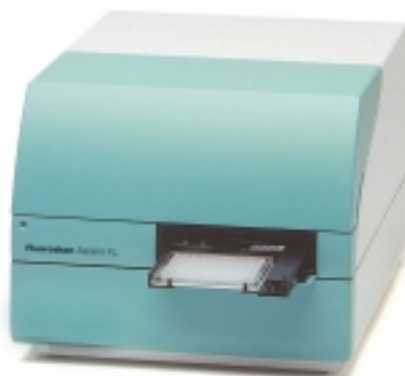

Fig. 3.4. Labsystems Ascent Fluoroskan Microtiterplate Reader

3.2.7. Measurements

Stock solutions with a concentration of c = $2.1 \cdot 10^{-5}$ mol/L of the dyes HPTS, carboxyfluorescein, fluorescein and fluamin were prepared. In case of absorption and emission spectra, solutions of c = $1.4 \cdot 10^{-5}$ mol/L were used. Dilutions were prepared by mixing 2 mL of dye stock solutions with 1 mL of respective buffer. Absorbance measurements were performed in the range from 350 to 700 nm; emission spectra were recorded from 500 to 600 nm with an excitation wavelength of 480 nm for all dyes.

Cross-sensitivity towards ionic strength of all dyes was measured in 96-well-microtiterplates. The concentration of the indicator was kept very low and dilutions of the stock solutions were used. In each well, 10 µL of dye solutions and 200 µL of the respective buffers were pipetted to give a total dye concentration of c = $1.0 \cdot 10^{-6}$ mol/L. Measurements were taken immediately after filling. Mean values and standard deviations were calculated from at least four measurements.

Ionic strength of the phosphate buffer systems was varied in the range from 25 mM to 400 mM. In general, for the absorption and emission spectra phosphate buffers of IS = 50 mM were used, if not stated otherwise.

3.3.   Results and discussions

3.3.1. Choice of Indicators

HPTS and fluorescein derivatives were chosen because of their spectral similarity in absorption and emission. Thus, mixtures of the dyes can be checked towards their effect of ionic strength by using the same excitation and emission wavelength.

The dissociation constants of the dyes are in the physiological range around pH 7.0 and can therefore the dyes can be applied in sensors for biotechnical and medical applications. Numerous other fluorescent indicators with neutral pK_a's like coumarins, modified anthracenes, cyanines, SNARFs and SNAFLs exist, but these indicators do not have overlapping absorption/excitation spectra and emission spectra with the Ru(dpp)$^{2+}$ complex. This is a prerequisite for the DLR scheme described in chapter 2 and chapter 6. HPTS and fluoresceins fulfill this requirement and have been chosen for the pre-study described in this chapter.

3.3.2. Effects of Ionic Strength on HPTS

The absorption and emission spectra of HPTS in buffers of varying pH are shown in Figure 3.5. Depending on pH, HPTS shows two different absorption maxima at 455 nm for the basic form and 405 nm for the acidic form, respectively, and an explicit isosbestic point at 418 nm. The emission spectra show only one maximum at 510 nm for both forms. Therefore, HPTS can be used for single intensity measurements and ratiometric double-excitation measurements.
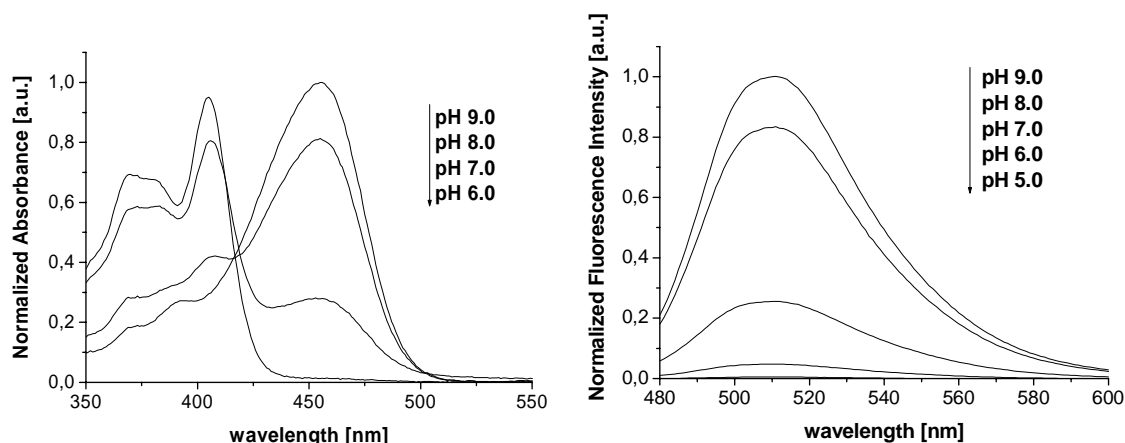
Fig. 3.5. Absorption spectra (left) and fluorescence emission spectra (right) of HPTS in presence of PBS of varying pH and constant ionic strength.

The calibration plots for the experiments with varying ionic strength are shown in Figure 3.6. Calibration plots were normalized and the resulting pK_a values were displayed versus the respective ionic strength in order to ease comparison.
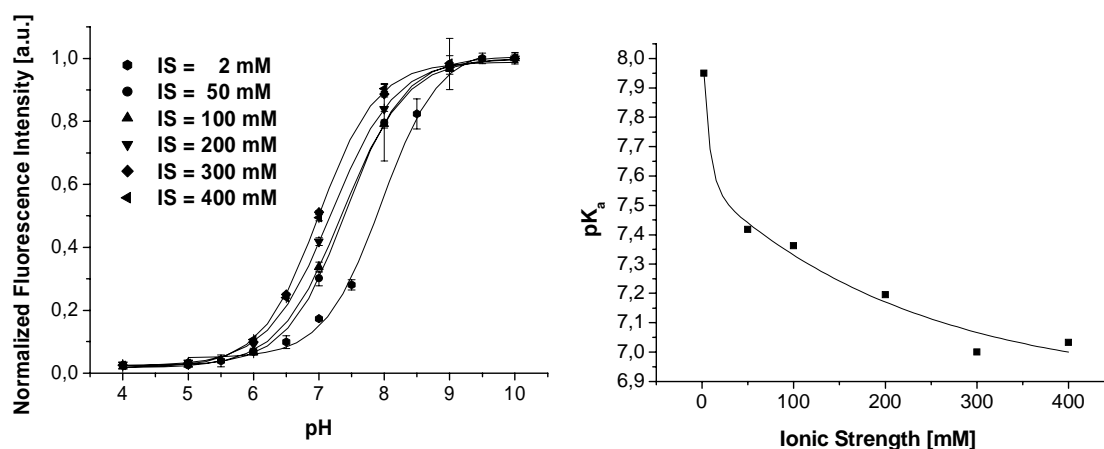
Fig. 3.6. Normalized calibration plots of a 10^{-6} M HPTS solution in dependence of pH and ionic strength (left). Shift of apparent pK_a values with increasing ionic strength from 2 mM to 400 mM (right).

Due to the highly negatively charged structure of HPTS in its acidic and basic form (-3/-4), changes in ionic strength cause a notable shift on the dissociation constant which is given in Table 3.4 and shown graphically in Figure 3.6. (right). Taking the calibration plot of 200 mM as mean value, variation of IS in the range from 50 mM to 400 mM causes a pH error of ca. 0.2 pH units.

Tab. 3.4. Effect of IS on the dissociation constant of HPTS in the range from 2 mM to 400 mM.

Ionic strength [mM]	Apparent pK_a
2	7.95
50	7.42
100	7.36
200	7.20
300	7.00
400	7.03

3.3.3. Effects of Ionic Strength on Carboxyfluorescein

The absorption and emission spectra of carboxyfluorescein in buffers of varying pH are shown in Figure 3.7. In contrast to HPTS, carboxyfluorescein shows only two different absorption maxima at 492 nm for the basic form and 452 nm for the acidic form in the range from pH 9 to 5. For pH lower than 4 the chromophore lactonizes and the total intensity diminishes. The emission spectra display only one maximum at 518 nm for both forms.


Fig. 3.7. Absorption spectra (left) and fluorescence emission spectra (right) of carboxyfluorescein in presence of phosphate buffers of varying pH and constant ionic strength.

The calibration plots for the experiments with varying ionic strength are shown in Figure 3.8. Calibration plots were normalized and the resulting pK_a values were plotted versus the respective ionic strength in order to ease comparison.

Fig. 3.8. Normalized calibration plots of a 10^{-6} M carboxyfluorescein solution in dependence of pH and ionic strength (left). Shift of apparent pK_a values with increasing ionic strength from 2 mM to 400 mM (right).

In comparison to HPTS the carboxyfluorescein chromophore carries one negative charge less for both, acidic and basic form (-2/-3). This "charge reduction" has a noticeable effect on the cross-sensitivity towards ionic strength. The apparent dissociation constants are given in Table 3.5 and are shown graphically in Figure 3.8 (right). Taking the calibration plot of 200 mM as mean value, variation of IS in the range from 50 mM to 400 mM causes a pH error of ca. 0.12 pH units.

Tab. 3.5. Effect of IS on dissociation constant of carboxyfluorescein in the range from 2 mM to 400 mM.

Ionic strength [mM]	Apparent pK_a
2	6.82
50	6.49
100	6.42
200	6.34
300	6.26
400	6.25

3.3.4. Effects of Ionic Strength on Fluorescein

The absorption and emission spectra of fluorescein in phosphate buffers of varying pH are shown in Fig. 3.9. In analogy to carboxyfluorescein, fluorescein shows the absorption maxima at 492 nm for the basic form and 452 nm for the acidic form in the range from pH 9 to 5. For pH lower than 4 the fluorescein chromophore also lactonizes and the total intensity diminishes. The emission spectra display only one maximum at 518 nm for both forms.
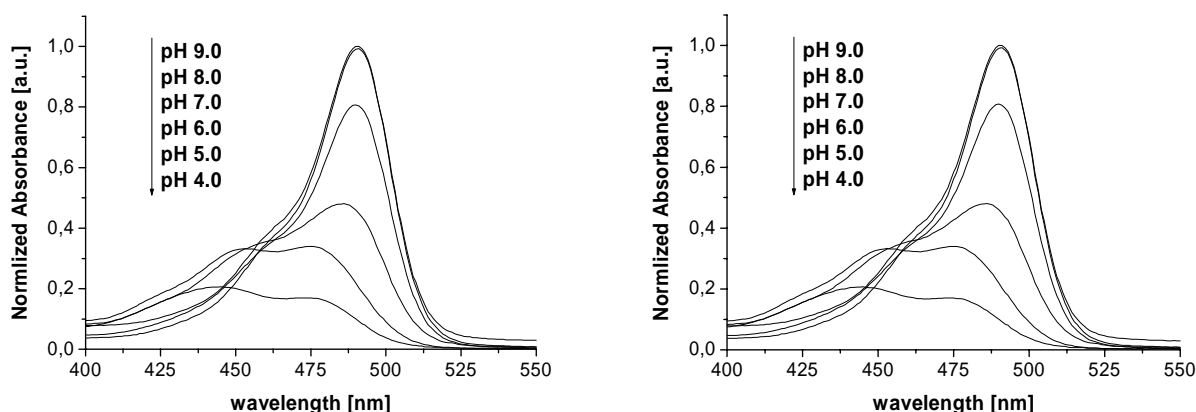
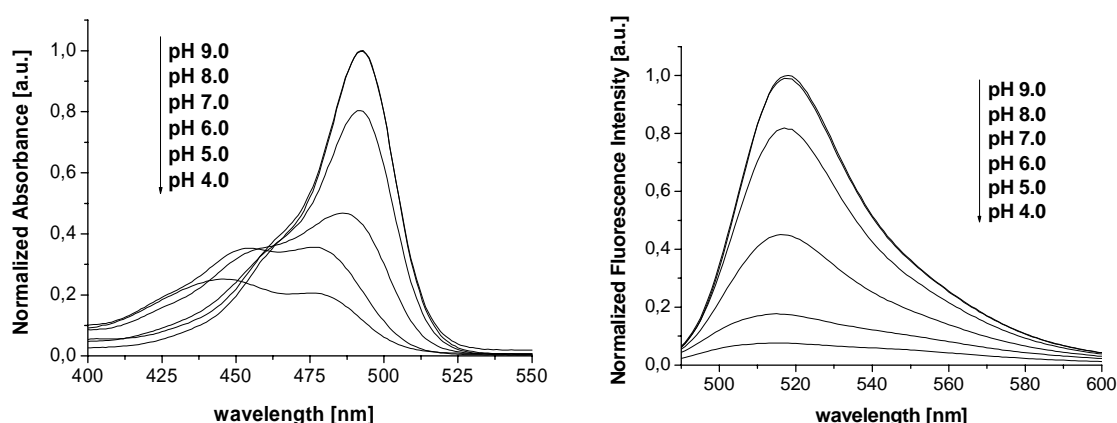**Fig. 3.9.** Absorption spectra (left) and fluorescence emission spectra (right) of fluorescein in presence of phosphate buffer of varying pH and constant ionic strength.

The calibration plots for the experiments with varying ionic strength are shown in Fig 3.10. Calibration plots were normalized and the resulting pK_a values were plotted versus the respective ionic strength in order to ease comparison.
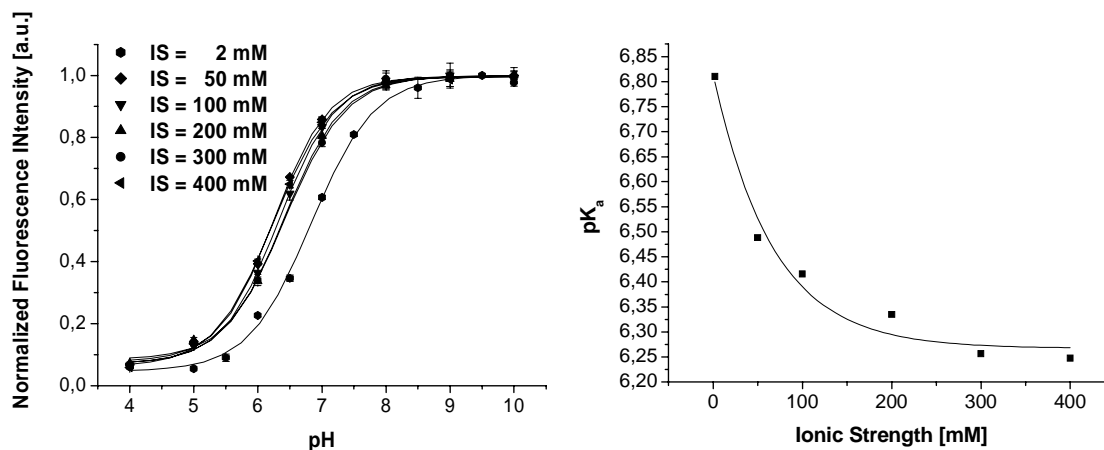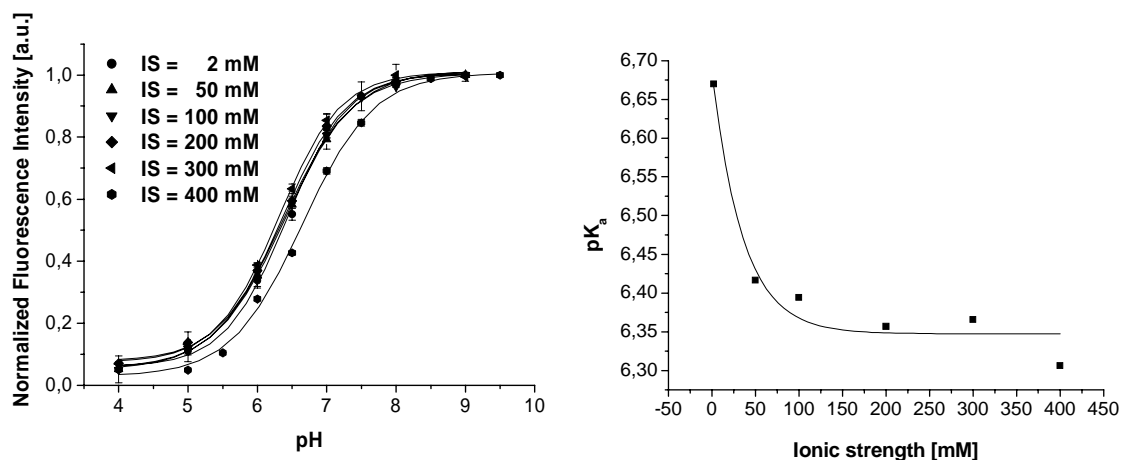

Fig. 3.10. Normalized calibration plots of a 10^{-6} M fluorescein solution as function of pH and ionic strength (left). Shift of apparent pK_a values with increasing ionic strength from 2 mM to 400 mM.

Fluorescein carries least negative charges of all investigated indicators in this series. The missing carboxy group in 5'- or 6'-position reduces the charges to -2 (basic) and -1 (acidic). Compared to HPTS and carboxyfluorescein, fluorescein is less affected by ionic strength. The shift of the dissociation constant with varying IS is given in Table 3.6 and shown graphically in Figure 3.10 (right). Again, taking the calibration plot of 200 mM as mean value, variation of IS in the range from 50 mM to 400 mM causes an pH error of ca. 0.05 pH units. This error is acceptable and therefore fluorescein is a suitable indicator for pH measurements in aqueous solutions. The small cross-sensitivity of fluorescein is in accordance with the Debye-Hückel theory. Assuming that $1 \gg B \cdot I^2$ for low concentrations, equation 3-2 can be simplified to equation 3-4.

$$\log f_x (I) = -z_i^2 \cdot A \cdot I^{\frac{1}{2}} \qquad (3\text{-}4)$$

By means of this equation one can predict the tendency of the activity coefficients of the indicators. In table 3.7. constant A was set to be 0.001 and virtual activity coefficients for the basic form of the indicators were calculated. It can be seen that Debye-Hückel coefficients (and thus pK_a) and experimental data correspond. First, for HPTS, the activity coefficients differ stronger with increasing IS than for fluorescein. Second, the biggest difference for $\ln(f_i)$ (and thus pK_a) is between low IS (2 mM) and higher IS (50 – 400 mM). The same effect can be seen in the calibration curves of HPTS, carboxy fluorescein and fluorescein. (Fig. 3.6., Fig. 3.8., Fig. 3.10.)

Tab. 3.6.   Effect of IS on dissociation constant of fluorescein in the range from 50 mM to 400 mM.

Ionic strength [mM]	Apparent pK_a
2	6.67
50	6.42
100	6.39
200	6.36
300	6.37
400	6.31

Tab. 3.7.   Calculated activity coefficients (A= 0.001) based on eq. 3-4 and their logarithmic form.

IS [mM]	f_{HPTS} (z = -4)	f_{Carbfl} (z = -3)	$f_{Fluor.}$ (z = -2)	$\ln f_{HPTS}$	$\ln f_{Carbfl}$	$\ln f_{Fluor.}$
2	0,98	0,99	0,99	-0,023	-0,013	-0,006
25	0,92	0,96	0,98	-0,080	-0,045	-0,020
50	0,89	0,94	0,97	-0,113	-0,064	-0,028
100	0,85	0,91	0,96	-0,160	-0,090	-0,040
200	0,80	0,88	0,95	-0,226	-0,127	-0,057
400	0,73	0,84	0,92	-0,320	-0,180	-0,080

3.3.5. Effects of Ionic Strength on Fluamin

Initially, another chromophore was planned to be checked for its cross-sensitivity towards IS. A non-carboxylated xanthene dye (*NC-Fluorescein*) was synthesized to follow consequently the series of indicators that have been already checked. Benzene aldehyde was chosen instead of phthalic acid for the ring closure to give a fluorescein-like chromophore. The exact structure is given in Figure 3.11. The overall charge of the indicator was reduced to -1 for the basic form and 0 for the acidic form.
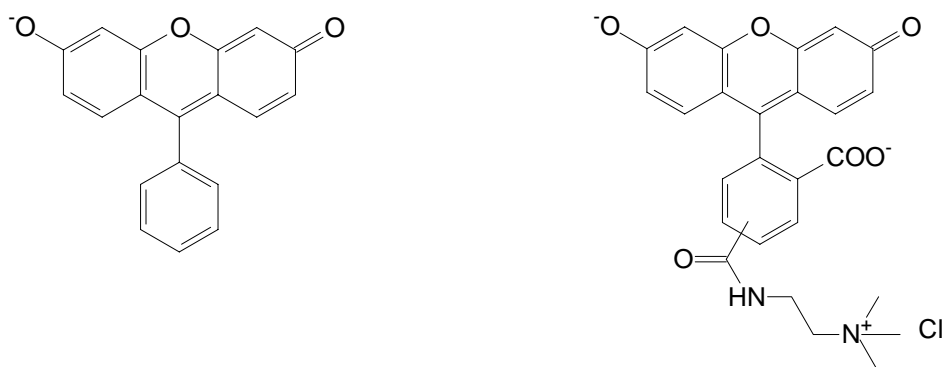
Fig. 3.11. Structures of the non-carboxylated fluorescein derivative NC-fluorescein (left) and of fluamin (right).

Unfortunately, the dye was not very well soluble in pH solutions and precipitated upon lowering the pH. Therefore it was not possible to characterize the cross-sensitivity. Carboxyfluorescein was reacted with (2-aminoethyl)trimethylammonium chloride to give the new dye fluamin (Figure 3.11) to obtain a similar low-charged indicator. The carbonamide bond neutralizes the negative charge of the carboxy group in 5' or 6'-position and the permanently positive charged trimethylammonium group compensates another negative charged group. Thus, the chromophore of fluamin is zwitterionic in its acidic form and still water soluble. The overall charge of the indicator is the same as for the non-carboxylated fluorescein. The absorption and emission spectra of fluamin in presence buffers of varying pH are shown in Fig. 3.12. In analogy to other fluoresceins, fluamin has an absorption maximum at 492 nm for the basic form and 452 nm for the acidic form in the range from pH 9 to 5. For pH lower than 4 the fluorescein chromophore also lactonizes and the total intensity diminishes. The emission spectra show only one maximum at 518 nm for both forms.
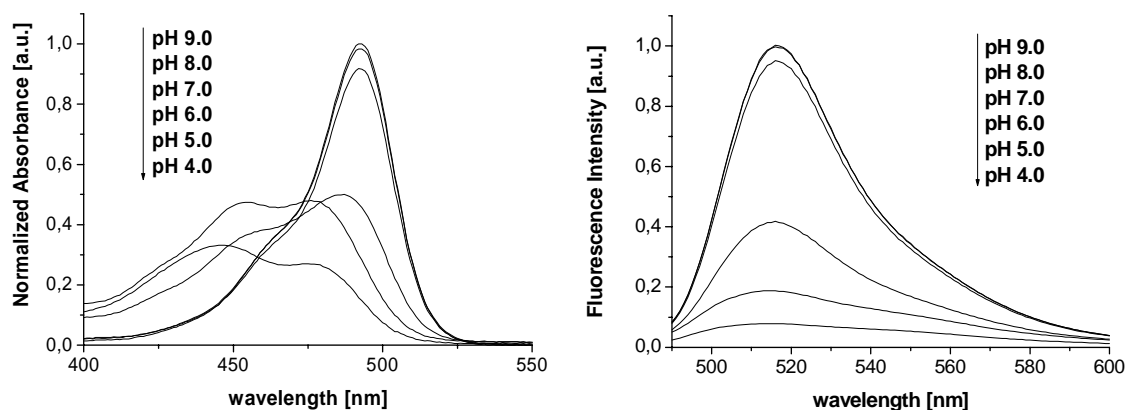
Fig. 3.12. Absorption spectra (left) and fluorescence emission spectra (right) of fluamin in presence of phosphate buffers of varying pH and constant ionic strength.

The calibration plots for the experiments with varying ionic strength are shown in Fig 3.6. Calibration plots were normalized and the resulting pK_a values were displayed versus the respective ionic strength in order to ease comparison.
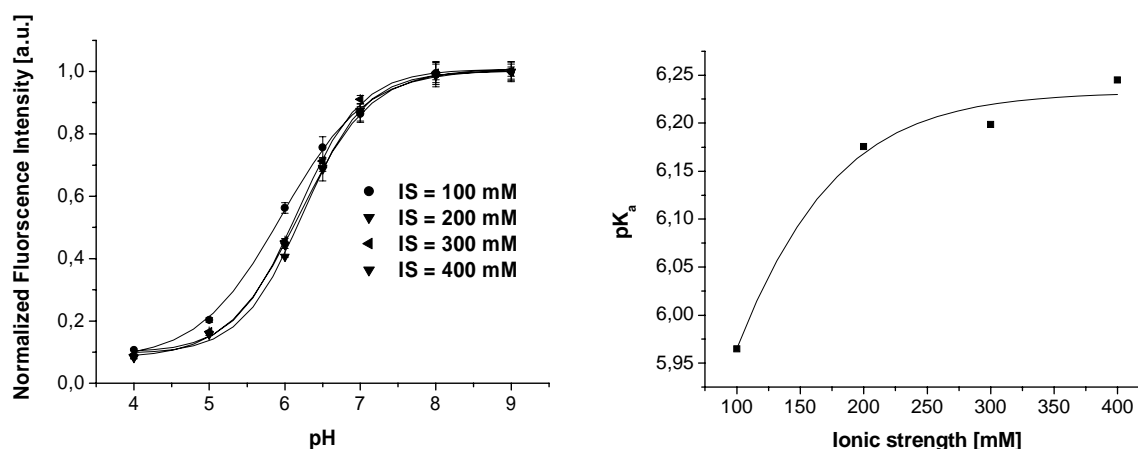
Fig. 3.13. Normalized calibration plots for a 10^{-6} M fluamin solution in dependence of pH and ionic strength (left). Shift of apparent pK_a values with increasing ionic strength from 50 mM to 400 mM.

Fluamin shows a non-expected behavior when changing ionic strength. Instead of a minimization of the pK_a shift, the direction of the pK_a shift has turned. Usually, the pK_a of the negative indicators decreases with increasing IS. For fluamin, pK_a increases with increasing IS. It seems that the positively charged group not only compensates the negative group, indeed it seems to have a different effect on the dissociation constant of the indicator than the negative charges and causes a contrary behavior. This fact was used in a

mixture of a negative and a positive dye as described in the next paragraph. The "positive" shift of the dissociation constant with varying IS is given in Table 3.8. and shown graphically in Figure 3.13. (right). The apparent pK_a of IS = 50 mM was not determined. Variation of IS in the range from 100 mM to 400 mM causes a pH error of ca. 0.15 pH units.

Tab. 3.8. Effect of IS on dissociation constant of fluamin in the range from 50 mM to 400 mM.

Ionic strength [mM]	Apparent pK_a
50	n. d.
100	5.97
200	6.18
300	6.20
400	6.25

3.3.6. Effects of Ionic Strength on an Equimolar Mixture of Fluamin and Carboxy-fluorescein

Due to the fact that carboxyfluorescein and fluamin have a contrary behavior in pK_a shift, an equimolar mixture of both dyes was checked on its cross-sensitivity towards ionic strength. 100 µL of each stock solution was pipetted in a well and filled up to 210 µL with buffer.

Figure 3.13 shows the normalized calibration plot of the mixture in range from IS = 100 to 300 mM. On the left side, the IS-dependencies of fluamin, carboxyfluorescein and the 1:1 mixture are shown.
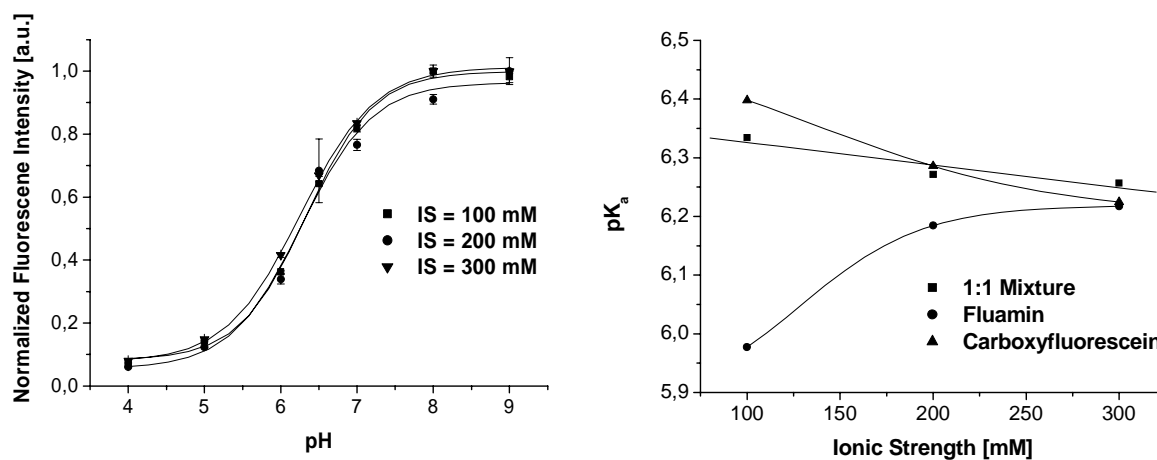

Fig 3.13. Normalized calibration plots for an equimolar mixture of fluamin and carboxyfluorescein as a function of pH and ionic strength (left). The total dye concentration was 10^{-6} M. Shift of apparent pK_a values with increasing ionic strength from 100 mM to 300 mM.

Mixing the two differently charged indicators results in an indicator system that is less affected by changes in IS than the indivial dyes. Obviously, by making use of an appropriate ratio of two differently charged indicators, a minimisation effect from the ionic strength on the measured signal can be obtained and the different deflection of pK_a's of the two individual dyes can be nearly compensate for each other. Reasons, for the mixture not to form exactly a "bisecting line" (Fig. 3.13) are manifold. The most likely reasons are different purity grade, different fluorescence quantum yields and pipetting errors. Table 3.9. lists the shift of the dissociation constant with varying IS. The values for 50 and 400 mM were not determined.

Tab. 3.9. Variance of the dissociation constants of fluamin, carboxyfluorescein and a 1:1 mixture of both dyes in the range from IS = 100 mM to 300 mM.

Ionic strength [mM]	Fluamin	Carboxy-fluorescein	1:1-Mixture
100	5.97	6.42	6.33
200	6.18	6.34	6.27
300	6.20	6.26	6.26
ΔpK_a	0.23	0.16	0.07

3.4. Conclusion and Outlook

In conclusion the experiments with water-soluble indicators have shown two ways to reduce the effect of ionic strength on pH-indicators. First, the results of the indicator set HPTS $\rightarrow$ carboxyfluorescein $\rightarrow$ fluorescein have shown that reduction of the charge in the chromophore system results in a noticable reduction of the effect of IS on the measurement signal. Concerning the cross-sensitivity towards ionic strength fluorescein is the most suitable indicator so far. The elimination of the carboxy group resulted in a poor water-soluble indicator, this fact is less severe for optical sensors wherein the indicator is embedded in an polymeric, lipophilic microenvironment. Fluorescein carries two negative charges, but the negative charge of the carboxy group in 2'-position does not contribute to the pH-sensitivity of the chromophore and can be used for covalent, lipophilic or electrostatic immobilization. In chapter 5, fluoresceins were made lipophilic by esterification and embedded in a charge-free, proton-permeable polymer to give fluorescent optical pH sensors, almost insensitive to ionic-strength.

Second, the results of the set carboxyfluorescein, fluamin and their 1:1 mixture have shown that contrary effects and tendencies can be compensated by mixing in an appropriate ratio. This fact could be used in optical sensors using two differently charged support materials or polymers. In chapter 4, results are reported on carboxyfluorescein was covalently immobilized on a positvely and a negatively charged cellulose. Both materials were mixed and the overall effect of IS was checked.

3.5. Syntheses

3.5.1. Synthesis of Non-carboxylated Fluorescein (NC-Fluorescein)

C_7H_5ClO $C_6H_6O_2$ $C_{19}H_{12}O_3$
140.57   110.11   288.30
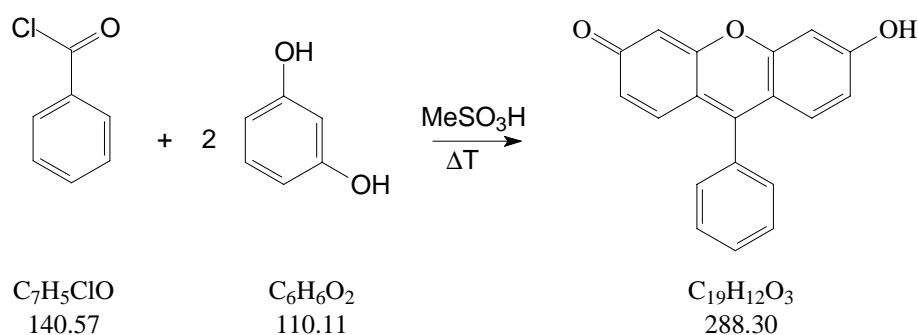
146 mg (1.04 mM) of benzoyl chloride and 229 mg (2.08 mM) of resorcine were placed in 10 mL round bottom flask. Methanesulfonic acid (5 mL) was then added and the resulting suspension was heated to 130 °C. At elevated temperature all materials went into solution, which subsequently went dark into color. After stirring for 30 min, the solution was cooled to room temperature and then added dropwise to rapidly stirring water (20 mL). The resulting fine precipitate was filtered and dried. Column chromatography using a mixture of ethanol:$CHCl_3$ (v/v 1:20) yielded pure NC-fluorescein.

Yield: 115 mg (38%), $C_{19}H_{12}O_3$ (288.3 g/mol)
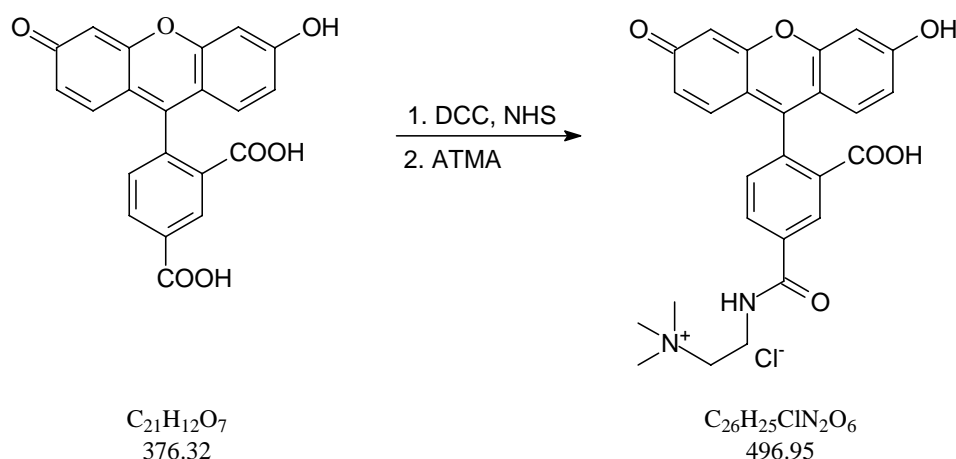
R_f (silica gel, EtOH:$CHCl_3$ (v/v 1:20): 0.11

^{1}H-NMR (MeOD)   7.65 (d, 1 H, aromatic), 7.63 (dd, 2 H, aromatic), 7.47 (d, 2 H, aromatic), 7.45 (dd, 2 H, aromatic), 7.05 (d, 2 H, aromatic), 7.45 (m, 4 H, aromatic)

ESI-MS: (M[-], anion) calc. for $C_{19}H_{12}O_3$ 288.3, found 288.0

3.5.2. Synthesis of Fluamin

$C_{21}H_{12}O_7$
376.32

$C_{26}H_{25}ClN_2O_6$
496.95

100 mg (265 µmol) of 5-(and 6-)carboxyfluorescein are dissolved in 5 mL of dry DMF. Portions of 100 mg of N-hydroxy-succinimide (NHS, 868 µmol) and dicyclohexyl carbodiimide (DCC, 484 µmol) are added and stirred slowly. 100 µL (73 mg, 728 µmol) of freshly distilled triethylamine are added dropwise and stirring is continued for five hours.

    50 mg of (2-aminoethyl)trimethylammonium chloride hydrochloride (ATMA, 285 µmol) and another 100 µL triethylamine are added and stirring is continued for 12 hours. The red solution is transferred into 25 mL of doubly distilled water and filtered. The greenish filtrate is evaporated and fluamin is purified by MPLC, using MeOH : H_2O (v/v 90:10, pH 8-9) as eluent.

Yield: 76 mg (58%), $C_{26}H_{24}ClN_2O_6$ (495.94 g/mol)

R_f (silica gel RP-18, MeOH:water (v/v 90:10, pH 8-9)): 0.3

ESI-MS: (M^+, cation) calc. for $C_{26}H_{24}N_2O_6$ 461.5, found 461.1

3.6. References

1.   G. Bugge, **Der Alchemist – Die Geschichte Leonhard Thurneyssers, des Goldmachers von Berlin**, Wilhelm-Limpert-Verlag, Berlin, **1943**.

2.   H. Friedenthal, **Die Bestimmung der Reaktion einer Flüssigkeit mit Hilfe von Indikatoren,** Z. Elektrochem., **1904**, 10, 113-119.

3.   http://palimpsest.stanford.edu/byorg/abbey/phpens.html

4.   C. R. French, J. J. Carr, E. M. Dougherty, L. A. K. Eidson, J. C.Reynolds, M. D. DeGrandpre, **Spectrophotometric pH measurements of freshwater,** Anal. Chim. Acta, **2002**, 453(1), 13-20.

5.   W. Yao, R. H. Byrne, **Spectrophotometric Determination of Freshwater pH Using Bromocresol Purple and Phenol Red,** Environ. Sci. Technol., **2001**, 35(6), 1197-1201.

6.   T. A. Haines, J. J. Akielaszek, S. A. Norton, R. B. Davis, **Errors in pH measurement with colorimetric indicators in low alkalinity waters,** Hydrobiologia, **1983**, 107(1), 57-61.

7.   E. Schmidt-Marton, A. Halasz, **Photometric pH measurement of natural waters,** Hungarian Scientific Instruments, **1974**, 30, 53-55.

8.   G. S. Konovalov, **Colorimetric determination of the pH in natural waters,** Gidrokhim. Materialy, **1955**, 24, 18-19.

9.   J. Kramer, A. Tessier, **Acidification of aquatic systems: a critique of chemical approaches,** Environ. Sci. Technol., **1982**, 16(11), 606A-615A.

10.   R. E. Stauffer, **Electrode pH error, seasonal epilimnetic pCO2, and the recent acidification of the Maine lakes,** Water, Air, and Soil Pollution, **1990**, 50(1-2), 123-148.

11.   W. Davison, C. Woof, Colin, **Performance tests for the measurement of pH with glass electrodes in low ionic strength solutions including natural waters,** Anal. Chem., **1985**, 57(13), 2567-2570.

12.   T. E. Edmonds, N. J. Flatters, C. F. Jones, J. N. Miller, **Determination of pH with acid-base indicators: implications for optical fiber probes,** Talanta, **1988**, 35(2), 103-107.

13.   R. G. Bates, **Determination of pH-Theory and Practice,** Wiley, New York, **1964**.

14.   M. Kilpatrick, **The colorimetric determination of hydrogen-ion concentration in aqueous solution,** Chem. Rev., **1935**, 16, 57-66.

15.   N. Sugimoto, **pH indicator for measuring intracellular pH,** Jpn. Kokai Tokkyo Koho 2004117217, **2004**.

16.   K. P. Yip, I. Kurtz, **Confocal fluorescence microscopy measurements of pH and calcium in living cells,** Method. Cell Biol., **2002**, 70, 417-427.

17.   Z. Diwu, J. J. Twu, G. Yi, L. D. Lavis, Y. W. Chen, K. J. Cassutt, **Fluorescent pH indicators and their use in intracellular assays,** Eur. Pat. Appl. 1281712, **2003**.

18.   R. M. Andersson, K. Carlsson, A. Liljeborg, H. Brismar, **Fluorescence lifetime imaging of pH in cells: investigation of factors influencing the pH calibration lifetime,** Proc. SPIE Opt. Eng., **2000**, 3921, 242-248.

19.   C. W. Davies, **The extent of dissociation of salts in water. VIII. An equation for the mean ionic activity coefficient of an electrolyte in water, and a revision of the dissociation constants of some sulfates,** J. Am. Chem. Soc., **1938**, 2093-2098.

Chapter 4

Minimizing the Effect of Ionic Strength in an Optical pH Sensor for Physiological pH's

The cross-sensitivity towards ionic strength on the calibration curve depends on the charge of the indicator substance and its environment, e.g. the immobilization matrix. We present two methods to minimize the cross-sensitivity: First, mixing two oppositely charged matrices loaded with a fluorescent pH-indicator. Second, the opposite charges are immobilized onto the same matrix. Changing ionic strength from 25 mM to 500 mM results in an error of less then 0.15 pH units between pH 5 and pH 8.

4.1. Introduction

Optical pH sensors can be easily miniaturized, they are non-invasive, and they can have a larger resolution than that of electrodes[1]. Nowadays, optical pH sensors become attractive for the parallel measurement in high-throughput arrays and the pictographically, two or three dimensional data logging in imaging schemes. Recently, optical pH sensors have been described for a large field of applications, e.g. for controlling of bioreactors[2,3], biotechnological and clinical applications[4-8], and sea water studies[9].

Otherwise, optical sensors have one decisive drawback in comparison to the pH glass electrode: The measurement signal is dependent on the ionic strength of the sample. While electrodes measure the activity of protons in an aqueous solution, the signal of optical sensors is based on the ratio of concentrations of acid and base form of a pH-sensitive dye.

In optical sensors additional bulk-surface interactions and the relationship between the bulk and the surface pH have to be taken into account. The difference between surface and bulk pH is described by the surface potential Ψ, which depends on the concentration profile of all ionic species in the interface, i.e. diffuse double layer and ionizable groups on the surface (Equation 4-1). Thus, the surface itself possesses acid-base properties that are reflected in the pH_{surf}[10, 11].

$$pH_{surf} = pH_{bulk} + \frac{Ne\Psi}{2.3 \cdot RT} \qquad (4\text{-}1)$$

In this chapter, the surface potential was decreased to a minimum by reduction of the charge density of the fixed, ionizable groups. This was performed by compensation of negatively charged groups by positively charged groups and results in optical sensors that are less sensitive towards ionic strength of the analyte solution. An interesting study for electrically charged lipid monolayers was described by Fromherz et al.[12], wherein monomolecular films of various charge densities were prepared by mixing methylstearate with long chain sulfate and quaternary ammonium ions. The lipophilic fluorescence pH indicator 4-heptadecylumbelliferone was embedded in the charged interface. Interfacial pH changes were detected as a function of the charge density of the monolayer and the NaCl concentration of the subphase.

This chapter describes pH sensors that are based on one pH-indicator, covalently linked to differently charged celluloses. A highly negative charged carboxymethylcellulose was modified with ethylene diamine and loaded with a fluorescent pH-indicator. A throughout positive charged cellulose matrix was obtained by the reaction of negative charged cellulose with an excess of a quaternary ammonium salt via EDC linking[13]. The negatively and positively charged celluloses were mixed in a different ratio and embedded in a charge-neutral, polyurethane-based hydrogel.

In a second approach varying amounts of positively charged ammonium groups were covalently bound to a dyed, negatively charged carboxymethylcellulose. The dyed celluloses were embedded in a charge-free hydrogel.

Our intention was to prove that an optimal ratio of negative and positive charges in the environment of the indicator leads to a reduced charge density and results in a sensor that is widely independent of variations in ionic strength. Additional, zeta potentials of the celluloses were measured to compare the pK_a shift of the indicator of each cellulose with the correspondent charge density.

4.2. Material and Methods

4.2.1. Chemicals

N-(3-Dimethylaminopropyl)-N'-ethyl-carbodiimide hydrochloride (EDC, product no. 03449), (2-aminoethyl)trimethylammonium chloride hydrochloride (AETA, product no. 06730), fluorescein (product no. 46955), 5(6)-carboxyfluorescein (product no. 21877) and ethylenediamine dihydrochloride (product no. 03580) were purchased from Fluka (Buchs,

Switzerland; www.fluka.com). The carboxymethyl cellulose Servacel CM52 (product no. 45209) was from Serva (Heidelberg, Germany; www.serva.de). The polymer Hydromed D4 (formerly known as Hydrogel D4) was received from Cardiotech Inc. (Woburn, MA, USA; www.cardiotech-inc.com) by request. The polyester support (product no. LS 1465585, polyethyleneterephthalate ("PET" or "Mylar")) was obtained from Goodfellow (Cambridge, UK; www.goodfellow.com). Ethanol, sodium hydroxide and hydrochloric acid were also of analytical grade. Aqueous solutions were prepared from doubly distilled water.

4.2.2. Apparatus

An Aminco-Bowman Series 2 luminescence spectrometer from SLM (Rochester, NY, USA; www.thermo.com) was used to record the fluorescence. The excitation light passed through a monochromator and was focused to one branch of a bifurcated fiber bundle of randomized glass fibers ($\varnothing$ 6mm). The fiber bundle was fixed to the back of the sensor membrane, mounted in a home-made flow through cell[14] as shown in Figure 4.1 (bottom).
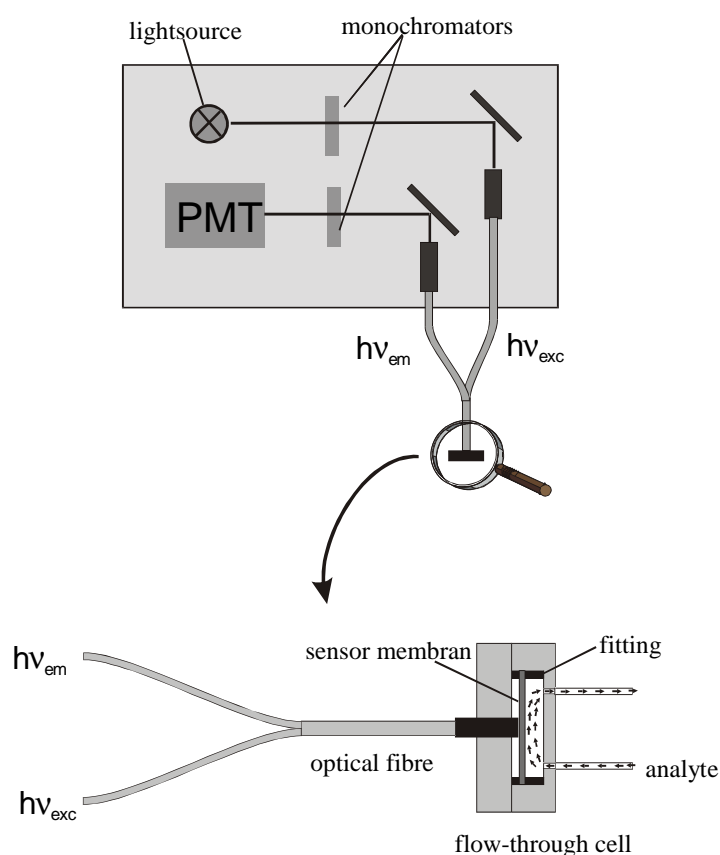

Fig. 4.1. Schematic representation of the instrumental set-up.

The flow rate was kept constant at 1 mL/min using a Minipuls-3 peristaltic pump (Gilson, Villiers, France; www.gilson.com). The emitted light was guided by the other branch of the fiber bundle through a monochromator to the photomultiplier tube inside the spectrometer. If not stated otherwise, measurements were performed at excitation and emission wavelengths of 500 and 530 nm, respectively. The pH values of solutions were checked using a digital pH meter (Schott, Mainz, Germany, www.schott.de) calibrated with standard buffers of pH 7.00 and 4.00 (VWR, Darmstadt, Germany; www.vwr.de) at 20 ± 2 °C. Measurements of zeta potentials were carried out on a Malvern Instruments Zetasizer 3000 (Malvern Instruments, Worcestershire, UK; www.malvern.co.uk).

4.2.3. Fitting function and calibration curves

Calibration curves were fitted according to Eq. 3-3 described in chapter 3.2.4.

4.2.4. Preparation of amino-modified Carboxycellulose
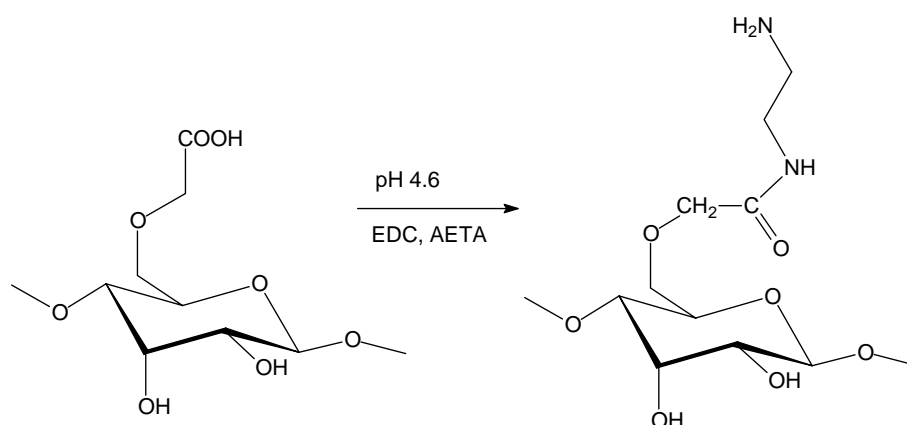
10 g of the Carboxycellulose CM52 were suspended in 200 mL of water. 4 g of ethylenediamine dihydrochloride were added in small portions. After ten minutes, 350 mg of EDC were added and pH of the solution was set to 4.6 by addition of 0.1 M hydrochloric acid. The solution was stirred for four hours ($\equiv$ cellulose AC1) and two hours ($\equiv$ cellulose AC2) under pH control. The cellulose was filtered, resuspended in 200 mL of water, stirred for 15 min and sucked off. This step was repeated five times. Afterwards, the cellulose was washed three times with 1 M NaOH and water. Finally, the powder was washed with 100 mL of ether and dried over silica gel in a desiccator.

4.2.5. Photometric Determination of the Content of Amino Groups

ninhydrine   Ruhmann's purple
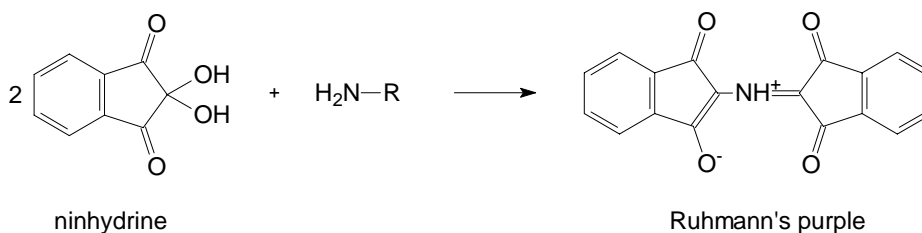
Based on the principle of the Moore-Stein analysis[15], two test reagents were prepared for the photometric determination of amino groups on the carboxycellulose. 1 g of ninhydrine was dissolved in 70 mL of ethylene glycol, and 70 mg of hydrindantin was dissolved in 5 mL methyl cellosolve. Both solutions were combined in a 100 mL graduated flask and filled up with 4 mol/L sodium acetate buffer pH 5.5. 100 mg of the amino-modified cellulose were suspended in 1 mL water and 0.5 mL of the ninhydrine reagent. At the same time the test was repeated with carboxycellulose as blank sample. The suspensions were incubated for 15 min in a water bath. 5 mL of an EtOH/water mixture (σ(EtOH) = 0.5) were added and the cellulose suspensions were transferred quantitatively into a 50 mL graduated flask. After the cellulose was sedimented, the absorbance of the supernatant liquid was measured at 570 nm against EtOH/water (σ(EtOH) = 0.5) as reference. The content of aminogroups was calculated according to the concentration of the dye Ruhemann's purple (ε = 8750 l mol^{-1} cm^{-1}). Mean values and standard deviations were calculated from at least three measurements.

4.2.6. Covalent Immobilization of the Indicator
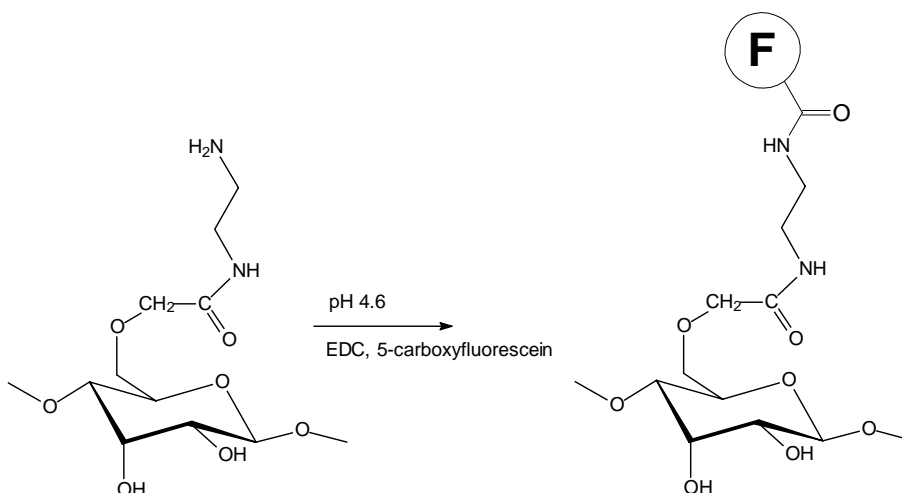
4 g of the amino-modified celluloses (AC1 and AC2) in 100 mL of water were reacted with 124 mg (328 µmol) 5(6)-Carboxyfluorescein (**F**) in the presence of 63 mg of EDC for

four hours at pH 4.6. The cellulose powder was filtered off and washed thoroughly with water, 1 M HCl and 1 M NaOH solutions, rinsed with brine and finally treated with ethanol until the filtrate was colorless. After drying overnight at a temperature of 60 °C, the colored celluloses CFAC1 and CFAC2 were obtained.

4.2.7. Covalent Immobilization of the positively charged Amino Groups

The positive charged AETA was coupled to the negative charged, dyed celluloses by the same method as described for the modification with ethylene diamine. The reactants and reaction times for the preparation of the different charged celluloses are shown in Table 4.1.

Table 4.1. Reactants and reaction times for the preparation of the different charged celluloses C1 to C6

Cellulose	m (dyed cellulose) [mg]	m (ATEA) [mg]	m (EDC) [mg]	V H$_2$O [mL]	Reaction time [h]
C1	500 (CFA1)	1000	850	40	24
C2	350 (CFA2)	176	193	30	24
C3	350 (CFA2)	15	16	30	4
C4	350 (CFA2)	45	50	30	4
C5	350 (CFA2)	90	193	30	4
C6	350 (CFA2)	105	205	30	4

4.2.8. Membrane preparation

Hydrogel cocktails were prepared from 100 mg D4 hydrogel and 100 mg of the respective charged cellulose in 1.08 g ethanol and 0.12 g water. The mixtures were vigorously stirred at room temperature overnight. 100 µl of each cocktail were knife-coated onto dust-free, 125 µm polyester supports as shown in Figure 4.2. 120 µm spacers were used to set the thickness of the layer.
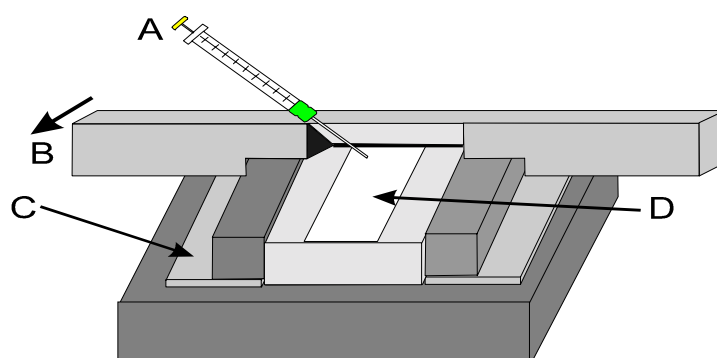
Fig. 4.2. Schematic view of the knife coating device, with A= pipette containing the membrane cocktail, B = coating device, C= spacer and D= polyester support (Mylar)

The membranes were dried for two hours before characterization. Spots of 25 mm diameter were cut with a hollow punch and mounted in the flow-through cell. Table 4.2 gives information about the membrane compositions.

Table 4.2. Sensor Membrane compositions

Membrane	cellulose	m (dyed cellulose) [mg] in 100 mg hydrogel
M1	CFA1	100
M2	C1	100
M3	CFA1/C1	17/85
M4	CFA2	100
M5	C2	100
M6	C3	100
M7	C4	100
M8	C5	100
M9	C6	100

4.2.9. Buffer preparation

Phosphate buffers with varying ionic strength and NaCl as background electrolyte were prepared according to the procedure described in chapter 3.2.2.

4.3.   Results and Discussion

4.3.1. Choice of indicator and polymeric support

HPTS, carboxyfluorescein, and fluorescein are suitable indicators for fluorescence-based pH sensors. In chapter 3, solutions of the indicators in phosphate buffers were checked on their cross-sensitivity towards ionic strength in the range from 50 to 400 mM. The results are summarized in Table 4.3. It can be seen that the error of fluorescein is about 0.1 pH units.

Table 4.3. Effect of ionic strength on apparent pK_a of fluorescent indicators ($c_{dye} = 1 \cdot 10^{-6}$ M) using phosphate buffers of varying NaCl concentration.

Ionic strength [mM]	Apparent pK_a HPTS	Apparent pK_a Carboxyfluorescein	Apparent pK_a Fluorescein
50	7.42	6.49	6.42
100	7.36	6.42	6.39
200	7.20	6.34	6.36
300	7.00	6.26	6.37
400	7.03	6.25	6.31
ΔpK_a	0.39	0.24	0.11

There are three widely used methods for immobilization of a pH indicator on/in a solid substrate: adsorption, entrapment and covalent binding. Covalent binding results in sensors which are free of leaching phenomena[16]. Therefore covalent immobilization was chosen.

In this chapter, HPTS was not used as pH-indicator due to the facts that (a) immobilization is quite complicated and involves several steps and (b) the high cross-sensitivity of the chromophore towards IS. The tested fluorescein indicators show a lower cross-sensitivity and possess suitable photophysical properties which include high absorption coefficients ($\varepsilon > 80000$ L mol^{-1} cm^{-1}) and fluorescence quantum yields of typically higher than 0.9[17]. For the optical sensor, carboxyfluorescein was chosen as the indicator because of its ease of immobilization. The 5-(or 6)carboxy group in carboxyfluorescein can be activated by conventional peptide activating reagents such as EDC to make it reactive towards amino groups[18-20]. Another reason is the fact that bound carboxyfluorescein shows the same ionic valency like fluorescein and therefore the effect of the indicator in the sensor on the overall cross-sensitivity towards ionic strength is minimal. Effects of IS higher than that of fluorescein are caused by charges of the matrix.

Further on, the pK_a of the free dye in aqueous solution is around pH 6.4 which matches the physiological range from pH 6.5 to 7.5.

Celluloses are suitable and often used supporting material for optical sensors. Either cellulose acetate films[21-24] or aminomodified cellulose fibers[25-28] can be used. Dyed, microcrystalline fibers can be embedded in a polymeric matrix and act as sensing element. To obtain functional cellulose, the ion-exchanger carboxymethyl-cellulose CM52 was reacted with ethylene diamine. In order to prevent cross-linking between the cellulose fibers, only a small amount of ethylene diamine was used. It is also favorable to keep the number of reactive sites low to prevent that too high indicator concentration is loaded on the cellulose and fluorescence quenching occurs at higher pH. According to manufacturer's information, the capacity of the cellulose is 96 µmol carboxygroups per 100 mg cellulose. Since acid-base titration methods to determine the content of aminogroups failed because no explicit equivalence point was observed, the capacity of aminogroups was estimated to be 3.22 ± 0.09 µmol per 100 mg cellulose by means of the photometric method. This means that about 3.5% of the carboxygroups were converted to amino-functional groups. Fig. 4.3 shows the absorption spectra of the supernatant liquids of modified and non-modified carboxycellulose. Since the ninhydrine reaction is specific for primary amino groups, it was proved by the appearance of Ruhemann's purple that a noticeable amount of ethylenediamine was linked one-sided to the carboxycellulose in spite of the risk of cross-linking.
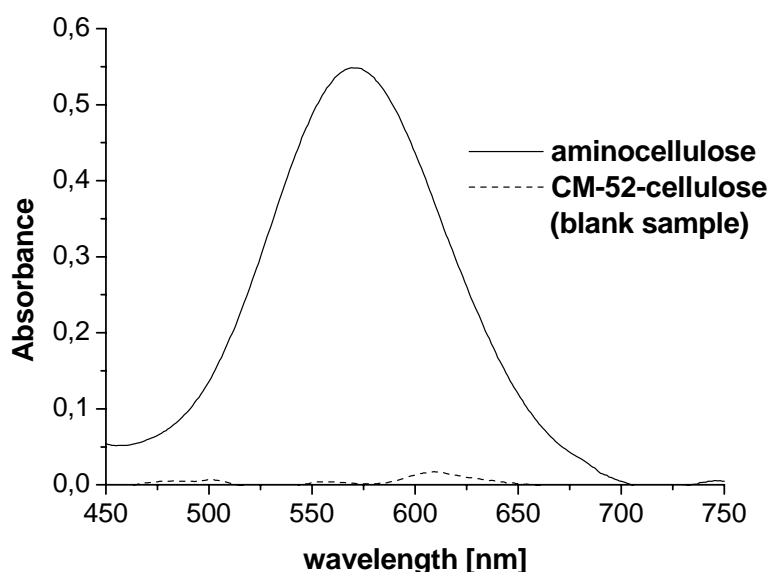

Fig. 4.3. Absorption spectra of the supernatant liquid of carboxycellulose CM-52 and the amino-modified cellulose.

In the past, PVC and sol-gels were used as polymers for optical pH sensors. Both materials have severe drawbacks: In general, a PVC-based sensor consists of 1/3 PVC and 2/3 plasticizer (e.g. Bis-(2-ethylhexyl sebacate, DOS) to increase the permeability of the membrane. Therefore, the term PVC-membran is delusive. The sensitivity of these mebranes is based on a co-extraction mechanism, wherein a proton and an anion, as counterpart, are extracted into the lipophilic membrane due to electroneutrality. The sensors suffer from leaching of the plastizer out of the membrane, which reduces the permeability of the membrane and changes its sensitivity. Second, sol-gels suffer from their poor long-term stability due to dye leaching and aging effects, i.e. changes of the gel structure[29, 30].

In addition to sol-gel and PVC-based polymers, hydrogels serve as alternative polymeric matrices for pH-sensitive membranes. They are soluble in non-toxic solvents such as ethanol and due to the high water uptake, water content and swelling, they exhibit excellent ion permeability[31]. We chose the polyurethane based hydrogel D4, because the polymer structure is uncharged according to the manufacturer's information and with respect to its stability in varying conditions of pH and temperature.

4.3.2. Minimizing the effect of ionic strength with the mixed-matrix compensation method (MMCM)

Figure 4.4 shows a cross-section the membranes (left) and a picture of membrane M1 (right) taken with a Leica DMRE Fluorescence microscope and a Leica digital camera DC 200 with 50-fold magnification. The picture shows that the dyed fibers were inhomogenously distributed in the membrane. This fact reduces reproducibility and the spatial resolution of the sensor.
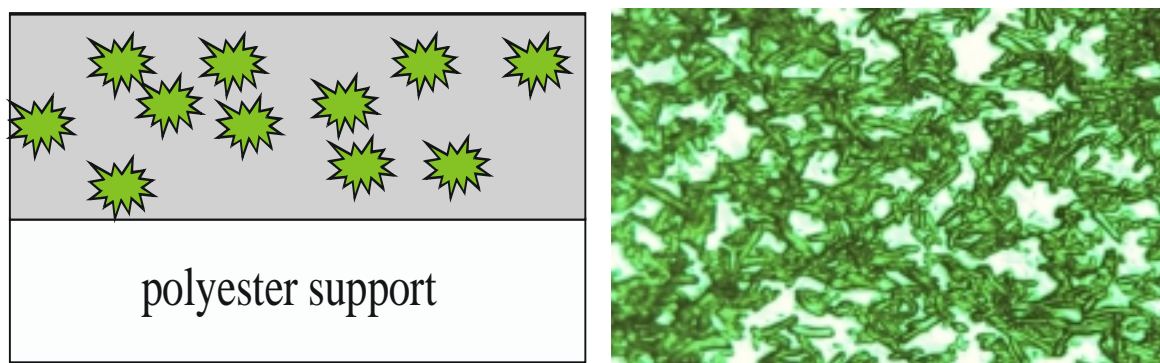

Fig. 4.4. Left: Schematic cross-section of the sensor membranes (⭐ carboxy-fluorescein dyed cellulose fibers; ▨ hydrogel matrix; ☐ inert, transparent mylar foil). Right: Fluorescent image of membrane M1 (taken with bandpass-filters 470 nm exc. / 515 nm em.)

All membranes were tested in a flow-through cell with respect to the response to various pH-values ranging from 9.0 to 4.0. Ionic strength varied from 25 to 500 mM. Figure 4.5 shows the excitation and emission spectra of membrane M1 for varying pH with PBS solutions of IS = 100 mM.
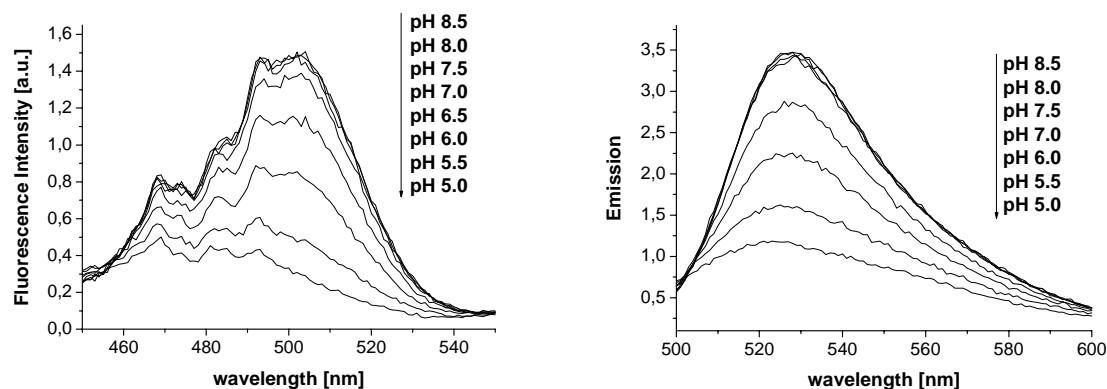
Fig. 4.5. Fluorescence excitation (left; λ_{em}= 580 nm) and emission spectra (right; λ_{exc} = 480 nm) of membrane M1.

Titration plots were determined from a series of time traces with ten seconds resolution, where fluorescence intensity depending on change of pH was measured. The response curve of membrane M1 is shown in Figure 4.6.

Fig. 4.6. Time trace with respective fluorescence intensities of membrane M1 for PBS of IS = 50 mM.

Figure 4.7 shows the calibration plot of membrane M1 for ionic strength from 25 mM to 500 mM. In general, all signals were taken as mean of at least 100 seconds. The sensor shows a high cross-sensitivity towards ionic strength due to the fact that both, cellulose and pH-indicator are negatively charged. It is obvious that wi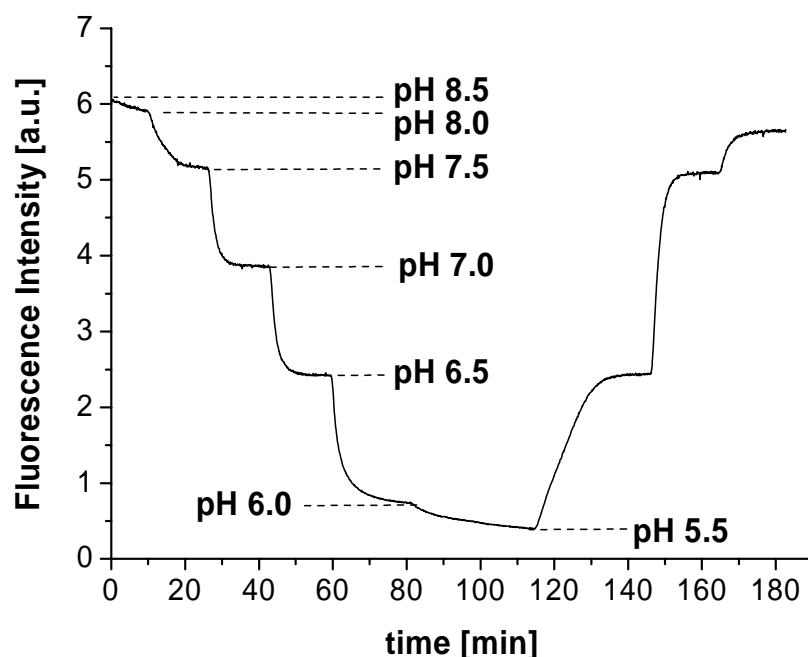th increasing ionic strength the pK_a of the sensor is strongly shifted towards acidic pH. The noticeable shift between 25 mM and 500 mM can not only be caused by changes of activity of the two forms of the indicator. It is reasonable that the numerous negative charges of the cellulose matrix have a destabilizing effect on the basic form of the indicator. For lower IS, the charges of the carboxy groups of the cellulose are weakly shielded by the background electrolyte and it is possible that there is a repulsion between negative cellulose and negative charged indicator. Therefore, protonation occurs for lower H^+-concentrations and the apparent pK_a of the indicator is shifted to higher pH. With increasing ionic strength, more carboxy groups of the cellulose are shielded by the background electrolyte and the destabilizing effect decreases and the apparent pK_a is shifted towards lower pH. At higher IS the pK_a of the membrane becomes nearly equal to the pK_a of water-soluble fluorescein.
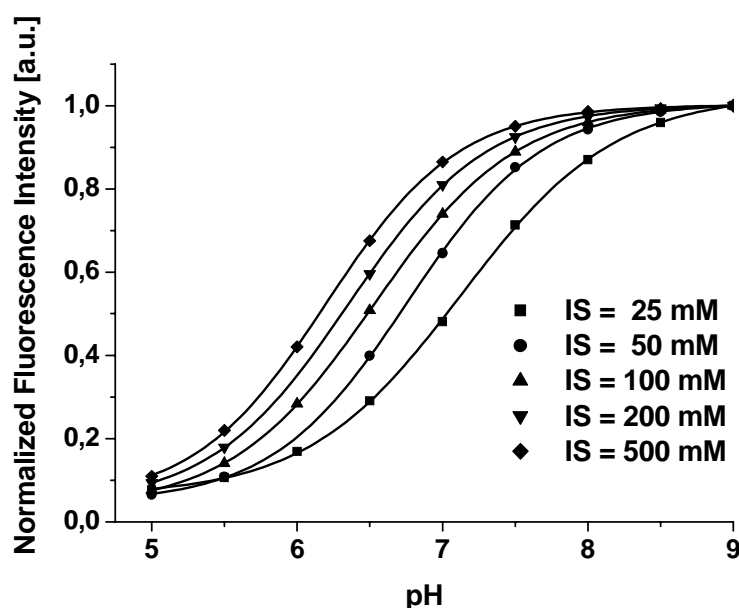
Fig. 4.7. Titration plots of membrane M1 with phosphate buffers of varying ionic strength.

In contrast, membrane M2 carries a maximum of positive ammonium groups, which are surrounding the negatively charged indicator and changing its microenvironment. This results in a different behavior of the membrane when exposed to buffers of varying ionic strength.

The apparent pK_a is shifted towards basic pH when the ionic strength is increasing. In case of the positively charged matrix, it is reasonable that the positively charged ammonium

groups the modified cellulose matrix have a stabilizing effect on the basic form of the indicator. For lower IS, the ammonium groups of the cellulose are weakly shielded by the background electrolyte and there is an attraction between the positively charged cellulose and the negatively charged indicator. Therefore, higher H^+-concentrations are needed to protonate the indicator and therefore the apparent pK_a of the indicator is shifted to lower pH. With increasing ionic strength, more ammonium groups of the cellulose are shielded by the background electrolyte and the stabilizing effect decreases and the apparent pK_a is shifted towards higher pH.

In low ionic strength buffered solutions (25-100 mM) the membranes M1 and M2 display contrary behavior. This matter of fact is utilized in Membrane M3 wherein a mixture of positively and negatively charged celluloses is combined. By means of the Microsoft Excel program, fluorescence intensities of negatively and positively charged cellulose were added virtually. Several virtual mixtures were tested in real membranes. The optimum ratio between the celluloses CFA1 and C1 was found out to be 1:5 (w/w). Fig. 4.8 shows the virtual titration plot of M3 for a ratio of CFA1/C1 = 1:5 and Figure 4.9 shows the real titration plot of sensor membrane M3 when exposed to phosphate buffers of varying ionic strength.

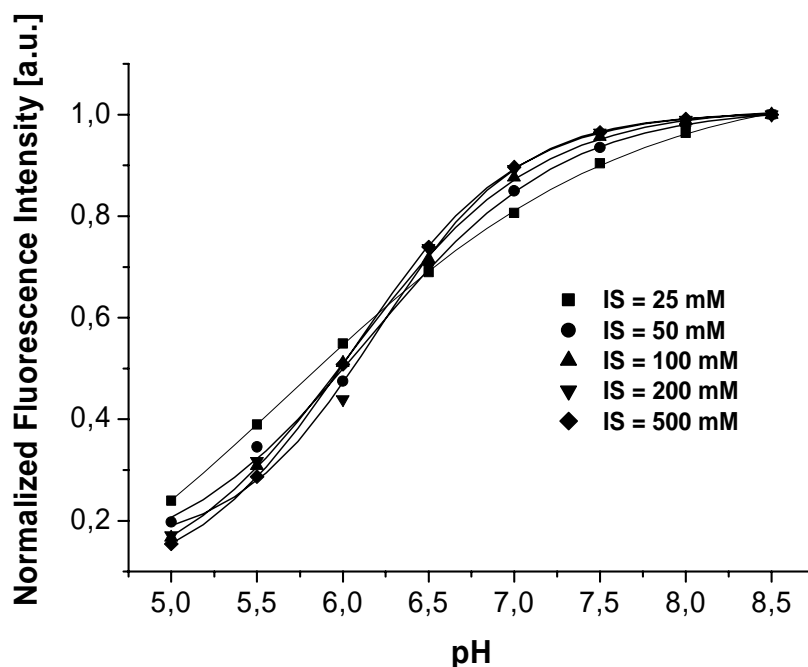**Fig. 4.8.** Excel-generated, virtual titration plot of membrane M3 for various ionic strength.
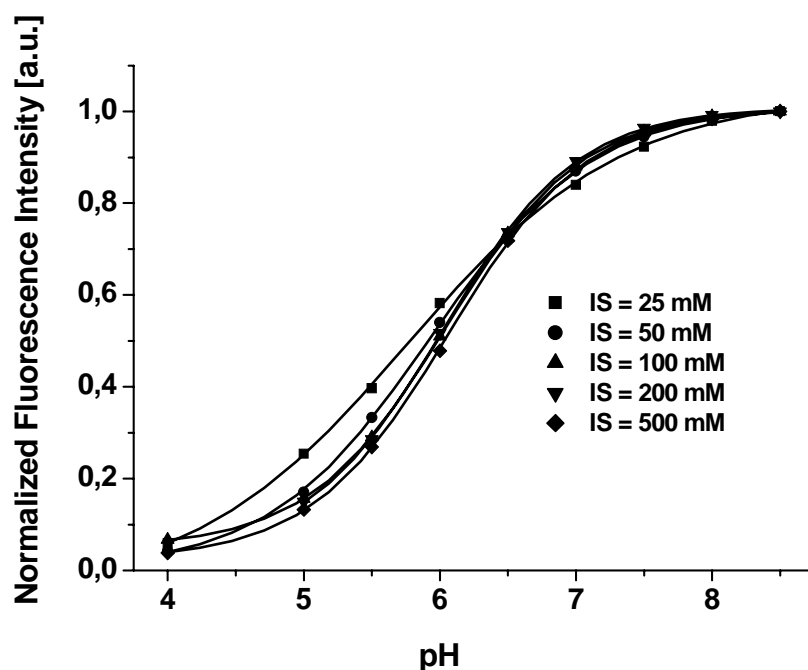
Fig. 4.9.   Titration plots of membrane M3 with phosphate buffers of varying ionic strength.

In comparison to the membranes consisting of either CFA1 or C1 the cross-sensitivity towards ionic strength of the mixed hybrid membrane M3 could be minimized in the range from pH 6.0 to 8.0. The method works very good for pH 6.5 because the maximum pH error caused by varying IS is less than 0.05 pH units. An obvious deviation of the signals can be seen at lower pH for an ionic strength of 25 mM in Figure 4.9. This signal difference can be explained by the fact that the pK_a's at 25 mM IS of the positively and negatively charged matrices show a difference of more than 1.5 pH units. Therefore, the dynamic ranges of membrane M1 and M2 are less overlapping than for higher ionic strengths. Based on the fact that the fluorescent signal of membrane M3 is an additive signal of two different sensors, namely M1 and M2, the deviant curve progression of sensor M3 for IS = 25 mM can be explained. The additive signals show a sigmoidal plot when the pK_a's of M1 and M2 are close together. In the case of IS = 25 mM the titration plot shows a more linear shape between pH 5 and 7 than a typical sigmoidal plot. This circumstance can be seen in Fig. 4.10, where the individual titration plots of negatively, positively celluloses and their mixture are displayed. Figure 4.11 illustrates the contrary behavior of pK_a's of the different charged membranes (M1, M2) upon increasing ionic strength. The effect of ionic strength was compensated by mixing both materials as can be seen for membrane M3.
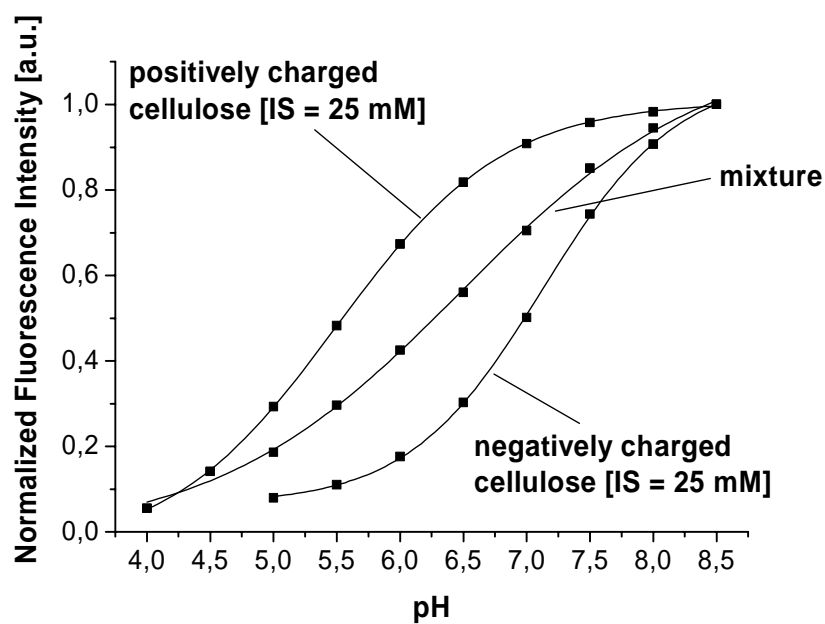
Fig. 4.10. Comparison of the calibration plots of M1, M2 and M3 for IS = 25 mM.
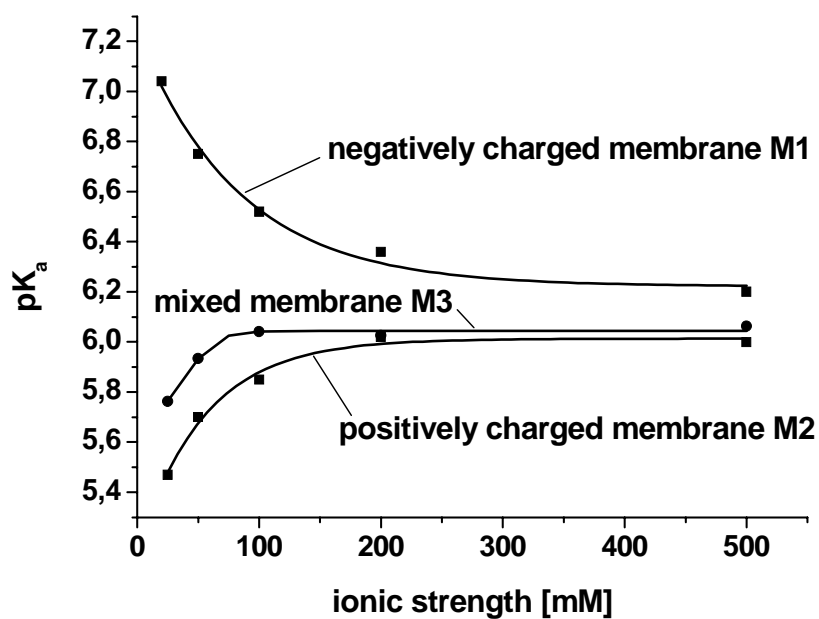
Fig. 4.11. Effect of ionic strength on the pK$_a$'s of the membranes M1, M2 and M3.

To estimate the pH error caused by the effect of ionic strength on the sensor signal of sensor membrane M3, the fluorescence intensities of phosphate puffers of constant pH, but different ionic strength were compared one after the other in 500 second time intervals in a time trace (Figure 5). Towards acidic pH, the differences between the intensities of low and high ionic strength rise. This circumstance can also be explained by the fact that the pK_a of negative and positive matrix at low ionic strength are rather away from each other.
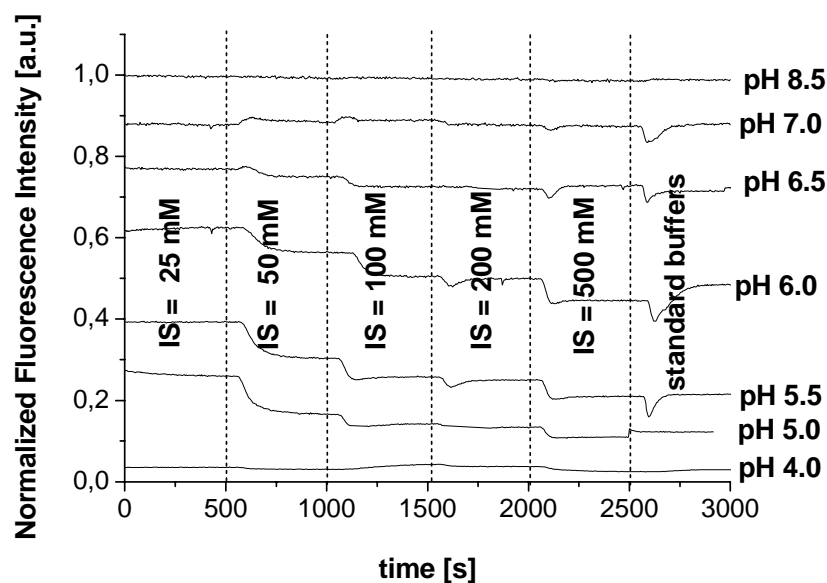
Fig. 4.12. Time trace of membrane M3 at constant pH and rising ionic strength.

The normalized fluorescence intensities of IS = 100 mM were used to create a new calibration plot. This calibration plot was used because it almost represents the average of all calibration plots. The resulting Boltzmann fit-function was rearranged to obtain an equation that converts fluorescence intensities into pH units. By means of this equation the intensities in Fig. 4.12. were calculated into pH units. The divergences $\Delta pH = pH_{real}$-$pH_{calculated}$ are exemplified in Figure 4.13.
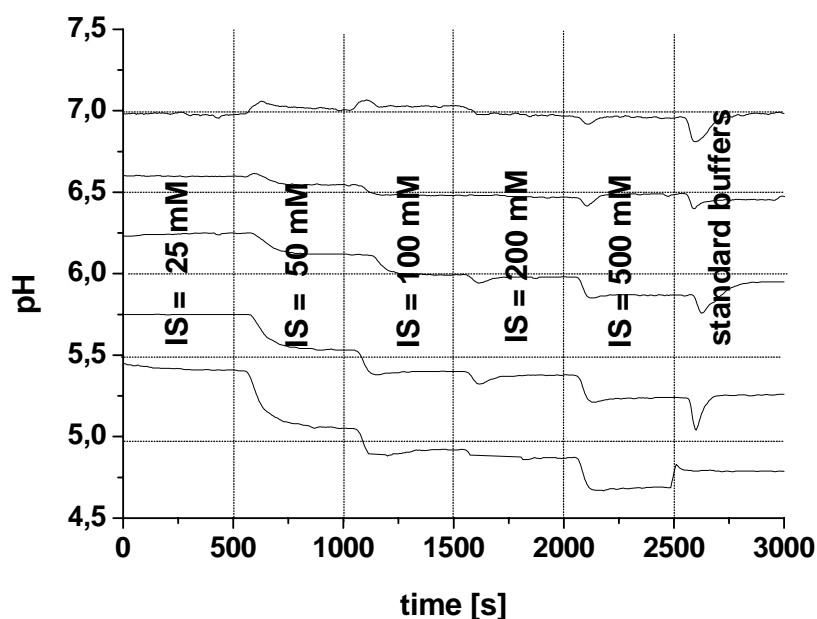
Fig. 4.13. Calculated deviation of pH at constant pH of the buffer solutions, but varying ionic.

In the range from pH 6 to 7 and for ionic strengths from 50 to 500 mM the maximum pH error is 0.15 pH units. At lower pH and lower ionic strength the maximum error rises to almost 0.5 pH units. Table 4.4 shows the deviation of measured pH from the real value if the calibration curve of IS = 100 mM is used.

Table 4.4. Calculated deviation of pH of Sensor Membrane M3

	Ionic strength [mM]				
pH	25	50	100	200	500
7,0	-0,06	-0,02	-	-0,06	-0,07
6,5	0,11	0,07	-	0,01	0,01
6,0	0,25	0,12	-	0,03	-0,14
5,5	0,35	0,13	-	-0,02	-0,15
5,0	0,49	0,13	-	-0,05	-0,24

4.3.3. Minimizing the effect of ionic strength using the direct immobilization compensation method (DICM)

Instead of mixing contrary charged materials, the charges of the free carboxy groups can be compensated by immobilized positively charged ammonium groups on the same cellulose strand. In this case, defined amounts of a positively charged amine were coupled

to a dyed and negatively charged carboxycellulose. The corresponding membranes M4-M9 were prepared as described in chapter 2.6. The shift of pK_a with increasing ionic strength is plotted in Fig. 4.14. for the membranes M4-M9. The optimum ratio results in a charge density that is close to zero. The titration plots of membrane M7 are displayed in Figure 4.15. The curves of membrane M7 run parallel for all ionic strengths and the shift towards acidic pH with increasing ionic strength is very low.

In comparison to the mixed membrane M3, the pK_a values of membrane M7 deviate less for lower ionic strengths (25 – 50 mM). The plots for M3 show a change in shape between the plots of higher and lower ionic strength (Fig. 4.9.) and at IS = 25 mM the deviation of the sensor signal is remarkably higher than for M7 in Figure 4.15.
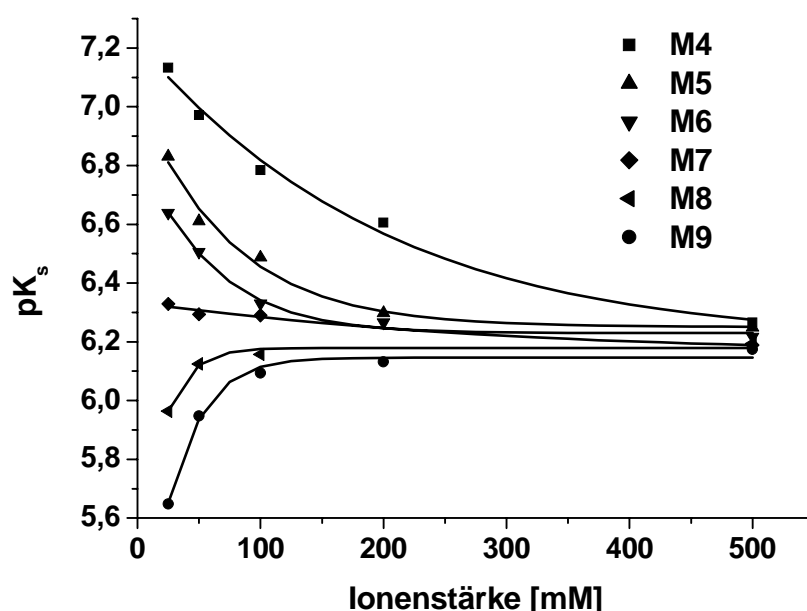
Fig. 4.14. Effect of ionic strength on the pK_a's of the membranes M4-M9.
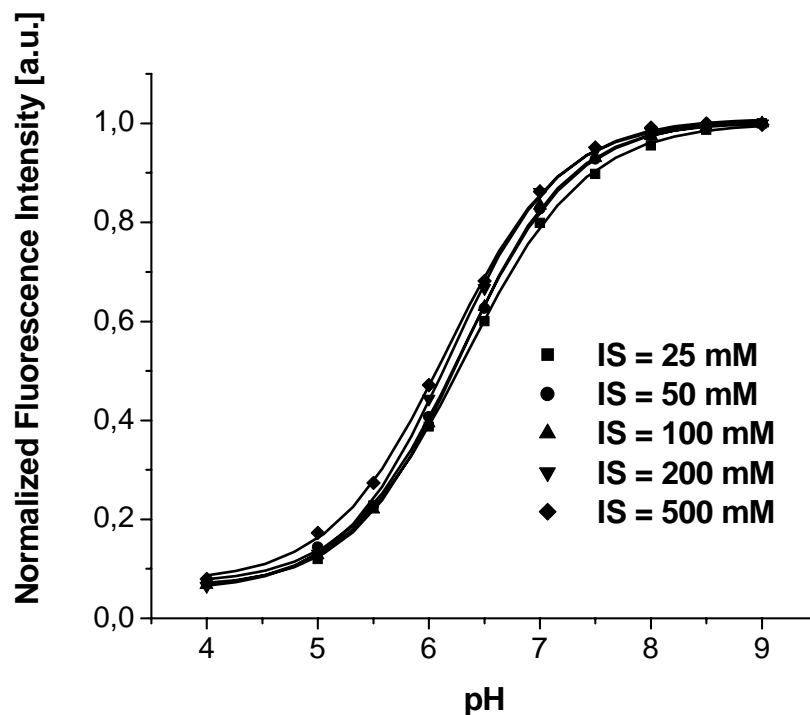
Fig. 4.15. Titration plots of membrane M3 with phosphate buffers of varying ionic strength.

In analogy to sensor membrane M3, the fluorescence intensities of phosphate puffers of constant pH, but different ionic strength were compared one after the other in 500 second time intervals in a time trace. Again, the normalized fluorescence intensities of IS = 100 mM were used to create a new calibration plot. The resulting Boltzmann fit-function was rearranged to obtain an equation that converts fluorescence intensities into pH units. By means of this equation the intensities were calculated into pH units. The divergences $\Delta pH = pH_{real}-pH_{calculated}$ are shown in Figure 4.16.
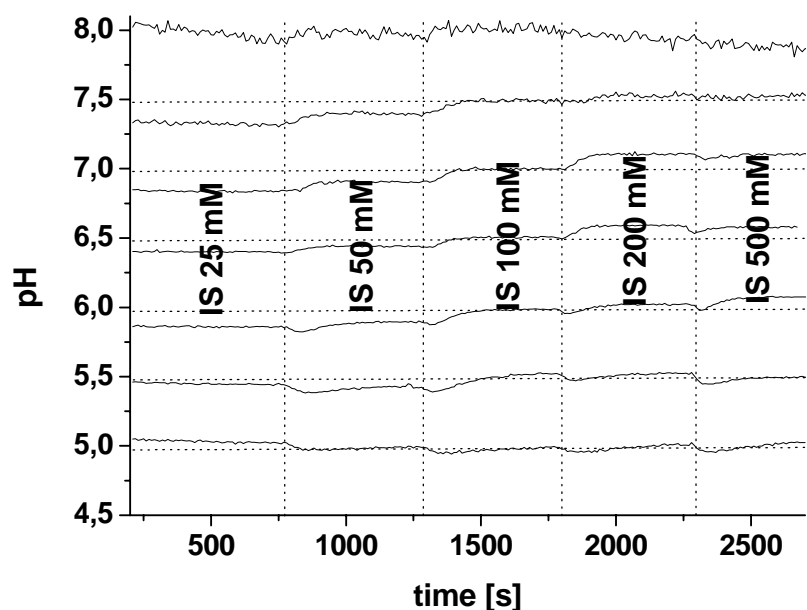
Fig. 4.16. Calculated deviation of pH at constant pH of the buffer solutions, but varying ionic strength (membrane M7).

While the maximum error for membrane M3 was up to 0.5 pH units, the direct coupling in a certain ratio of positive charges in the closer environment of indicator and negative charged carboxy groups generated a sensor membrane wherein the maximum error is less than 0.15 pH units for the whole range of ionic strength. The data is shown is table 4.5.

While the maximum error for membrane M3 was up to 0.5 pH units, the direct coupling in a certain ratio of positive charges in the closer environment of indicator and negative charged carboxy groups generated a sensor membrane wherein the maximum error is less than 0.15 pH units for the whole range of ionic strength.

Table 4.5. Calculated deviation of pH of Membrane 7

	Ionic strength [mM]				
pH	25	50	100	200	500
7,0	-0,15	-0,11	-	0,10	0,10
6,5	-0,11	-0,06	-	0,09	0,07
6,0	-0,14	-0,11	-	0,02	0,07
5,5	-0,06	-0,08	-	0,02	0,01
5,0	0,02	-0,02	-	0,00	0,02

In order to test the long-term stability, the membrane was exposed to PBS buffer pH 8.0 (IS = 100 mM) with 1% m/m BSA in a time trace with continuous illumination and analyte flow. The sensor is suitable for long-term measurements because the signal only dropped by 2 % after 15 h.

4.3.4. Zeta potentials

The zeta potentials of suspensions of 50 mg cellulose (CFA2, C2-C6) in 5 mL millipore water were analyzed. Measurements were made at a temperature of 25 °C; the cell field was set to 29 V/cm with a current of 0.1 mA. The resulting zeta potentials and the dependency of pK_a from ionic strength of each membrane are listed in Table 4.6.

Table 4.6. Zeta potentials of different charged celluloses

Cellulose	CFA2	C2	C3	C4 (M7)	C5	C6
Zeta potential [mV]	-59.6	-45.4	-14.9	-3.6	25.6	41.3
$\Delta pK_a = pK_{a,\ 25\ mM} - pK_{a,\ 500\ mM}$	0,87	0,58	0,42	0,14	-0,23	-0,53

An increasing pK_a shift to more basic pH comes along with increasing negative zeta potential when reducing the ionic strength of the solution. A positive zeta potential indicates a pK_a shift to more acidic pH. Cellulose C4 (incorporated in sensor membrane M7) displays the smallest zeta potential and the smallest shift of pK_a with IS. This is in accordance with the prediction previously mentioned.

4.4. Conclusion

Two methods have been developed to decrease the effect of ionic strength on an optical pH sensor. The mixed-matrix compensation method is based on the contrary behavior of the apparent pK_a's of two matrices when ionic strength decreases. Therefore, the compensation is a mathematical correction based on the addition of two hyperbolic functions. The method works well for ionic strengths from 50 to 500 mM, but it lacks for lower IS. The best results for this method are achieved when the mean of pK_a with varying IS of negative and positive matrix results in a constant value. Otherwise, the mixed matrix are not completely compensated and the pK_a shift will be influenced by the stronger bended

hyperbolic curve of one of the starting components. These problems have been alleviated by the direct immobilization compensation method. This method uses a more homogenous matrix because the compensation is realized on one cellulose strand by partial modification of negative charges. Therefore, the pK_a shift of the sensor is not depending of the characteristics of two starting materials, but it is defined by the local microenvironment of the indicator, affected by the total number of negative and positive charges. For measurements in lower IS it was found that the titration plots of the best sensor results in an pH error of less than 0.15 pH units. Therefore, the sensor is applicable to monitor pH changes in a physiological sample solution as long as ionic strength is in the range from 25 to 500 mM.

In conclusion it can be said that the performance of an optical sensor has been improved. Other the other hand there are a few drawbacks of the sensor that make its use still difficult: First, the cellulose fibers are inhomogenously distributed in the sensor membrane. Secondly, the sensor chemistry is quite complicated, involves several immobilization steps and is therefore susceptible for errors in reproducibility. Thirdly, the membrane is based on single intensity measurements, because the indicator carboxyfluorescein shows only one excitation and emission maximum and is therefore not suitable for dual wavelength measurements. Experiments to reference the signal via DLR failed due to photobleaching.

4.5. References

1. O.S. Wolfbeis, **Fiber Optic Chemical Sensors and Biosensors**, Vol. I, CRC Press, Boca Raton, **1991**, pp. 359.

2. A. S Jeevarajan, S. Vani, T. D. Taylor, M. M. Anderson, **Continuous pH monitoring in a perfused bioreactor system using an optical pH sensor,** Biotech. & Bioeng., **2002**, 78(4), 467-472.

3. A. Holobar, B. H. Weigl, W. Trettnak, R. Benes, H. Lehmann, N. V. Rodriguez, A. Wollschlager, P. O'Leary, P. Raspor, O. S. Wolfbeis, **Experimental results on an optical pH measurement system for bioreactors,** Sens. Actuat. B, **1993**, B11(1-3), 425-430.

4. J. A. Ferguson, B. G. Healey, K. S. Bronk, S. M. Barnard, D. R. Walt, **Simultaneous monitoring of pH, CO_2 and O_2 using an optical imaging fiber,** Anal. Chim. Acta, **1997**, 340(1-3), 123-131.

5.   K. L. Michael, D. R. Walt, **Combined Imaging and Chemical Sensing of Fertilization-Induced Acid Release from Single Sea Urchin Eggs,** Anal. Biochem., **1999**, 273(2), 168-178.

6.   F. Baldini, S. Bracci, F. Cosi, P. Bechi, F. Pucciani, **Controlled-pore glasses embedded in plastic optical fibers for gastric pH sensing purposes,** Appl. Spectrosc., **1994**, 48(5), 549-552.

7.   H. E. Posch, M. J. P. Leiner, O. S. Wolfbeis, **Towards a gastric pH-sensor: an optrode for the pH 0-7 range,** Fresen. J. Anal. Chem., **1989**, 334(2), 162-5.

8.   J. I. Peterson, S. R. Goldstein, R.V. Fitzgerald, R. V. Buckhold, **Fiber optic pH probe for physiological use**,   Anal. Chem.*,* **1980**, 52, 864-867.

9.   S. Hulth, R. C. Aller, P. Engstrom, E. Selander, **A pH plate fluorosensor (optode) for early diagenetic studies of marine sediments,** Limnol. Oceanogr., **2002**, 47(1), 212-220.

10.   J. Janata, **Do Optical Sensors Really Measure pH,** Anal. Chem., **1987**, 59, 1351.

11.   J. Janata, **Ion Optodes,** Anal. Chem., **1992**, 64, 921A.

12.   P. Fromherz, B. Masters, **Interfacial pH at electrically charged lipid monolayers investigated by the lipoid pH-indicator method,** Biochim. Biophys. Acta**, 1974**, 356(3), 270-275.

13.   G. T. Hermanson, **Bioconjugate Techniques**, Academic Press, **1996**, pp. 100.

14.   T. Mayr, T. Werner, **Highly selective optical sensing of copper(II) ions based on fluorescence quenching of immobilized Lucifer Yellow,** Analyst, **2002**, 127(2), 248-252.

15.   S. Moore, W. H. Stein, **Photometric ninhydrin method for use in the chromatography of amino acids,** J. Biol. Chem., **1948**, 176, 367-388.

16.   A. Lobnik, I. Oehme, I. Murkovic, O. S. Wolfbeis, **pH optical sensors based on sol-gels. Chemical doping versus covalent immobilization,** Anal. Chim. Acta, **1998**, 367(1-3), 159-165.

19.   W. C. Sun, K. R. Gee, D. H. Klaubert, R. P. Haugland, **Synthesis of fluorinated fluoresceins,** J. Org. Chem., **1997**, 62(19), 6469-6475.

18.   J. C. Sheehan, J. Preston, P. A. Cruickshank, **Rapid synthesis of oligopeptide derivatives without isolation of intermediates.**,   J. Am. Chem. Soc., **1965**, 87(11), 2492-3.

19.   H. Offenbacher, O. S. Wolfbeis, E. Fuerlinger, **Fluorescence optical sensors for continuous determination of near-neutral pH values,** Sens. Actuat., **1986**, 9(1), 73-84.

20.   O. S. Wolfbeis, N. V. Rodriguez, T. Werner, **LED-compatible fluorosensor for measurement of near-neutral pH values,** Mikrochim. Acta, **1992**, 108(3-6), 133-141.

21.   Y. Kostov, A. Neykov, **Rapid covalent method for fabrication of optical pH sensitive membranes,** Anal. Lett., **2000**, 33(3), 413-423.

22.   Y. Kostov, S. Tzonkov, L. Yotova, M.Krysteva, **Membranes for optical pH sensors,** Anal. Chim. Acta, **1993**, 280(1), 15-19.

23.   A. A. Ensafi, A. Kazemzadeh, **Optical pH Sensor Based On Chemical Modification of Polymer Film**, Microchem. J., **1999**, 63(3), 381-388.

24.   W. Wroblewski, E. Rozniecka, A. Dybko, Z. Brzozka, Zbigniew, **Cellulose based bulk pH optomembranes,** Sens. Actuat. B, **1998**, B48(1-3), 471-475.

25.   S. G. Schulman, S. Chen, F. Bai, M. J. P. Leiner, L. Weis, O. S. Wolfbeis, 27. **Dependence of the fluorescence of immobilized 1-hydroxypyrene-3,6,8-trisulfonate on solution pH: extension of the range of applicability of a pH fluorosensor,** Anal. Chim. Acta, **1995**, 304(2), 165-70.

26.   G. J. Mohr, O. S. Wolfbeis, **Optical sensors for a wide pH range based on azo dyes immobilized on a novel support,** Anal. Chim. Acta, **1994**, 292(1-2), 41-8.

27.   T. Werner, O. S. Wolfbeis, **Optical sensor for the pH 10-13 range using a new support material,** Fresenius' J. Anal. Chem., **1993**, 346(6-9), 564-568.

28.   H. E. Posch, M. J. P. Leiner, O. S. Wolfbeis, **Towards a gastric pH-sensor: an optrode for the pH 0-7 range,** Fresenius' J. Anal. Chem., **1989**, 334(2), 162-165.

29.   M. Cajlakovic, A. Lobnik, T. Werner, **Stability of new optical pH sensing material based on cross-linked poly(vinyl alcohol) copolymer,** Anal. Chim. Acta, **2002**, 455(2), 207-213.

30.   G. E. Badini, K. T. V.Grattan, A. C. Tseung, **Characteristics of dye-impregnated tetraethylorthosilane (TEOS) derived sol-gel coatings,** J. Sol-Gel Sci. Technol., **1996**, 6(3), 269-272.

31.   N.A. Peppas, **Preparation, Methods & Structures of Hydrogels**, CRC Press, Boca Raton, 1986.

Chapter 5

Fluorescent pH Sensors with Negligible Sensitivity to Ionic Strength

Optical pH determination has the fundamental disadvantage of measuring a signal that is depending on the ionic strength of the sample. The problem originates from the complex relationship between the proton activity and the concentration of the pH-sensitive dye. The effect of ionic strength on the signal depends on the charge of the indicator and its environment, e.g. the immobilization matrix. We present novel lipophilic fluorescein esters carrying one negative charge. They are embedded in an uncharged, highly proton-permeable hydrogel to give optical pH sensors that show a negligible cross-sensitivity towards ionic strength. The fluorescent dyes differ in their substituents. This variation of substituents results in dissociation constants between 5.5 and 8.5. The indicators were made lipophilic by esterification of the carboxy group with a C_{18} alkyl chain. Since their spectral properties are quite similar, two indicators may be used in one sensor. This results in an optical pH sensor with a dynamic range that extends from pH 4.5 to 8.

5.1. Introduction

The Henderson-Hasselbalch equation Eq. 2-3 relates the concentration ratio of a pH-sensitive indicator to pH of the sample.

$$pH = pK_a + \log \frac{c(A^-)}{c(HA)} + \log \frac{f_{A^-}}{f_{HA}} - \log a_{H_2O} \qquad (2-3)$$

One consequence of this equation is that the dynamic range of most optical sensors is limited to $pK_a \pm \sim 1.5$. However, in this range the sensitivity (ΔSignal/ΔpH) of optical sensors is better due to the large slope of the sigmoidal titration plot compared to the linear (Nernstian) response of electrochemical sensors. A more serious consequence is the fact that the signal of optical sensors is affected by ionic strength. Recently, optical pH sensors have been presented wherein a change of ionic strength from 10 mM to 3 M caused a pK

shift of 1.23 pH units[1].

Many attempts have been made to overcome this problem. A technique was reported[2] that works for aqueous solutions, wherein two differently charged indicators where used to determine both pH and ionic strength. Later, two sensors were described based on one indicator with different surface chemistries[3]. In the first sensor, the indicator is embedded in an uncharged micro-environment. This sensor is highly sensitive to changes in ionic strength. In the second sensor, the indicator is placed in a highly charged environment. This sensor is less sensitive towards changes in ionic strength. The optical pH determination using two sensors or indicators which respond to different degrees of a measurement solution requires complex equipment and additional calculations.

In 1988, Janata[4, 5] critically reviewed optical sensors and pointed out that the signal in optical sensors originates from bulk-surface interactions. Therefore, in optical sensors these interactions and the relationship between the bulk and the surface pH have to be taken into account. The difference between surface and bulk pH is described by the surface potential Ψ, that depends on the concentration profile of all ionic species in the interphase, i.e. double layer and ionizable groups on the surface (Equation 4-3).

$$pH_{surf} = pH_{bulk} + \frac{Ne\Psi}{2.3RT} \qquad (4\text{-}3)$$

Therefore, the difference between pH_{surf} and pH_{bulk} should be especially large for sensors having highly charged surfaces. According to equation 4-3, the best results will be achieved if $pH_{surf} \sim pH_{bulk}$, in other words if the surface potential Ψ is close to zero. In this paper, we present a method to design pH optical sensors with the surface potential reduced to a minimum and therefore with a minimized effect of ionic strength.

We also describe the syntheses of novel, lipophilic fluorescein derivatives and their esterification with long alkyl chains. This ester-modification results in three characteristic features: First, the number of charges is reduced to one negative charge because the carboxy group becomes an ester; this results in a negligible cross-sensitivity towards ionic strength. Second, the modification of the carboxy group prevents lactonization of the chromophore. Therefore, the indicators show different absorbance maxima for the basic and the acidic form, respectively. This is desirable with respect to internal referencing via ratiometric measurements see (Chapter 2.2.1.1.). Third, the lipophilic character of the dyes prevents their leaching out of the polymer matrix. The indicators can be embedded in the hydrophobic blocks of a suitable polymer matrix. Thus, covalent coupling is not needed

which facilitates sensor preparation.

5.2. Materials and Methods

5.2.1. Chemicals

Fluorescein (product no. 46955), 2',7'-dichlorofluorescein (DCF (**6**), product no. 35848), methanesulphonic acid (product no. 64285), 5-(octadecanoylamino)fluorescein were purchased from Fluka (Buchs, Switzerland; www.fluka.com). 4-chlororesorcin (product no. C7,060-6), 4-hexylresorcin (product no. 20,946-5) and 1-iodooctadecane (product no. 25,198-4) were from Aldrich (Taufkirchen, Germany; www.sigmaaldrich.com). Phthalic anhydride (product no. 800592) was from VWR-Merck (Darmstadt, Germany; www.vwr.de). The polymer Hydromed D4 (formerly known as Hydrogel D4) was received from Cardiotech Inc. (Woburn, MA, USA; www.cardiotech-inc.com) by request. According to the manufacturer's specification the hydrogel is of the polyurethane type. The mechanical support (product no. LS 1465585) a foil of polyterephtalate (125 μm thick) was obtained from Goodfellow (Cambridge, UK; www.goodfellow.com). Phosphate buffer solutions of defined pH were prepared from respective sodium salts from hydrogen phosphate and dihydrogen phosphate (total concentration of phosphate = 10 mM) of analytical grade from VWR-Merck (Darmstadt, Germany; www.vwr.de) according to the buffers described in Chapter 3.2.2. The ionic strength of buffer solutions was adjusted with sodium chloride as background electrolyte. Dimethylsulphoxide (DMSO), ethanol, sodium hydroxide and hydrochloric acid also were of analytical grade. Aqueous solutions were prepared from doubly distilled water.
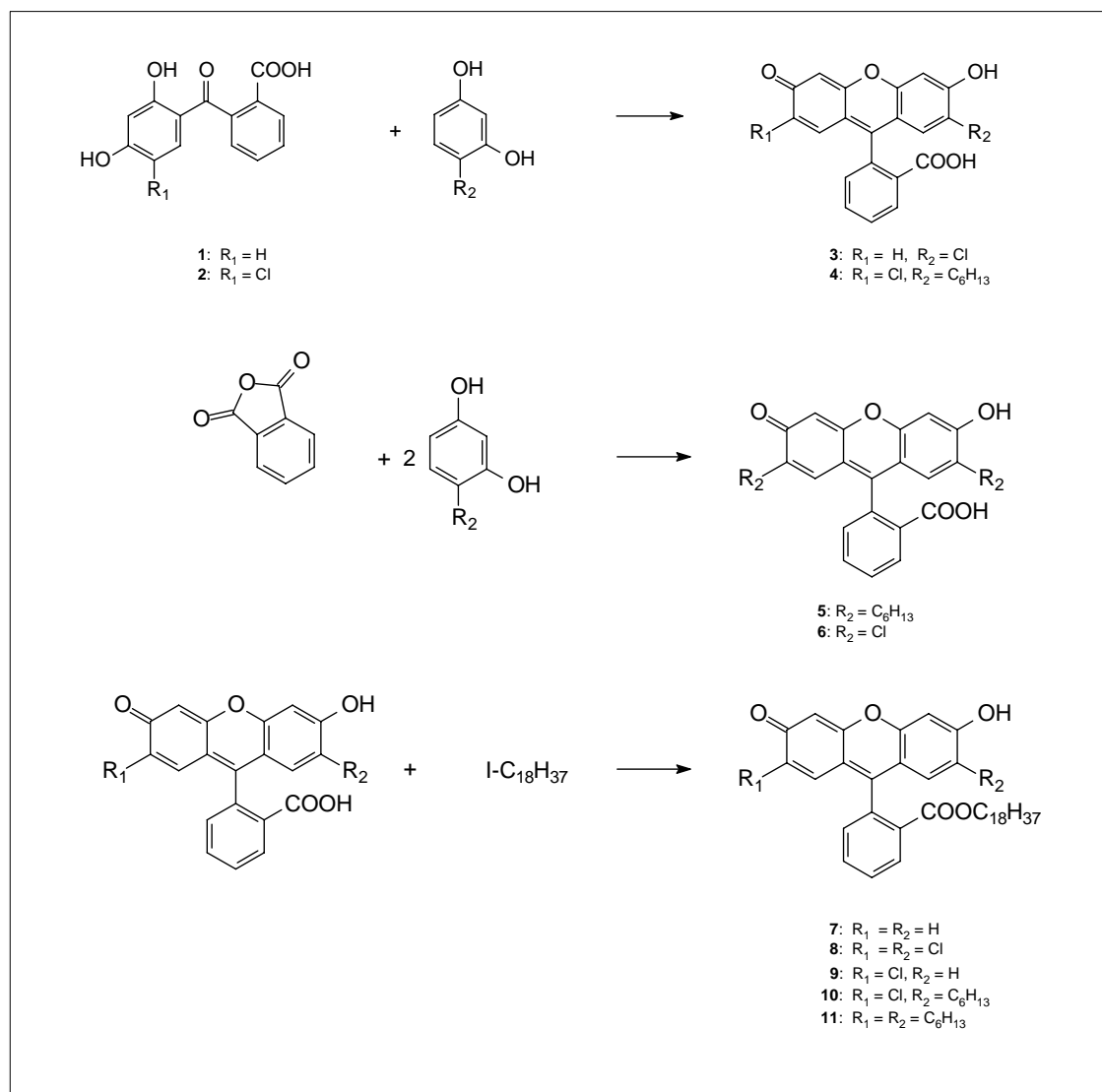
Scheme 5.1. Structure of the dyes and corresponding reaction schemes.

5.2.2. Apparatus

An Aminco-Bowman Series 2 luminescence spectrometer from SLM (Rochester, NY, USA; www.thermo.com) was used to record fluorescence spectra. The excitation light passed a monochromator and was focused to one branch of a bifurcated fiber bundle of randomized glass fibers ($\varnothing$ 6 mm). The fiber bundle was directed to the backside of the sensor membrane mounted in a home-made flow through cell, as described in chapter 4.2.2. The flow rate was kept constant at 1 mL/min using a Minipuls-3 peristaltic pump (Gilson, Villiers, France). The emitted light was guided by the other branch of the fiber bundle through a monochromator to the photomultiplier tube inside the spectrometer after having passed the emission monochromator. Unless stated otherwise, measurements were performed at excitation wavelengths of 530 and 470 nm and at an emission wavelength of 550 nm, respectively. Microtiterplates were analyzed with a Labsystems Fluoroskan

Ascent reader. Decay times were measured on a LF 401 NanoScan microplate reader from IOM (Berlin, Germany; www.iom-berlin.de). Absorption spectra were recorded with a Perkin Elmer Lambda 14 UV/VIS spectrophotometer. The pH values of solutions were checked using a digital pH meter (Schott, Mainz, Germany) calibrated with standard buffers of pH 7.00 and 4.00 (Merck) at 20 ± 2 °C.

5.2.2. Buffer preparation

MES and MOPS buffers with a total buffer salt concentration of 2 mM and 10 mM, respectively and with sodium chloride to adjust ionic strength were used. Buffers were prepared by mixing two stock solutions of defined ionic strength. A basic stock solution A was prepared by dissolving 0.4344 g of Na-MES-salt (2.312 g Na-MOPS-salt) and sodium chloride in 1 L of water. 0.3904 g of MES-salt (2.0927 g of MOPS-salt) and sodium chloride were dissolved in 1 L of water for a acidic stock solution B. Table 3 gives the corresponding amounts of sodium chloride for each stock solution to adjust the desired ionic strength. Ionic strength of the buffers was calculated by means of an EXCEL sheet according to the equation of Debye and Hückel.

Table 5.1.   Amounts of additional sodium chloride to adjust the total ionic strength of the stock solutions A and B.

Ionic strength [mM]	Amount of NaCl for solution A [g]	Amount of NaCl for solution B [g]
25 mM (MES)	1.3441	1.461
25 mM (MOPS)	0.8766	1.461
150 mM (MOPS)	8.6491	8.766

Stock solutions A and B of the same ionic strength were mixed, controlled by a pH meter, to obtain the desired pH solutions.

5.2.4. Experimental Set-up for measurements at low Ionic Strength

In order to determine the performance of the sensors at low ionic strength (2-25 mM) the experimental set-up was changed. Instead of using the flow-through cell, a sensor foil (M_{DCFOE}) was fixed with silicone at the edge of a graduated beaker. The beaker was placed in a black, wooden box, with a nitrogen in- and outlet, two openings for a funnel and a stirrer. On the left side of the black box was an opening for the fiber bundle of the AB2

fluorometer. By means of an elevating platform, the membrane was positioned opposite of the fiber bundle. After calibration with MES buffer 25 mM solutions, the beaker was filled with MES buffer 2 mM pH 5.5. Ionic strength of the buffer was changed by addition of NaCl in 1 mM steps up to 25 mM through a funnel. The solution was permanently stirred and the black box was flushed with nitrogen to prevent pH changes caused by CO_2 introduction. Scheme 5.2. shows the experimental set-up.
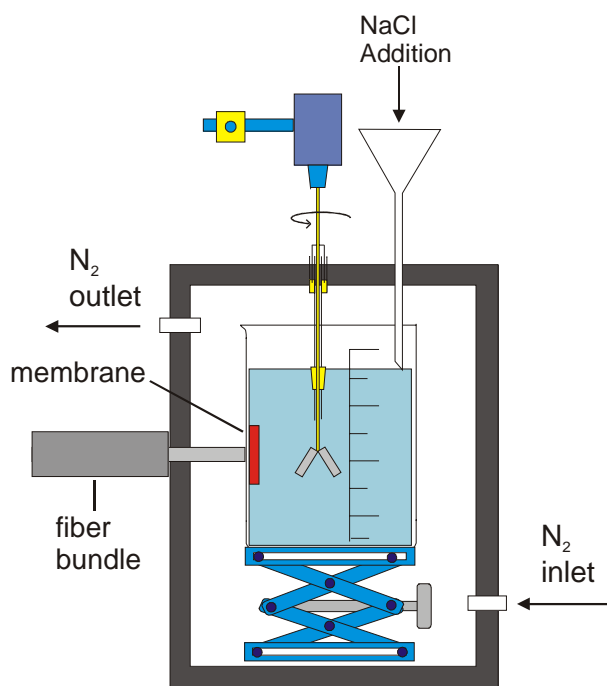
Scheme 5.2. Experimental set-up for measurements at low ionic strength.

5.2.5. Determination of the molar absorbance

The purified dyes were dissolved in 100 mL of ethanol. From this stock solution, three dilutions (1:20, 1:50, and 1:100) were made, and the molar absorbance was measured. The extinction coefficients were calculated according to Lambert-Beer's law (E = ε·c·d).

5.2.6. Determination of Quantum Yields

The quantum yields ϕ of the dyes were measured in ethanol relative to fluorescein as the reference fluorophore whose QY is 0.97 in basic ethanol[6]. The quantum yields ϕ_X of the dyes were determined using the following formula[7]:

$$\varphi_X = \varphi_R \frac{A_R \times I_X \times n_X^2}{A_X \times I_R \times n_R^2}$$

(5-1)

where ϕ_R is the quantum yield of the reference, A_R and A_X are the absorbences of the reference and the dye, respectively, at the excitation wavelength, I_R and I_X are the integrated areas of the corrected emission spectra of the reference and the dye, respectively, and n_R and n_X are the refractive indices of the solvent of the reference and the dye, respectively.

5.3. Syntheses

These were carried out according to the methods reported by Matray et al.[8] or Wang et al.[9]. The dyes are of orange colour and their ^{1}H-NMR and mass spectra are in agreement with the assumed chemical structure. The general sytheses strategy is shown in scheme 5.1. The reaction schemes for the precursors 2,4-Dihydroxy-2'-carboxybenzophenone (1) and 5-Chloro-2,4-dihydroxy-2'-carboxybenzophenone (2) are shown beneath. In the following, the chemical names of the pH indicators, their numbers and acronyms, the starting material and the method used, the yields (in %) and melting points are summarized.

5.3.1. Synthesis of 2,4-Dihydroxy-2'-carboxybenzophenone (1):
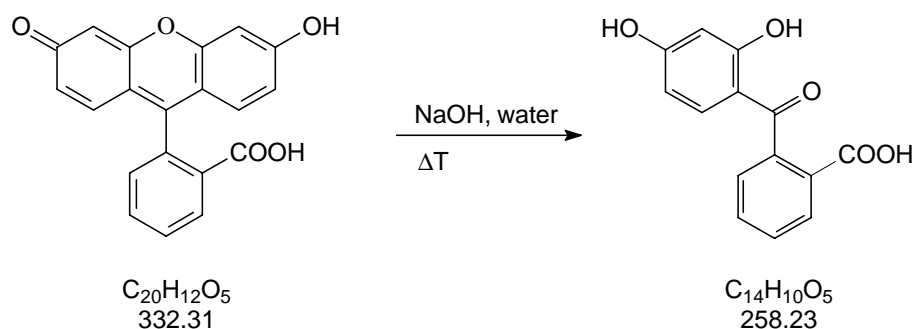
The synthesis was carried out according to Matray et al.[8] with a slightly modification. Instead of 5(6)-Carboxyfluorescein, 10 g of Fluorescein were used. Finally, the product was recrystallized in methylene chloride to give 6.85 g (88%); mp. 203 °C.

5.3.2. Synthesis of 5-Chloro-2,4-dihydroxy-2'-carboxybenzophenone (2):

$C_{20}H_{10}Cl_2O_5$
401.20

$C_{14}H_9ClO_5$
292.68
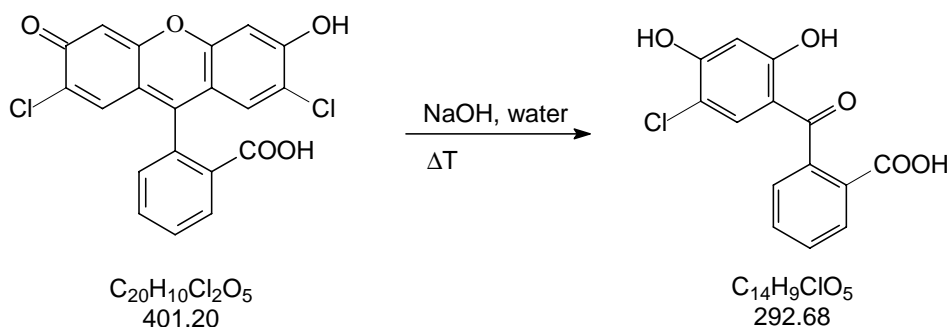
5 g of DCF and 10 g of NaOH were combined in 10 mL of water and heated for 2h at 175 °C. Afterwards, 50 ml of water were added and the solution was cooled to room temperature. Acidification with concentrated hydrochloric acid precipitated a tan solid. The crude product was recrystallized twice (CHCl$_3$:MeOH 1:1) to give 2.66 (73%) of light brown powder. ^{1}H-NMR (CD$_3$OD) δ 8.26 (1 H, d, aromatic): 7.82 (td, 2 H, aromatic), 7.45 (d, 1 H, aromatic), 7.06 (s, 1 H, aromatic), 6.58 (s, 1 H, aromatic). ESI-MS: m/e (M+, cation) for $C_{14}H_{10}ClO_5$, calcd. 292.7, found 293.3.; mp. 238 °C.

5.3.3. Synthesis of 2'-Chlorofluorescein (3; MCF):

4-chlororesorcinol (0.64 g, 5.08 mmol) and 2,4-dihydroxy-2'-carboxybenzophenone (1.32 g, 5.08 mmol) were put into a 100 mL round bottom flask. Methanesulfonic acid (25 mL) was added and the resulting suspension was heated to 130 °C using an oil bath. After allowing the reaction to stir for 30 min, the solution was cooled to room temperature and then added drop wise to rapidly stirring water (100 mL). The resulting fine dark precipitate was filtered and dried. MPLC (ethanol) yielded the product as an orange powder (0.23 g, 12%). ESI-MS: m/e (M+, cation) for $C_{20}H_{11}ClO_5$, calcd. 366.8, found 366.1; mp. 251 °C.

5.3.4. Synthesis of 2'-Chloro-7'-hexylfluorescein (4; CHF):

4-hexylresorcinol (493 mg, 2.54 mmol) and 5-chloro-2,4-dihydroxy-2'-carboxy-benzophenone (743 mg, 2.54 mmol) were put into a 50 mL round bottom flask. Methanesulfonic acid (10 mL) was added and the resulting suspension was heated to 130 °C using an oil bath. After allowing the reaction to stir for 30 min, the solution was cooled to room temperature and then added drop wise to rapidly stirring water (50 mL). The resulting orange precipitate was filtered and dried. Column chromatography (silica gel, methanol:CHCl$_3$ 1:9 v/v) yielded the product as a orange powder (0.94 g, 82%). TLC R$_f$ =

0.48 (silica plate, methanol:CHCl$_3$ 1:9 v/v). ^{1}H-NMR (CD$_3$OD) δ 8.19 (1 H, d, aromatic): 7.88 (m, 2 H, aromatic), 7.31 (d, 1 H, aromatic), 6.86 (s, 1 H, aromatic), 6.71 (dd, 2 H, aromatic), 6.51 (s, 1H, aromatic), 2.52 (t, 2 H, aryl-CH$_2$), 1.64 (m, 8 H, -CH$_2$-CH$_2$-CH$_2$), 0.95 (t, 3 H, -CH$_3$). ESI-MS: m/e (M+, cation) for C$_{26}$H$_{23}$ClO$_5$, calcd. 450.9, found 451.1 (100%) and 453.1 (35%); mp. 242 °C.

5.3.5. Synthesis of 2',7'-Dihexylfluorescein (5; DHF):

4-hexylresorcinol (2 g, 10.4 mmol) and phthalic anhydride (770 mg, 5.2 mmol) were put into a 50 mL round bottom flask. Methanesulfonic acid (20 mL) was added and the resulting suspension was heated to 130 °C using an oil bath. After allowing the reaction to stir for 30 min, the solution was cooled to room temperature and then added drop wise to rapidly stirring water (100 mL). The resulting fine orange precipitate was filtered and dried to afford 2', 7'-dihexylfluorescein (1.76 g, 67%). ^{1}H-NMR (CDCl$_3$) δ 8.31 (1 H, d, aromatic): 7.75 (m, 2 H, aromatic), 7.26 (s, 3 H, aromatic), 6.86 (s, 2 H, aromatic), 2.39 (t, 4 H, aryl-CH$_2$), 1.31 (t, 4 H, aliphatic), 1.11 (t, 12 H, aliphatic) 0.77 (t, 6 H, -CH$_3$). ESI-MS: m/e (M+, cation) for C$_{32}$H$_{36}$O$_5$, calcd. 500.6, found 501.3.; m.p. 113 °C.

5.3.6 Synthesis of 2',7'-Dichlorofluorescein octadecylester (8; DCFOE):

The synthesis was carried out according to Wang et al.[9]

5.3.7. Synthesis of 2'-Chlorofluorescein octadecylester (9; MCFOE):

A mixture of 2'-monochlorofluorescein (200 mg, 0.55 mmol) and 1-iodooctadecane (209 mg, 0.55 mmol) in 5 ml of DMSO and K$_2$CO$_3$ solid (140 mg) was stirred in an oil bath at 65°C for 20 h. The red precipitate that formed upon addition of 10 ml saturated NaCl was filtered, washed with deionized water and redissolved in ethyl acetate with 1 M HCl. The yellow orange, organic phase was separated, washed with phosphate buffer (pH 7.4) and deionized water, and evaporated to dryness under reduced pressure. 100 mg of the reaction mixture were purified using MPLC with ethanol as eluent to yield pure MCFOE (17 mg, 5%). R$_f$=0.61 (RP-silica plates, ethanol). ^{1}H-NMR (CDCl$_3$), 8.34 (d, 1 H, aromatic): 7.81 (m, 2 H, aromatic), 7.47 (d, 1 H, aromatic), 7.20 (s, 2 H, aromatic), 7.12 (s, 2 H, aromatic), 4.02 (t, 2 H, -O-CH$_2$-), 1.34 (m, 32 H, aliphatic, -CH$_2$-), 0.89 (t, 3 H, CH$_3$). ESI-MS: m/e (M+, cation) for C$_{38}$H$_{47}$ClO$_5$, calcd. 619.2, found 618.3.; m.p. 142 °C.

5.3.8. Synthesis of 2'-Chloro-7'-hexylfluorescein octadecylester (10; CHFOE):

A mixture of 2'-chloro-, 7'-hexylfluorescein (482 mg, 1.07 mmol) and 1-iodooctadecane (380 mg, 1.07 mmol) in 5 ml of DMSO and K_2CO_3 solid (290 mg) was stirred in an oil bath at 65°C for 20 h. The red precipitate that formed upon addition of 10 ml saturated NaCl was filtered, washed with deionized water and redissolved in ethyl acetate with 1 M HCl. The yellow orange, organic phase was separated, washed with phosphate buffer (pH 7.4) and deionized water, and evaporated to dryness under reduced pressure. The product was purified by column chromatography with methanol:$CHCl_3$ 1:9 v/v as eluent to yield pure CHFOE (92 mg, 13 %). R_f=0.70 (silica plates, methanol:$CHCl_3$ 1:9 v/v). ^{1}H-NMR ($CDCl_3$), 8.29 (d, 1 H, aromatic): 7.70 (dd, 2 H, aromatic), 7.29 (d, 1 H, aromatic), 7.21 (d, 2H, aromatic), 7.12 (s, 1 H, aromatic), 7.00 (s, 1 H, aromatic), 3.89 (t, 2 H, -O-CH_2-) 2.48 (t, 2 H, aryl-CH_2-), 1.37 (m, 2 H, aliphatic CH_2), 1.08 (t, 38 H, -CH_2-CH_2-CH_2-), 0.78 (t, 6 H, CH_3). ESI-MS: m/e (M+, cation) for $C_{44}H_{59}ClO_5$, calcd. 703.4, found 703.4.; m.p. 134 °C.

5.3.9. Synthesis of 2',7'-Dihexylfluorescein octadecylester (11; DHFOE):

A mixture of 2', 7'-dihexylfluorescein (535 mg, 1.07 mmol) and 1-iodooctadecane (380 mg, 1.07 mmol) in 5 ml of DMSO and K_2CO_3 solid (290 mg) was stirred in an oil bath at 65°C for 20 h. The red precipitate that formed upon addition of 10 ml saturated NaCI was filtered, washed with deionized water and redissolved in ethyl acetate with 1 M HCl. The yellow orange, organic phase was separated, washed with phosphate buffer (pH 7.4) and deionized water, and evaporated to dryness under reduced pressure. The product was separated from the byproducts by column chromatography with methanol:$CHCl_3$ 1:9 v/v as eluent to yield pure DHFOE (72 mg, 9%). R_f=0.59 (silica plates, methanol:$CHCl_3$ 1:9 v/v). ^{1}H-NMR ($CDCl_3$) δ 8.21 (1 H, d, aromatic): 7.65 (s, 2 H, aromatic), 7.26 (t, 3 H, aromatic), 6.75 (s, 2 H, aromatic), 3.91 (t, 2H, -O-CH_2-), 2.60 (t, 4 H, aryl-CH_2), 1.51-1.23 (t, 48 H, aliphatic) 0.91 (t, 9 H, -CH_3). ESI-MS: m/e (M+, cation) for $C_{50}H_{72}O_5$, calcd. 753.1, found 752.6; glassy orange mass whose mp. cannot be determined.

5.3.10. Preparation of sensor membranes

Hydrogel cocktails were prepared from 100 mg hydrogel dissolved in a mixture of 1.08 g ethanol and 0.12 g water. Starting from stock solutions of 1 mg dye in 1 mL ethanol, adequate volumina were added to the hydrogel cocktail to achieve dye concentrations of 2

mmol/kg of polymer. The cocktail compositions are summarized in Table 5.2. The mixtures were vigorously stirred at room temperature overnight. 100 µL of each cocktail were knife-coated onto dust-free, 125 µm thick polyester supports. The resulting membranes were dried on air for 2 h before characterization. Spots of 25 mm diameter were cut with a hollow punch and mounted in a flow-through cell.

Table 5.2 Cocktail compositions

membrane	indicator	V (stock sol.)/µL [*]
M_{DCFOE}	DCFOE	130.8
M_{MCFOE}	MCFOE	123.9
M_{CHFOE}	CHFOE	140.7
M_{DHFOE}	DHFOE	150.7
M_{HYBRID}	DCFOE / CHFOE	65.4 / 70.4

5.4. Results and Discussion

5.4.1. Choice of materials

There are three widely used methods for immobilization of a pH indicator on a solid substrate: adsorption, entrapment and covalent binding. The latter is more time consuming, because it includes several immobilization steps that complicate sensor chemistry. Embedding, in contrast, can be carried out fast and easily. In our method, ethanolic dye solutions are stirred with polymer solutions without any further chemical process. The resulting "cocktail" is cast, as a thin film, on an inert and transparent support and dried.

Derivatives of fluorescein were chosen among other fluorescent indicators because of their photophysical properties which include high absorption coefficients ($\varepsilon > 70000$ L mol^{-1} cm^{-1}) and fluorescence quantum yields of typically higher than 0.9 in dissociated form. The spectral and thermodynamic properties of fluorescein are governed by the substitution pattern of the xanthene structure[10]. Halides in 2',7' or 4',5' positions affect the dissociation constant of the indicator. For example, the pK$_a$ values of fluorescein, 2',7'-difluorofluorescein, 2',7'-dichlorofluorescein (**6**) and 2', 4', 5', 7'-tetrabromofluorescein are 6.5, 4.8, 5.0 and 3.8, respectively. Halides in 2',7'-position do not alter the QY's compared to fluorescein (QY ~ 1), whereas substitution in 4',5'-position results in decreased QYs[11]. To our knowledge, 4-fluororesorcinol, the starting material to obtain 2',7'-difluorofluorescein, is commercially not available and has to be synthesized in several steps from resorcin and a fluorinating reagent[12-15]. Therefore, we used 4-chlororesorcine to

obtain halogenated fluoresceins.

In addition to sol-gels and PVC-based polymers (see discussion chapter 4), hydrogels can serve as an attractive polymeric matrix for pH-sensitive and ion-sensitive membranes[16-20]. They are soluble in non-toxic solvents such as ethanol and exhibit excellent ion permeability due to the high water uptake and swelling[21]. The treatment made by Janata is based on the assumption of a well defined sensor-bulk interphase. This is true for many of the pH sensors reported so far. In case of a hydrogel, however, no discret interphase can be assumed because hydrogels can have a water-content up to 90% so that they may be considered as a kind of sponge. According to the manufacturer's information, our membrane has a water content of 50%. Therefore, the term Ψ in eq. 2 becomes less significant. We chose the polyurethane based hydrogel D4 as a polymer matrix due to its stability under varying conditions of pH and temperature and due to the fact that the polymer itself is uncharged. It is well soluble in 90% ethanol, but not in water. The structured polymer consists of hydrophilic and hydrophobic blocks and is capable of embedding lipophilic pH indicators without the need for covalent immobilization. This is demonstrated by the fact that sensor membranes M_{MCFOE}, M_{DCFOE} and M_{CHFOE} upon exposure to a buffer of pH 8.0 for 12 h showed a wash-out effect of less than 4% signal loss.

5.4.2. Membrane characteristics

DCFOE (**8**) has been used for optical determination of anions and protamins[9, 22], but not for optical sensing of pH. A comparison of the absorption spectra of DCFOE and its hydrophilic analogue DCF (**6**) reveals the effect of esterification at the C_2 carboxy group (Figure 5.1, Figure 5.2). The dye DCF in aqueous solution has absorption maxima for the deprotonated form at 502 nm. Lowering the pH does not result in a well-defined isosbestic point or in a new strong absorption band for the protonated (uncharged) form.
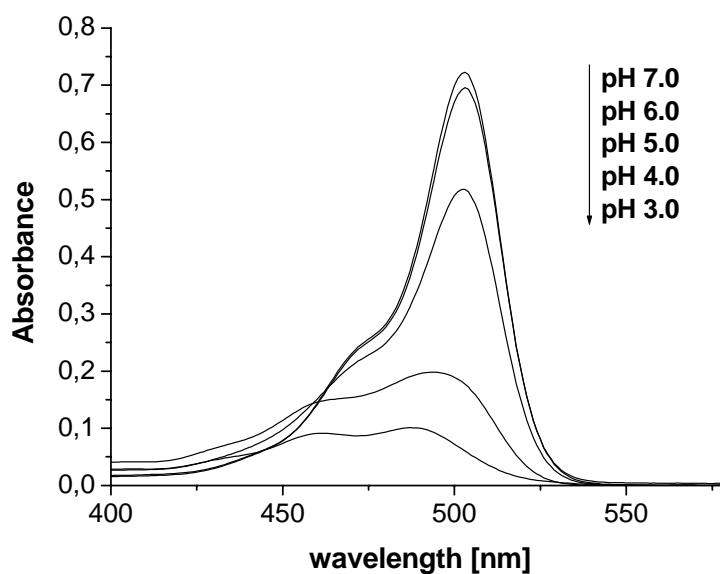
Fig. 5.1. Absorption spectra of DCF (c_{DCF} = 6 x 10^{-6} M) in a range of phosphate buffers (IS = 50 mM).

On the other hand, membrane M_{DCFOE} shows absorption maxima at 530 nm and 470 nm respectively for the basic and acidic form. If excited at the respective wavelengths, the membrane shows emission maxima at 544 nm and 524 nm (Fig. 5.3.).

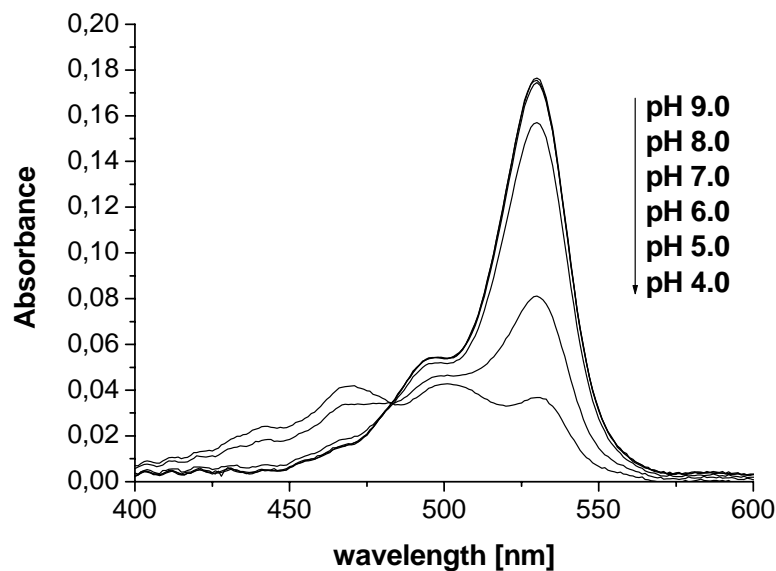**Fig. 5.2.** Absorption spectra of M_{DCFOE} (c_{DCFOE} = 2 mmol/kg) in a range of phosphate buffers (IS = 50 mM).
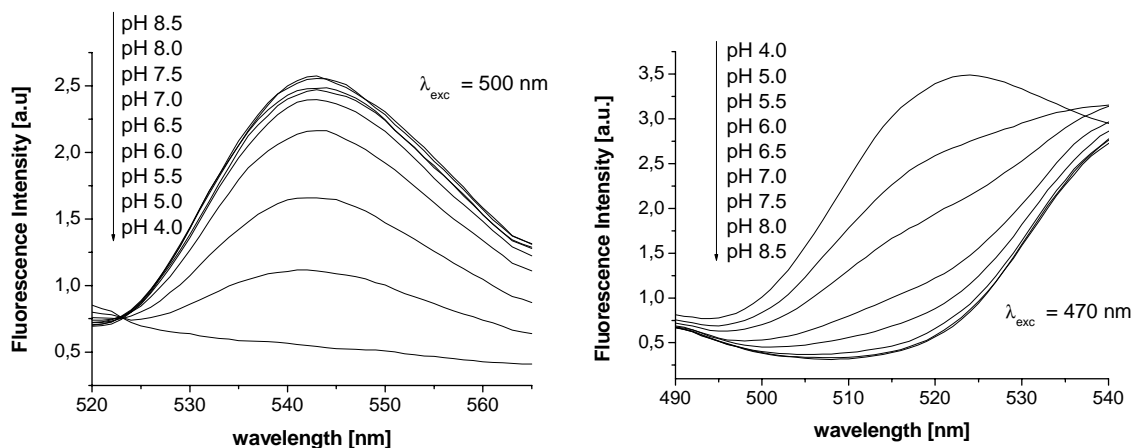
Fig. 5.3. Emission spectra of the basic (left) and the acid (right) form of membrane M_{DCFOE} .

Thus, the membrane is suitable for dual-wavelength measurements using either two excitation wavelengths and one emission wavelength, or one excitation wavelength and two emission wavelengths. We prefer excitation at 470 nm and 530 nm, and measuring the ratio of the two emission intensities at 550 nm. This ratio is independent of dye concentration (and therefore of dye leaching) and LED drifts. The apparent pK_a was determined from a plot of emission intensities vs. pH. Fig. 5.4. shows the resulting sigmoidal plot which gives a pK_a of 5.5 and a dynamic range from pH 4.5 to 7.0. Unfortunately, this is outside the near-neutral pH range.

Fig. 5.4. pH dependence of the calibration curve of the membrane M_{DCFOE}, M_{CHFOE}, and M_{DHFOE}. Due to the minimal difference in pK_a of membrane M_{MCFOE} and M_{CHFOE}, the plots can not be resolved properly. Therefore, only one plot is displayed.

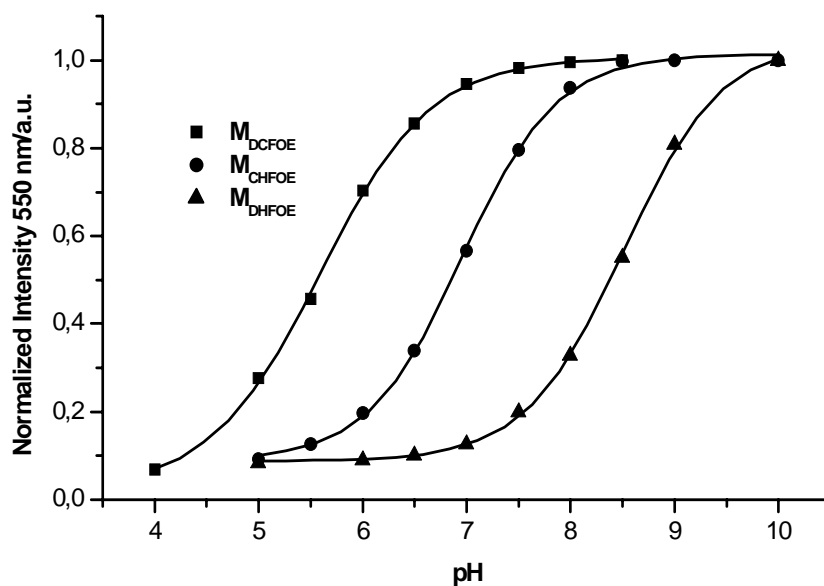It was perceived that the elimination of one chloro substituent of DCFOE should result in a pK_a of >5.5. Monochlorofluorescein octadecylester was prepared and placed into a hydrogel membrane (as described for DCFOE) to give membrane M_{MCFOE}. It shows absorption and emission maxima similar to those of M_{DCFOE} (Table 2), the wavelengths for the basic and acidic form being shifted shortwave by 5 nm. The membrane was excited at 530/470 nm and emission was collected at 550 nm. The membrane showed a pK_a of 6.8, which is almost ideal for sensing of physiological pHs.

In addition, fluoresceins were prepared with additional alkyl groups in order to increase the lipophilicy of the indicator and to better anchor the dye in the hydrophobic regions of the membrane. The absorption and emission maxima are similar to these of the other dyes, the apparent pK_a is 7.0 for CHFOE.

In DHFOE, both chloro substituents are replaced by hexyl groups. This dye displays the highest lipophilicity. The resulting membrane (M_{DHFOE}) shows the highest pK_a (8.5). This can be explained by the different inductive effects. A positive effect (ethyl-substituent) raises the electron density in the conjugated π-system and raises the dissociation constant. Vice versa, a -I-effect (Cl-substituent) lowers the dissociation constant. The spectral data for dyes and the corresponding membranes are listed in Table 5.3.

Table 5.3. Optical properties of pH indicators and corresponding membranes

Indicator / Membrane	λ_{max} (abs.) / nm	λ_{max} (em.) / nm	ε / L mol^{-1} cm^{-1} [1]	QY [1]
DCFOE	463 (ac.) / 523 (bas.) [1]	523 (ac.) / 541 (bas.) [1]	50000 (ac.) / 125000 (bas.)	0.52 (ac.) / 0.94 (bas.)
MCFOE	457 (ac.) / 516 (bas.) [1]	516 (ac.) / 535 (bas.) [1]	45000 (ac.) / 92000 (bas.)	0.57 (ac.) / 0.91 (bas.)
CHFOE	459 (ac.) / 519 (bas.) [1]	521 (ac.) / 540 (bas.) [1]	65000 (ac.) / 102000 (bas.)	0.58 (ac.) / 0.96 (bas.)
DHFOE	457 (ac.) / 515 (bas.) [1]	517 (ac.) / 543 (bas.) [1]	80000 (ac.) / 98000 (bas.)	0.67 (ac.) / 0.88 (bas.)
M_{DCFOE}	470 (ac.) / 530 (bas.) [2]	524 (ac.) / 543 (bas.) [2]	n.d.	n.d.
M_{MCFOE}	466 (ac.) / 523 (bas.) [2]	516 (ac.) / 540 (bas.) [2]	n.d.	n.d.
M_{CHFOE}	471 (ac.) / 526 (bas.) [2]	523 (ac.) / 545 (bas.) [2]	n.d.	n.d.
M_{DHFOE}	455 (ac.) / 520 (bas.) [2]	518 (ac.) / 548 (bas.) [2]	n.d.	n.d.

[1] in ethanolic solution; [2] in polyurethane hydrogel matrix;

5.4.3. Effect of ionic strength

The effect of IS on the response of the four membranes are shown in Figure 5.5.-5.8. The results show that changes in ionic strength affect the apparent pK_a only marginally. The small shifts in pK_a can be interpreted in terms of the change of the indicator which changes from zero to -1. Hence, the influence of the microenvironment charge of the indicator and

the surface potential of the membrane are reduced to a minimum and changes in IS alter the pK_a only marginally. The polymer is not expected to cause an effect at all. Table 5.4 summarizes the effect of ionic strength on the sensor membranes using phosphate buffer solutions with ISs of 25, 50, 100, 200 and 500 mM, respectively which cover the range of most clinical and biotechnical applications.
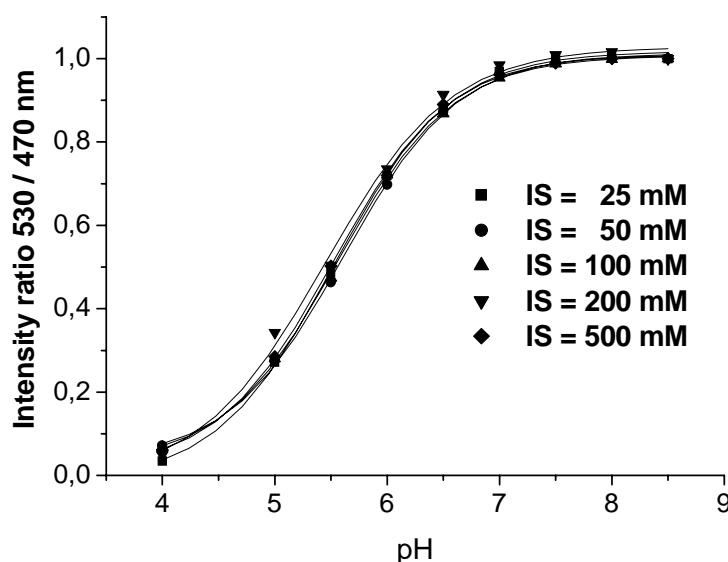
Fig. 5.5. Calibration curves of membrane M_{DCFOE} at ionic strengths from 25 to 500 mM.
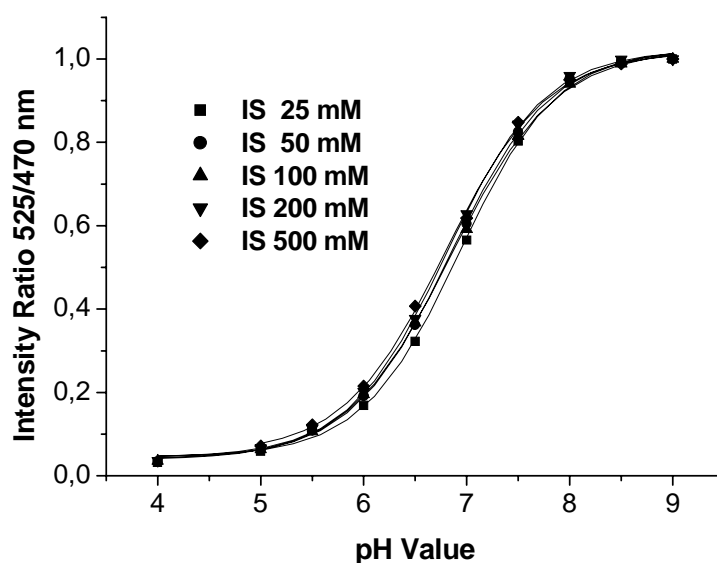
Fig. 5.6. Calibration curves of membrane M_{MCFOE} at ionic strengths from 25 to 500 mM.
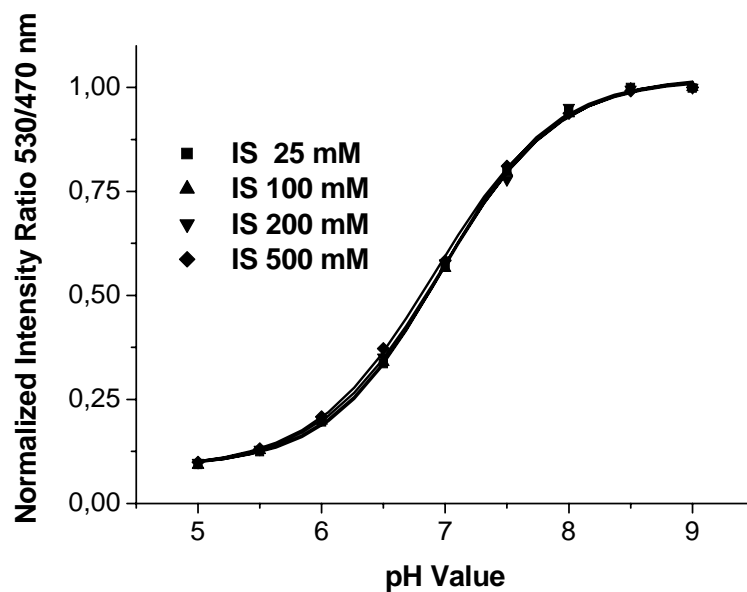
Fig. 5.7. Calibration curves of membrane M_{CHFOE} at ionic strengths from 25 to 500 mM.
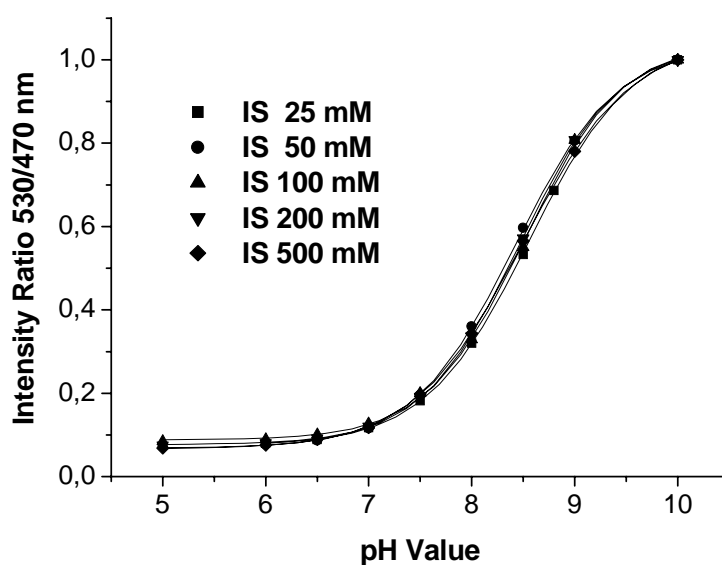
Fig. 5.8. Calibration curves of membrane M_{DHFOE} at ionic strengths from 25 to 500 mM.

Table 5.4. pK_a values of membranes at different ionic strengths

Membrane	Ionic strength				
	0.025 M	0.05 M	0.1 M	0.2 M	0.5 M
M_{DCFOE}	5.52	5.60	5.56	5.45	5.52
M_{MCFOE}	6.93	6.84	6.85	6.80	6.78
M_{CHFOE}	6.96	7.05	6.96	6.95	6.91
M_{DHFOE}	8.54	8.41	8.50	8.46	8.48
$M_{Fluorescein}$	7.66	7.58	7.68	7.55	7.42

In table 5.4. it can bee seen that esterification has an significant effect on the cross-sensitivity of the sensor. Compared with the reference membrane $M_{Fluorescein}$, consisting of the 2-fold negative charged indicator 5-(octadecanoylamino)fluorescein, embedded in hydrogel, the one-fold negative charged esters show a smaller shift of the apparent pK_a in the range from 25 mM to 500 mM.

5.4.4 Change of Sensor Signal at very low Ionic Strengths

The buffer system was changed from phosphate salts to MES, because the MES molecule carries one charge in its acidic form and is uncharged in its basic form. Therefore, the overall ionic strength can be kept very low. The sensor was calibrated in the new experimental setup with MES buffer (IS = 25 mM). Figure 5.9. shows the titration plot of the membrane.
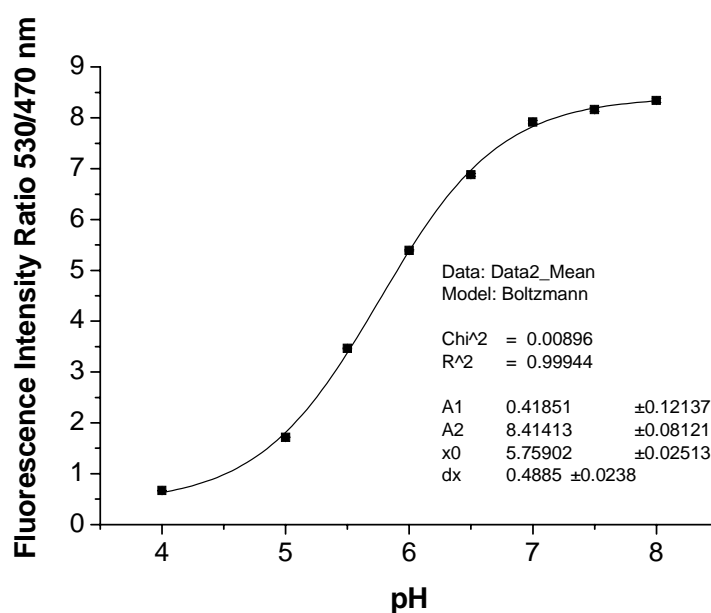
Fig. 5.9. Calibration plot of M_{DCFOE} in MES buffer (buffer capacity 2 mM, total ionic strength 25 mM).

After the calibration, the beaker was filled with MES buffer pH 5.5 (IS = 2 mM, no background salt), which is very close to the pK_a of the sensor membrane and therefore the membrane is very sensitive to changes in pH. In a time trace, the signal change of the sensor was recorded. After each addition of NaCl, the ratiometric signal increased (Figure 5.10.).
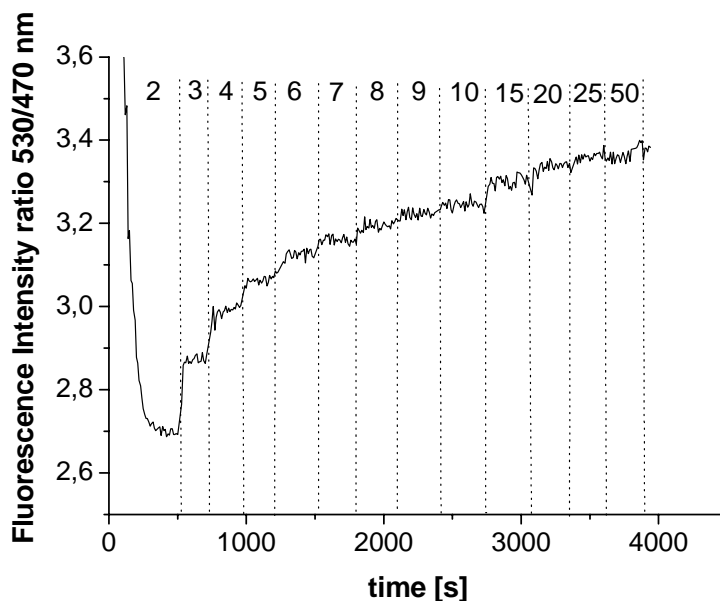
Fig. 5.10. Intensity changes of M_{DCFOE} due to addition of NaCl at pH 5.5.

By means of the Boltzmann-calibration function of 25 mM, the intensity changes were calculated into pH changes. The pH changes were set equal to shifts of the apparent pK_a, assuming that the other parameters of the calibration plot did not change. With this assumption, virtual titration plots for each ionic strength were calculated by means of an Excel sheet by taking x_0(new IS) = x_0(25 mM) for the new Boltzmann function. These virtual "calibration plots" are displayed in Figure 5.11.
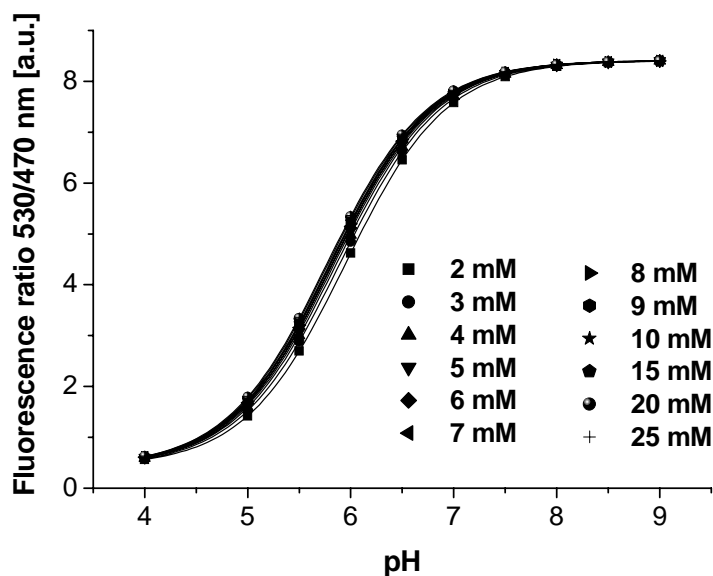
Fig. 5.11. Calculated calibration plots of M_{DCFOE} in the range from IS = 2 mM to IS = 25 mM.

Table 5.5. summarizes the intensity changes, the resulting pH changes and calculated pK_a values. It can be seen that with above mentioned assumptions, pH can be determined in the IS range from 2 mM to 25 mM with a precision of ca. 0.06 pH units when the sensor is calibrated at 25 mM.

Table 5.5. Fluorescence Intensity changes, calculated pH changes and assumed pK_a shift.

| Ionic strength [mM]	ΔIntensity	ΔpH	New apparent pK_a
2	-0,691	0,191	5,810
3	-0,500	0,135	5,764
4	-0,380	0,103	5,752
5	-0,310	0,082	5,761
6	-0,266	0,067	5,746
7	-0,228	0,060	5,769
8	-0,179	0,048	5,777
9	-0,157	0,042	5,781
10	-0,142	0,037	5,766
15	-0,071	0,021	5,740
20	-0,036	0,010	5,739
25	-0,0025	0,005	5,754

The experiments were repeated with M_{MCFOE} and M_{CHFOE} using MOPS buffer solutions of IS = 25 mM for calibration and buffer solutions of pH = 6.8 and pH = 7.2, respectively. Both membranes showed a similar small shift of calculated pK_a as listed for M_{DCFOE}. In comparison to the cross-sensitivity of water-soluble fluorescein, it can be said that the charge reduction by esterification reduced the pK shift in the range from 2 mM to 25 mM.

5.4.5. Reproducibility

To study reproducibility, 20 µL of hydrogel cocktails were pipetted into the wells of a 96-well microtiterplates. After drying, the bottoms were covered with a thin sensor film. The wells were filled with phosphate buffers of IS = 100 mM. For the membranes M_{DCFOE}, M_{MCFOE} and M_{CHFOE} the relative standard deviations (RSDs) of the pK_a values were less then 1.3 % for a set of four membranes (Table 4). Mean pK_a values, the standard deviations and RSDs are listed in Table 5.6. A maximum deviation of 1.22% is very good and therefore the sensor membranes are highly reproducible.

Table 5.6. Relative standard deviation of the pK_a Value for four patches of each sensor.

Membrane	Mean pK_a	S.D.	Relative S.D. [%]
M_{DCFOE}	5.54	0.07	1.22
M_{MCFOE}	6.97	0.02	0.29
M_{CHFOE}	7.28	0.02	0.27

5.4.6. Effect of proteins

Proteins and other macromolecules present in the analyte solution can affect the sensor membrane in two ways. First, proteins can bind indicators through their basic or acidic groups. Thereby, the indicator is extracted and leaches out of the membrane surface and the absorption intensity of the sensor decreases. Second, in case of a charged polymer a protein can be adsorbed to the surface of a membrane. This results in a change of (a) the microenvironment of the indicator at the membrane-bulk interphase, (b) the surface potential, and (c) of the apparent pK_a, respectively.

In order to study these phenomena, absorption spectra of the sensor membranes were recorded at pH 9.0 before and after storage for one week in phosphate buffer of pH 7.3 containing 3.8% (m/m) of BSA, which is a typical protein concentration in culture media used for biotechnical applications[23]. The changes in the absorption spectra of each membrane are listed in Table 5.5. It is found that the chromophores of higher lipophilicity (M_{CHFOE}, M_{DHFOE}) are less easily washed-out than the chlorinated derivatives in membranes (M_{DCFOE}, M_{MCFOE}). The maximum loss in absorption within one week was 5.2 % for membrane M_{DCFOE}. M_{DCFOE} was calibrated with phosphate buffers of IS = 100 mM again to obtain the pK_a shift caused by possible protein adsorption and gave an apparent pK_a of 5.49, indicating a pK_a shift of 0.05 pH units compared to the results given in Table 5.8.

Table 5.7. Absorption changes before and after storage in a solution of bovine serum albumin.

Membran	Absorption		Signal change
	before storage	after storage	$SC = (A_1-A_2)/A_2$ [%]
	A_1	A_2	
M_{DCFOE}	0.410	0.389	5.12
M_{MCFOE}	0.213	0.205	3.75
M_{CHFOE}	0.222	0.216	3.50
M_{DHFOE}	0.118	0.114	3.38

5.4.7. Sensor Stability

In order to test the sensor stability, two sensor foils based M_{DCFOE} were stored for 14 days at 30° C in the dark. One of the sensor foils (**#1**) was stored under dry conditions, the second one (**#2**) was stored in 100 mL of buffer PBS pH 7.0.

After 14 days, the sensor foils were characterized again under analogous conditions. Both sensors showed only a marginal effect of ionic strength on the signal, but the intensity ratio of sensor #1 decreased by 12% while sensor #2 showed no noticeable loss of intensity ratio. It seems to be superior to store the sensor foils in aqueous solution. The following table 5.8. compares the pK_a value before and after storage.

Table 5.8. pK_a of sensor foil #2 before and after storage in buffer PBS 7.0

Ionic strength [mM]	Sensors system 3 sensor (before storage)	Sensors system 3 (after aqueous storage)
25	5,52	5,56
50	5,60	5,62
100	5,56	5,56
200	5,45	5,59
500	5,52	5,47

Obviously, there is no significant pK_a change. It seems that the two-wavelength ratiometric method delivers stable signals, but it has to be mentioned that after storage the single emission intensities at 550 nm decreased by 25% when the sensor was excited at 530 nm and 470 nm. Figures 5.12. and 5.13. show the time traces of M_{DCFOE} before and after storage using buffers with a total ionic strength of 25 mM.
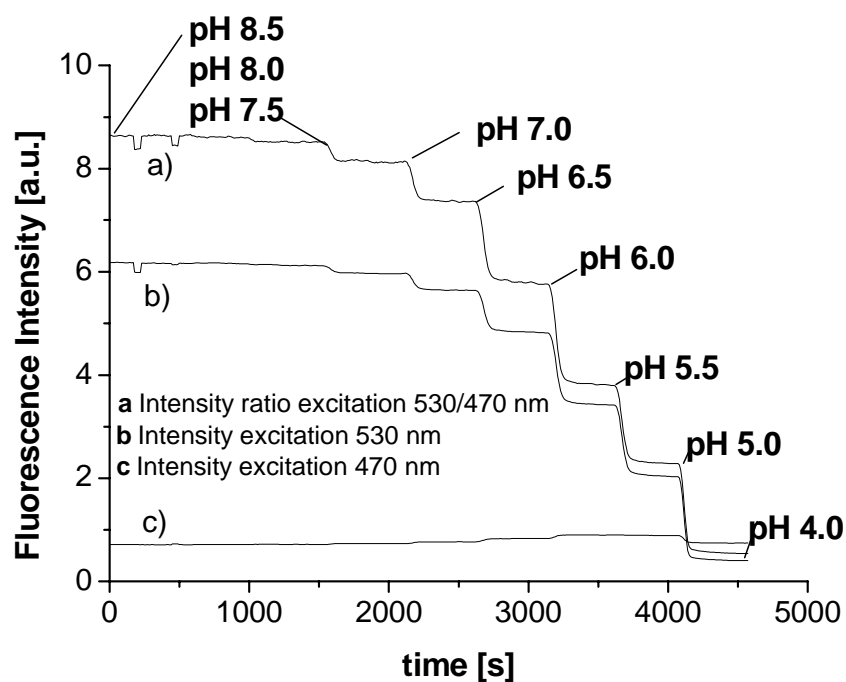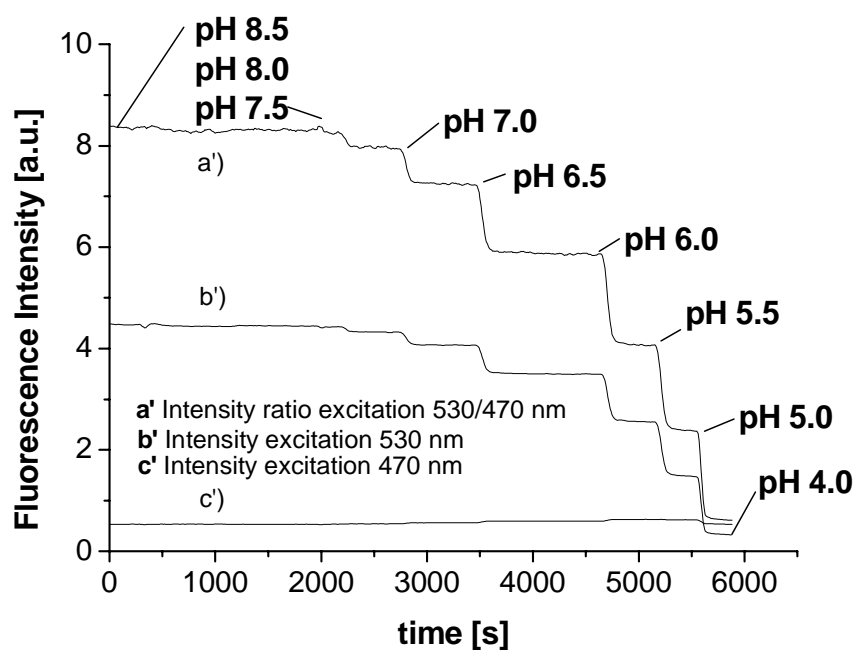
Fig. 5.12. Time trace before storage

Fig. 5.13. Time trace after storage

Figures 5.12. and 5.13. show that the intensity plots b) and c) are definitely higher than b')
and c') but the two ratios a) and a') only differ by a maximum of 3% from each other. It is

obvious that in the case of two-wavelength measurement the received signal is independent of dye concentration, dye leaching/bleaching and LED drifts.

5.4.8. Effect of Temperature

The color of many indicators depends on the temperature. This is mainly due to the fact that the ion product of water changes significantly with temperature. The second source for the observed temperature coefficient is the shift of the pK_a of the indicator itself. It is difficult to separate the temperature coefficient of the ion product of water and that of the dissociation constant (or pK_a) of the indicator.

In order to investigate the effect of temperature on the sensor M_{MCFOE}, sensor cocktails of defined concentrations, were deposited on the bottom of microtiterplates. These plates were dried on air at ambient temperature and used in a microtiterplate reader. For these experiments, readers are advantageous because the temperature in the reader can be easily controlled and kept constant. On the other side it is disadvantageous that optical readers use filters instead of monochromators. Therefore it is possible that the excitation or emission filter maxima do not exactly match the sensor excitation or emission maxima. This results in lower ratios than that measured with the flow-through cell in case of ratiometric measurements with the fluorimeter, but the turning point (=pK_a) is not affected. Fluorescence measurements in microplates were performed by means of an Ascent Fluoroscan microtiterplate reader from Labsystems (Helsinki, Finland) equipped with excitation filters at wavelengths of 460 and 530 nm and an emission filter at 570 nm. A quartz halogen lamp was used as the light source. Figure 5.14. shows the titration plots at 25 °C and 37 °C of M_{MCFOE} at IS = 100 mM.
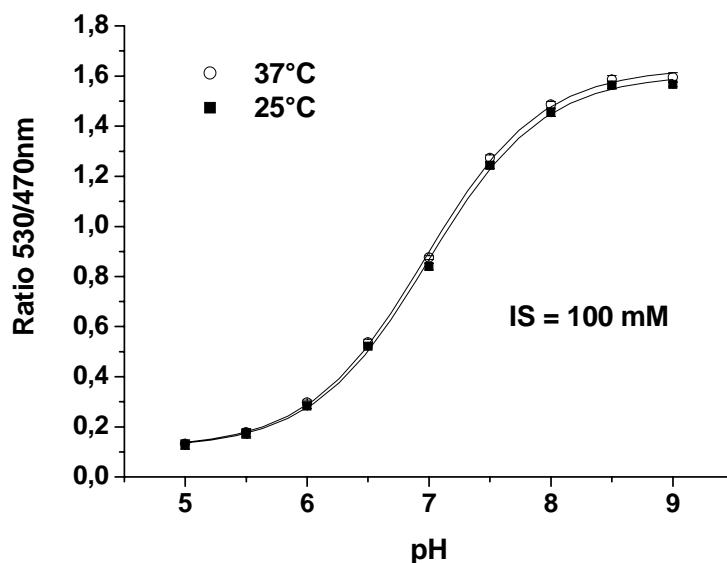
Fig. 5.14. Titration plots of sensor M_{MCFOE} at constant ionic strength and varying temperature.

Due to the fact that the phosphate buffer changes its pH with rising temperature by -0.0028 pH units per ^{o}C in the physiological range, the temperature effect in Fig. 5.10. is not only caused by the sensor. The difference in temperature between both measurements is 12 °C. Therefore, at 37 °C the pH should be 0.03 pH units lower than for 25 °C. In order to compare the sensor performance at both temperatures, the pH must be corrected for the higher temperature. Fig. 5.15. shows the corrected titration plots for both temperatures.
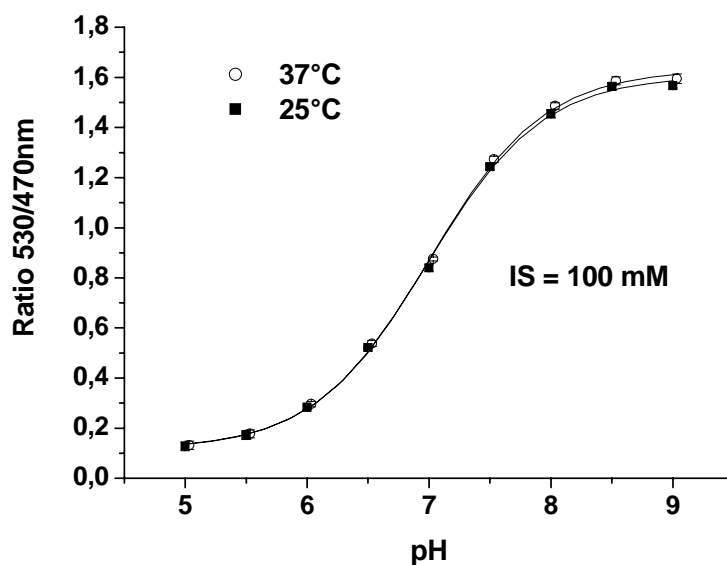

Fig. 5.15. Corrected titration plots of sensor M_{MCFOE} at constant ionic strength and varying temperature (corrections were made for 37 °C).

Obviously, there is only a negligible effect of temperature on the sensor system. The pH error caused by temperature change from 37 °C to 25 °C was calculated to be less than 0.1 pH units. The experiment was repeated for the sensor membranes M_{CHFOE}, M_{DCFOE}, and M_{DHFOE}. For all membranes no noticeable temperature effect of the sensor on the signal was found.

5.4.9. Response time

In order to determine the t_{100}-time of the sensor, a M_{MCFOE} foil was implemented in a flow through cell. The analyte solution in the cell was changed from pH 8.0 to pH 6.0 by means of the peristaltic pump. The fluid quantity was changed stepwise from 1 mL/min to the maximum of 5 mL/min. Table 5.9. shows the corresponding response times.

Table 5.9. Response time of M_{MCFOE} in dependence of analyte flow rate.

Fluid Quantity [ml/min]	Response time [s]
1	90
2	50
5	40

The response times are faster in reality since the cells used have a dead volume that is replaced in about 20 s. The real response time was determined via a reciprocal plot 1/(fluid quantity) (fq) vs. response time (rt) (Figure 5.16.).
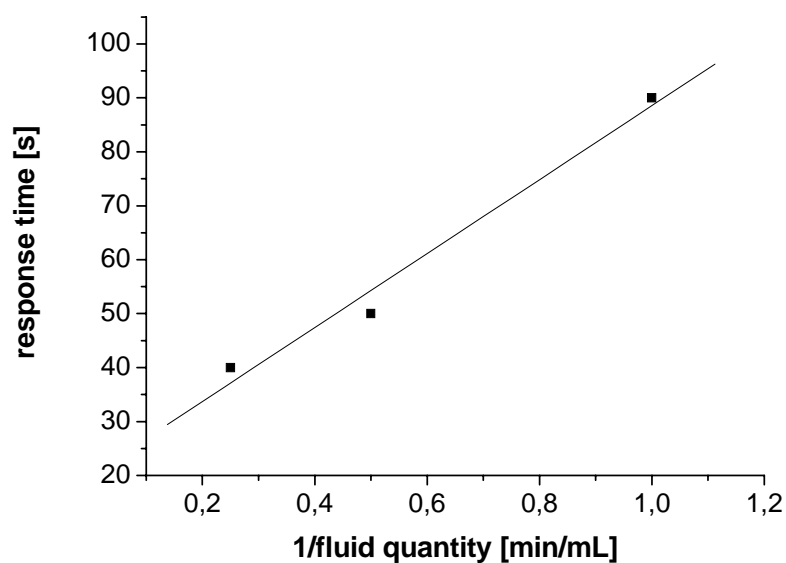

Fig. 5.16. Linear plot 1/fluid quantity vs. response time

The plot was best fitted by the following equation: rt = 20 + 60.57*fq. Thus, it is obvious that the response time for higher fluid quantities is 20 seconds.

5.4.10. Fluorescence decay times

To study the fluorescence decay time, 20 µL of hydrogel cocktails were pipetted as sensing film on the bottoms of the wells of a microtiterplate (as described above). After drying, wells were filled with phosphate buffers (IS = 100 mM) of pH 10.0 and pH 4.0. The membranes were excited at 488 nm (the isosbestic wavelength) and emission was collected at 535 nm with the IOM device. It can be seen that all four fluoresceins have decay times between 4 and 5 ns in both, the acidic and basic form. The decay times for basic and acidic form of each membrane are given in Table 5.10.

Table 5.10. Fluorescence Decay Times

Membrane	Fluorescence Decay Time [ns]	
	pH 4.0	pH 10.0
M_{DCFOE}	4.49	4.20
M_{MCFOE}	4.64	4.24
M_{CHFOE}	4.93	4.39
M_{DHFOE}	4.46	3.98

5.4.11. Photostability

The photostability of the membranes has been tested via two different methods: Firstly, the membrane was tested under continuous wave irradiation in the flow through cell for one hour. Secondly, the membranes were fixed in the Leica DMRE Fluorescence microscope and excitation light was focussed on the membranes by means of a lense combination of 500-fold magnification. Images of the membranes were taken with a Leica digital camera DC 200 in steps of 30 seconds. The excitation light was filtered by means of 505 nm bandpass-filter; the emitted response was filtered by a 570 nm bandpass filter. For both methods, the membranes were immersed into phosphate buffer pH 10.0 to ensure that only the deprotonated form of the indicators is present in the membrane. The photostability of membranes M_{MCFOE} and M_{DCFOE} is excellent. After 1 h of continuous illumination in the fluorometer at 530 nm with bandpass settings of 4 nm (i.e. the bandpass under which most experiments were performed) using a 150 W xenon lamp, the fluorescence intensity was

reduced to 95 % and 90 %. In the same time period, the signal of the membranes M_{CHFOE} and M_{DHFOE} is reduced to 79 % and 9 %, respectively. These signal losses do not limit the operational lifetime of the sensors, because ratiometric (2-wavelength) measurements compensate these effects. A membrane containing 5-(octadecanoylamino) fluorescein was used as reference (unsubstituted fluorescein chromophore) and showed a fluorescence signal of 35 % after 3 h ($\lambda_{exc} = 500$ nm, $\lambda_{em.} = 520$ nm). The fluorescein chromophore has a limited photostability and suffers from an irreversible photobleaching process, but the experiment showed that replacing one hydrogen atom by a chloro substituent does significantly increase photostability. Figure 5.17. shows the decay of fluorescence intensity of all membranes with time.
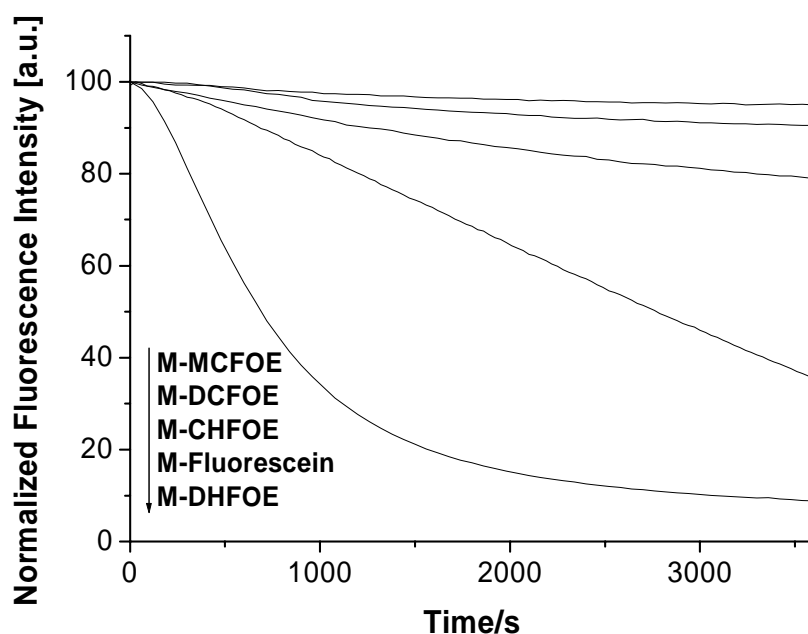
Fig. 5.17. Decay of fluorescence intensity for all membranes. Reference membrane contains a lipophilic
fluorescein derivative without substituents.

Figure 5.18. shows the images of the membranes, taken with the camera attached to the fluorescence microscope. Due to the fact that the light is focussed on a smaller area of the membrane, the indicator fades to black much faster compared to the experiments in the flow-through cell. The first picture in each column shows a 50-fold magnification, wherein the black spot is the irradiated area. The bleaching curves in Figure 5.20. were created from the data in Fig. 5.19. The intensity of each picture was estimated by calculating the mean value of the red channel taken from the overall luminosity of the picture. The values were calculated by Adobe's Photoshop 6.0 using the picture histogram.

Fig. 5.18. Images of all membranes when implemented in the fluorescence microscope using 500-fold magnification. Images were taken in 30 s steps. For the first pictures in each column magnification was reduced to 50-fold.

Figure 5.19. shows the calculated intensities of the microscope images. Although, the bleaching time is different compared to the flow-through cell experiment due to different experimental set-up, light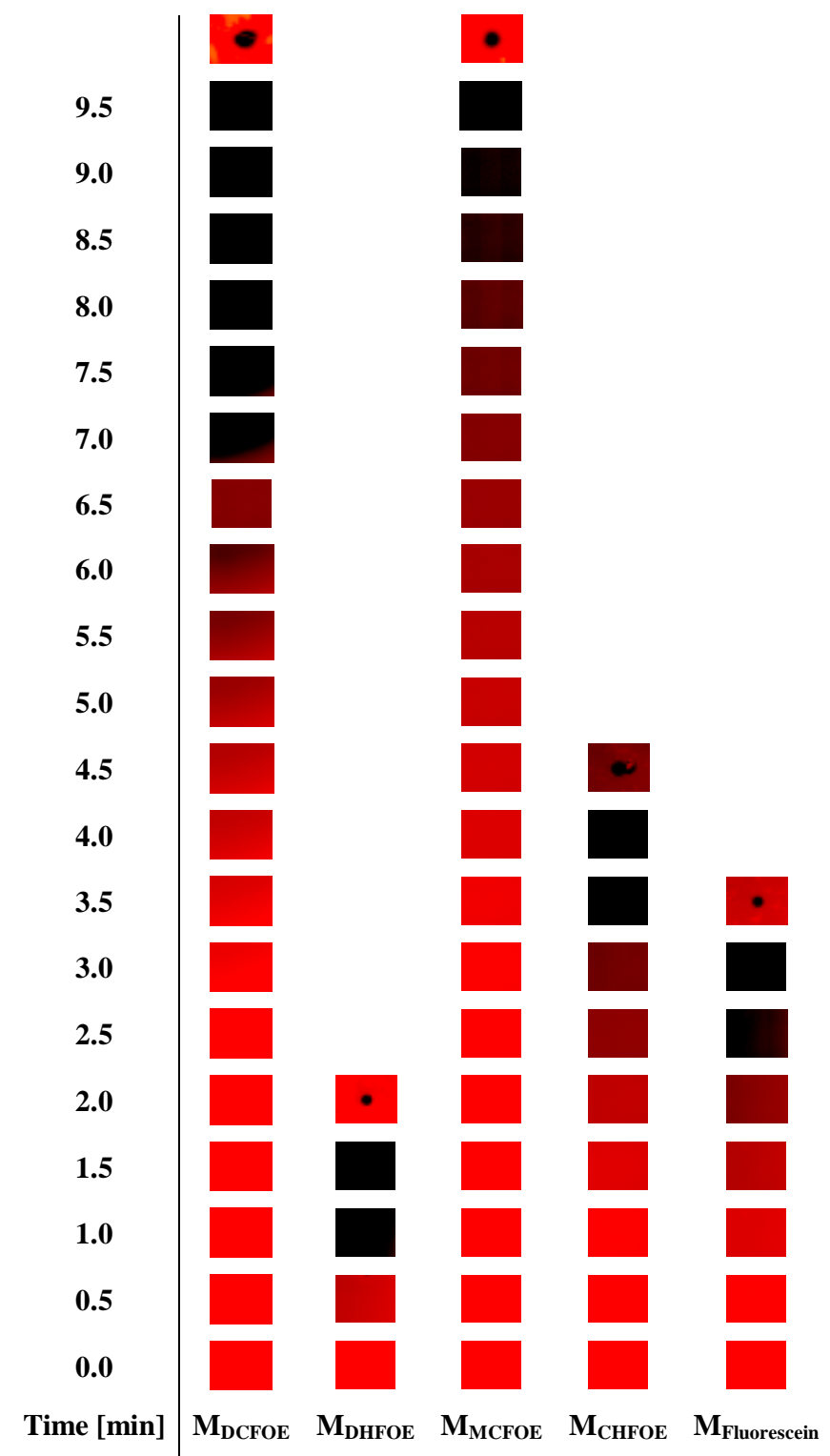 source and intensity of excitation light, the indicators show the same trend: The halogenated chromophores are much more photostable than the unsubstituted fluorescein. In case of M_{MCFOE} and M_{DCFOE}, it takes more than double the time to completely bleach the fluorophore. There, these sensors are very suitable for applications in fluorescence microscopy using high magnifications.
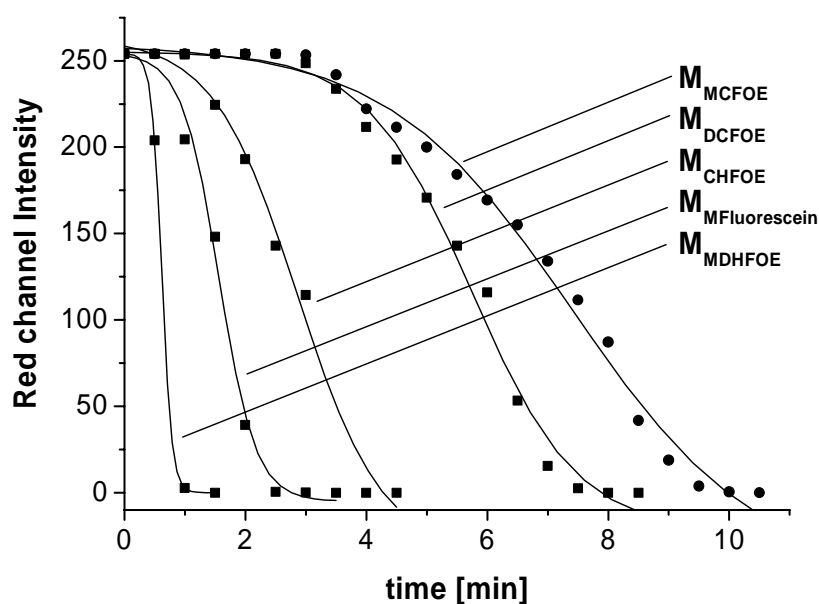
Fig. 5.19. Bleaching curves calculated from the intensities of fluorescence images shown in Fig. 5.15.

5.4.12. Sensor with enlarged dynamic range

Optical sensors have dynamic ranges usually not exceeding 3 pH units. Attempts have been made to extend the dynamic range of measurements in aqueous solutions using multiple pH indicators, or one indicator with multiple steps of indicator dissociation[24-26]. An optical pH sensor for the pH 0.5-13.5 working range was reported by Vishnoi et al[27]. The sensor is based on absorption dyes immobilized on ion exchanger IRA 400, placed in a PVC membrane. The sensor shows a linear response in the range from 0.5 to 13.5. On changing the ionic strength of the sample to 1 M, the calibration plot of the sensor is strongly bended and causes an error of approximately 4 pH units in the worst case. Lin et al.[28] reported a sensor wherein three indicators are entrapped in a sol-gel matrix to result in a sensor with a linear response between pH 6.3-9.8. The effect of ionic strength was not discussed. In most applications, such a broad dynamic range is not necessary. For

biotechnological applications, a dynamic range from 8.0 to 5.5 is adequate.

We have made a wide-range sensor by mixing the indicators DCFOE and CHFOE in equimolar ratios. The titration plot of membrane M_{HYBRID} is shown in Figure 5.20. Compared to the single-dye based membranes, M_{HYBRID} has a dynamic range that extends from pH 4.5 to 8.5. The low cross-sensitivity to IS is maintained in this sensor and the maximum errror is 0.1 pH units on varying ionic strength from 25 to 500 mM.
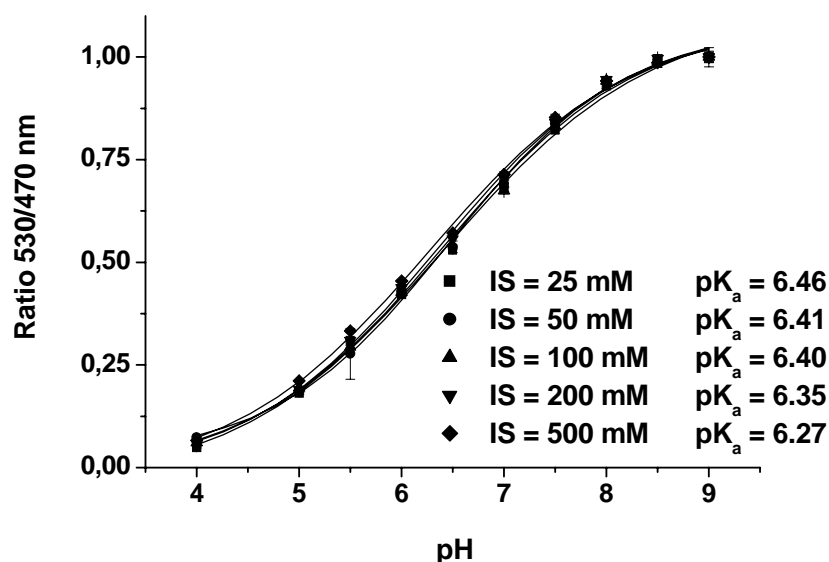
Fig. 5.20. Calibration curves of membrane M_{HYBRID} at ionic strength from 25 to 500 mM.

The sensor has on decisive drawback: The photostability of the two indicators are different and therefore the sensor calibration will alter due to different bleaching rates, when the sensor is used frequently under continuous wave irradiation. But it is useful for one-way usage or applications with pulsed excitation sources.

5.5. Applications

5.5.1. Determination of Blood Plasma pH

The blood volume of an adult human comprises 6 to 8 % of the body weight; 1 L of blood contains about 0.46 L red blood cells (erythrocytes) in males, 0.41 L in females. This value, which may also be expressed as a percentage (46 % in males), is called the hematocrit. Plasma is what is left after the cellular components have been centrifuged off.

Plasma consists of water in which high molecular proteins (6.5 to 8.0 %), low molecular weight uncharged molecules (glucose, urea, etc.) and ions are dissolved.

The balance of electrolytes is in close connection with the aqueous status of the human organism. If the composition of electrolytes is altered, the concentration of the other ions will deviate in a way that the total concentration of cations and the total concentration of anions will remain unchanged. Therefore, the status of electroneutrality will be preserved. Such changes always cause a change in the pH value of blood which will be compensated by the buffer systems in the blood as long as the buffer capacity of the blood is not exceeded. Normally, the electrolyte balance is regulated in a way that the pH will have a value of 7.40. Deviations may lead to alkalosis (pH > 7.40) or acidosis (pH < 7.40)[29].

Membrane M_{CHFOE} has an apparent pK_a of ca. 7.2. Therefore the sensor is suitable to determine the pH in plasma. The electrolytes of clinical importance in plasma are summarized in Table 5.11.

Table 5.11. Cations and Anions present in blood plasma of a human organism.

Cations	c_{Cation} *[mM]*	*Anions*	c_{Anion} *[mM]*
Sodium	150	Chloride	110
Potassium	10	Bicarbonate	30
Calcium	~ 5	Proteins	15
Magnesium	~ 5	inorg. Phosphate	~ 5
Hydrogen Ion	n.d.	Sulphate	~ 5
		Organic acids	~ 5

After calibration of the membrane M_{CHFOE} in the flow through cell with MOPS buffer solutions (IS = 150 mM, c_{MOPS} = 10 mM), the sensor was tested with nine different buffer solutions. While the pH and ionic strength were set to 7.3 and 150 mM (NaCl), respectively, different amounts of salts were added in the concentration described in Table 5.11. The last buffer solution contained all ingredients and was regarded as a kind of synthetic plasma solution. The time trace is shown in Fig. 5.21. There are three noticeable facts: First, there were no strong signal changes, when the electrolyte was changed to bivalent chloride salts. Therefore, the very good sensor performance regarding ionic strength effects is not affected when the background electrolyte is changed. Second, when the $MgCl_2$-buffer solution is replaced by the $NaHCO_3$-buffer or NaH_2PO_4 solution, two solutions with different pH, the response time is very fast. This is a critical point for sensors, especially for medical sensors. Thirdly, during the complete time trace, including the measurements for BSA and synthetic plasma, no wash-out effects were observed.

Therefore, the sensor is suitable for clinical or bioanalytical applications, because sensor components do not contaminate the sample solution. Regarding the signal for excitation at 470 nm, it can be said that changes of the background electrolytes do not change the reference signal.
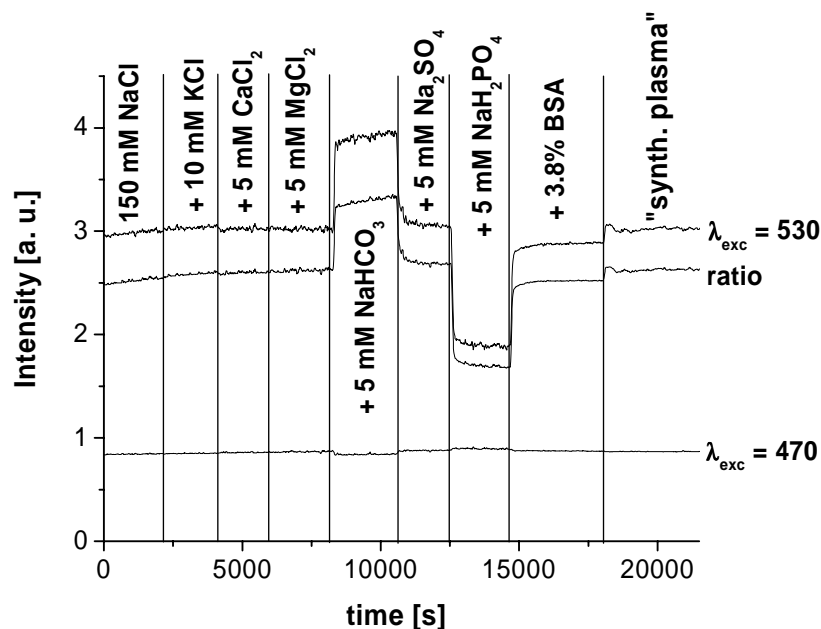
Fig. 5.21. Time trace of M_{CHFOE} with different background electrolytes contained in plasma, BSA and "synthetic plasma".

After each solution, the pH was controlled by the pH meter. Table 5.12. gives a comparison between the electrochemically and the optical determined pH. One can see, the measurements do not differ very much, except for the last buffer ("plasma"). This could be explained by absorption of protein on the sensor element, neither if it is an electrode or an optode. This "additional" layer alters the surface potential of the sensor element.

Table 5.12. Comparison of pH measurements in plasma by electrode and M_{CHFOE}.

Background	pH (optical)	pH (electrode)	ΔpH
150 mM NaCl	7.27	7.31	0.04
10 mM KCl	7.29	7.31	0.02
5 mM CaCl$_2$	7.27	7.32	0.05
5 mM MgCl$_2$	7.28	7.29	0.01
5 mM NaHCO$_3$	7.72	7.65	0.07
5 mM NaSO$_4$	7.28	7.28	0.00
5 mM NaH$_2$PO$_4$	6.78	6.77	0.01
3.8% BSA	7.23	7.22	0.01
synthetic plasma	7.33	7.22	0.11

5.5.2. Measurement of Enzyme Kinetics

The measurement of enzyme kinetics is another field of application for optical pH sensors. Microtiterplates with integrated pH sensors have been used to characterize the enzyme kinetic of glucose oxidase for the conversion from glucose to glucose-δ-lactone[30]. The effect of heavy metal ions as inhibitors for enzyme reactions was determined by means of optical pH sensors in cuvettes[31, 32]. In this paragraph, the membrane M_{HYBRID} was used to monitor the enzymatic cleavage of urea into carbon dioxide and ammonia by the enzyme urease (E.C.-Nr. 3.1.1.5.) according to the method described in ref.[33]. Membrane M_{HYBRID} was chosen due to its extended pH range and the minimal pH error caused by IS. Due to the formation of two molecules of ammonia and subsequent formation of OH^- ions (Scheme 5.3.) the pH changes during the reaction.

$$H_2N-\underset{\displaystyle O}{\overset{\displaystyle \|}{C}}-NH_2 \;+\; H_2O \;\xrightarrow{\text{urease}}\; 2\,NH_3 \;+\; CO_2$$

$$NH_3 \;+\; H_2O \;\rightleftharpoons\; NH_4^+ \;+\; OH^-$$
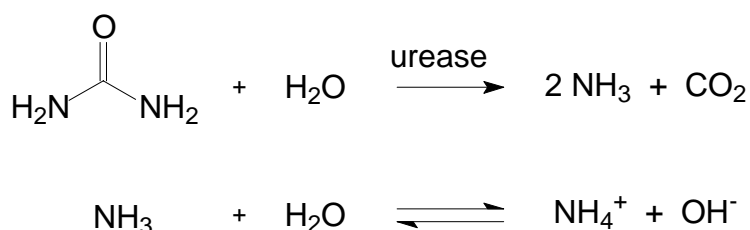
Scheme 5.3. Urease-catalysed cleavage of urea.

The bottoms of a 96-well microtiterplate were coated with a 2 mm/kg M_{HYBRID}-cocktail. The wells were filled with 100 µL urea solution (c = 5 mM, in 10 mM TRIS, 100 mM NaCl, pH 5.5). A stock solution of urease was prepared by dissolving 50 mg enzyme in 100 mL water. Three dilutions were obtained by diluting (v/v) 1:10, 1:100, and 1:200. Using to the manufacturer's specification, the activities of the three dilutions in 100 µL were calculated to be 0.051 U, 0.0051 U, and 0.0025 U. The measurement was started immediately after filling of the wells and interrupted after 5 minutes to add 10 µL of urease solution. Instead of phosphate buffers, TRIS buffer solutions were used because phosphate acts as an inhibitor for urease-catalysed reactions[34]. The analysis was repeated for each solution. The enzymatic reactions were pursued over 65 minutes (see Figure 5.22.).
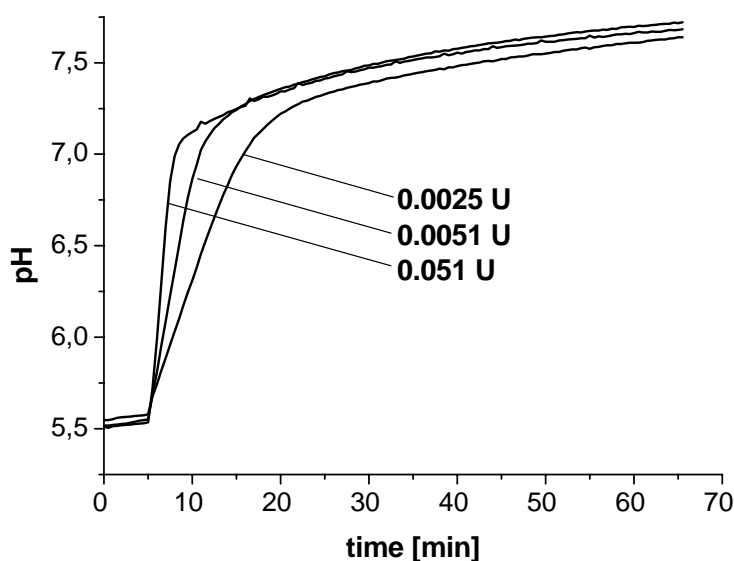
Fig. 5.22. Measurement of enzyme kinetic of urease by means of M_{HYBRID}, which was coated on the bottom of microtiterplates.

Fig. 5.22. shows the measurements for different amounts of enzyme. While the reaction times after addition of urease are very fast, a sensor with short response time is needed. The sensors based on lipophilic fluorescein ester fulfill this requirement. In this example, the extended measurement range of M_{HYBRID} is not fully used, but it may be important and useful, when the starting concentration of urea is increased (or unknown) and more ammonia molecules are released. Although, the enzymatic cleavage of urea was not completed after 65 min, because the fluorescence signal was still increasing, the principle that sensors based on lipophilic fluorescein ester embedded in MTPs, can be used to monitor enzyme reactions, has been proven.

5.6. Conclusion

New symmetrical and unsymmetrical derivatives of fluorescein were prepared in satisfactory yield. The results presented here clearly demonstrate that lipophilic esters of 2',7'-substituted fluoresceins can be used as pH-sensitive dyes in thin sensor membranes. Substitution of at least one hydrogen atom by chlorine in 2'-and 7'- position results in highly photostable chromophores.

The membranes can be prepared in a simple and reproducible way and show an extraordinarily low cross-sensitivity towards changes in ionic strength. The simplicity in

membrane preparation allows combinations of several indicators in one sensor without the need for covalent immobilization of indicator dyes.

The membranes can be used for bioanaylitcal applications, because the stability of the membranes towards wash-out was tested. The long-term stability is prolonged by the ratiometric measurement which compensates aging effects of the membranes.

5.7. References

1.   T. E. Edmonds, N. J. Flatters, C. F. Jones, J. N. Miller, **Determination of pH with acid-base indicators: implications for optical fiber probes,** Talanta, **1988**, 35(2), 103-107.

2.   N. Opitz, D. W. Luebbers, **New fluorescence photometrical techniques for simultaneous and continuous measurements of ionic strength and hydrogen ion activities,** Sens. Actuat., **1983**, 4(3), 473-479.

3.   O. S. Wolfbeis, H. Offenbacher, **Fluorescence sensor for monitoring ionic strength and physiological pH values**, Sens. Actuat., **1986**, 9(1), 85-91.

4.   J. Janata, **Do Optical Sensors Really Measure pH,** Anal. Chem., **1987**, 59, 1351.

5.   J. Janata, **Ion Optodes,** Anal. Chem., **1992**, 64, 921A-927A.

6.   P. G. Seybold, M. Gouterman, J. Callis, **Calorimetric, photometric and lifetime determinations of fluorescence yields of fluorescein dyes**, Photochem. Potobiol., **1969**, 9(3), 229-242.

7.   G. A. Crosby, J. N. Demas, **Measurement of photoluminescence quantum yields. Review,** J. Phys. Chem., **1971**, 75(8), 991-1024.

8.   T. Matray, V. Hernandez, S. Singh, **Electrophoretic tag reagents comprising fluorescent compounds,** U.S. Pat. Appl. Publ. 2002146726, **2002**.

9.   E. Wang, G. Wang, L. Ma, C. M. Stivanello, S. Lam, H. Patel, **Optical films for protamine detection with lipophilic dichlorofluorescein derivatives,** Anal. Chim. Acta, **1996**, 334(1-2), 139-147.

10. W. M. Fabian, S. Schuppler, O. S. Wolfbeis, **Effects of annulation on absorption and fluorescence characteristics of fluorescein derivatives: a computational study,** J. Chem. Soc. Perkin Trans. 2, **1996**, 5, 853-856.

11. W. C. Sun, K. R. Gee, D. H. Klaubert, R. P. Haugland, **Synthesis of fluorinated fluoresceins,** J. Org. Chem., **1997**, 62(19), 6469-6475.

12. J. J. Yang, D. Su, A. Vij, T. L. Hubler, R. L. Kirchmeier, J. M. Shreeve, **Synthesis of 4-fluororesorcinol and 4-trifluoromethylresorcinol,** Heteroat. Chem., **1998**, 9(2), 229-239.

13. G. S. Lal, G. P. Pez, R. G. Syvret, **Electrophilic NF Fluorinating Agents,** Chem. Rev., **1996**, 96(5), 1737-1755.

14. G. S. Lal, **Site-selective fluorination of organic compounds using 1-alkyl-4-fluoro-1,4-diazabicyclo[2.2.2]octane salts (selectfluor reagents),** J. Org. Chem., **1993**, 58(10), 2791-2796.

15. T. Umemoto, M. Nagayoshi, K. Adachi, G. Tomizawa, **Synthesis, Properties, and Reactivity of N,N'-Difluorobipyridinium and Related Salts and Their Applications as Reactive and Easy-To-Handle Electrophilic Fluorinating Agents with High Effective Fluorine Content,** J. Org. Chem., **1998**, 63(10), 3379-3385.

16. C. Huber, T. Werner, C. Krause, O. S. Wolfbeis, **Novel chloride-selective optode based on polymer-stabilised emulsions doped with a lipophilic fluorescent polarity-sensitive dye,** Analyst, **1999**, 124(11), 1617-1622.

17. C. Huber, I. Klimant, C. Krause, T. Werner, O. S. Wolfbeis, **Nitrate-selective optical sensor applying a lipophilic fluorescent potential-sensitive dye,** Anal. Chim. Acta, **2001**, 449(1-2), 81-93.

18. T. Werner, C. Huber, S. Heinl, M. Kollmannsberger, J. Daub, O. S. Wolfbeis, **Novel optical pH-sensor based on a boradiaza-indacene derivative,** Fresenius' J. Anal. Chem., **1997**, 359(2), 150-154.

19. C. Krause, T. Werner, C. Huber, O. S. Wolfbeis, **Emulsion-Based Fluorosensors for Potassium Featuring Improved Stability and Signal Change,** Anal. Chem., **1999**, 71(23), 5304-5308.

20. C. Krause, T. Werner, C. Huber, O. S. Wolfbeis, M. J. P. Leiner, **pH-Insensitive Ion Selective Optode: A Coextraction-Based Sensor for Potassium Ions,** Anal. Chem., **1999**, 71(8), 1544-1548.

21. N. A. Peppas, **Preparation, Methods & Structures of Hydrogels**, CRC Press, Boca Raton, **1986**.

22. E. Wang, C. Romero, D. Santiago, V. Syntilas, **Optical anion sensing characteristics of indium-porphyrin and lipophilic dichlorofluorescein doped polymer films,** Anal. Chim. Acta, **2001**, 433(1), 89-95.

23. A. Doyle and J. B. Griffiths, **Cell and Tissue Culture for Medical Research**, VCH Wiley, **2001**.

24. O. S. Wolfbeis, H. Marhold, **A new group of fluorescent pH-indicators for an extended pH-range,** Fresenius' J. Anal. Chem., **1987**, 327(3-4), 347-350.

25. S. Tucker, R. Robinson, C. Keane, M. Boff, M. Zenko, S. Batish, K. W. Street, **Colorimetric determination of pH,** J. Chem. Educ., **1989**, 66(9), 769-771.

26. S. S. Besar, S. W. Kelly, P. A. Greenhalgh, **Simple fibre optic spectrophoto-metric cell for pH determination,** J. Biomed. Eng., **1989**, 11(2), 151-156.

27. G. Vishnoi, T. C. Goel, P. K. C. Pillai, **A pH-optrode for the complete working range,** Proc. SPIE-Int. Soc. Opt. Eng., **1999**, 3538, 319-325.

28. J. Lin, D. Liu, **An optical pH sensor with a linear response over a broad range.** Anal. Chim. Acta, **2000**, 408(1-2), 49-55.

29. Brochure "Physiology" from AVL Medical Instruments, Reference No. DOC11.002.A, **1994.**

30. S. A. Piletsky, T. L. Panasyuk, E. V. Piletskaya, T. A. Sergeeva, A. V. Elkaya, E. Pringsheim, O. S. Wolfbeis, **Polyaniline-Coated Microtiter Plates for Use in Longwave Optical Bioassays**, Fresenius' J. Anal. Chem., **2000**, 366, 807-810.

31. C. Preininger, O. S. Wolfbeis, **Disposable Cuvette test with Integrated Sensor Layer for Enzymatic Determination of Heavy Metals**, Biosensors & Bioelectronics, **1996**, 11 (10), 981-990.

32. R. Koncki, O.S. Wolfbeis, **Composite Films ofPrussian Blue and N- Substituted Polypyrroles: Covalent Immobilization of Enzymes and Application to Near-Infrared Optical Biosensing**, Biosensors & Bioelectron., **1999**, 14, 87-92.

33. S. Arain, **Mikrotiterplatten mit integrierten optischen Chemosensoren**, Diploma thesis, University of Regensburg, **2001**.

34. D. Schomburg, M. Salzmann, **Enyzyme Handbook: Class 3: Hydrolases, 4**, Springer Verlag, Berlin, Heidelberg, **1991**.

Chapter 6

Dual Lifetime Referenced (DLR) Optical Sensor Membranes for the Determination of pH

This chapter describes the application of a new scheme to reference the fluorescence intensity of a pH-sensitive membrane. It is based on the conversion of the fluorescence intensity information into a phase-shift. A phosphorescent dye is added in the form particles to the sample. Both, the reference dye and the pH indicator are excited simultaneously by a blue-green LED, and an overall luminescence is measured. The two dyes have different fluorescence decay times, whereas the reference dye decays in µs. Therefore, the phase shift of the overall luminescence can be detected in the µs-domain, which eases the experimental set-up of the detection device.

6.1. Introduction

Fluorescence intensity is the most widely used parameter in bioanalytical assays and fluorescent sensing applications. According to Parker's law[1], fluorescence F is defined as

$$F = I_0 \cdot \varepsilon \cdot c \cdot d \cdot QY \cdot k \qquad (6\text{-}1)$$

where I_0 is the intensity of the excitation light, ε is the extinction coefficient of the fluorescent species, c is the concentration of the fluorescent species, d is the light pathway, QY is the quantum yield of the fluorescent species (0 - 1), and k is a geometric constant, depending on the geometry of the measurement set-up.

It is obvious that F is not an absolute magnitude. It is not only dependent on sensor specific parameters (ε, c, d, QY); but also on device-specific parameters (I_0, k). In order to ease reproducibility of experimental data, a referenced signal is preferred.

Drifts of the optoelectronic system, variable sample turbidity and color, and the effect of external quenchers are additional factors that affect fluorescence intensity. Sensors can be internally referenced by making use of ratiometric measurement, i. e., by rationing the intensities at two wavelengths. This approach is widely used, for example in calcium

assays using fluorophores displaying two excitation bands or two emission bands[2].

Alternatively, an inert fluorophore may be added with spectral properties different from those of the indicator. Again, rationing the intensities at two excitation or emission wavelengths results in a referenced parameter. The disadvantages of this method include the need for two separate optical channels, thus complicating the optical setup. For example, the drift in the sensitivity of both channels can be different, as can be the intensities at two excitation wavelengths. Light scatter and signal loss caused by fiber bending (e.g., in fiber optic sensors or certain microtiter plate readers) further contribute to effects not compensated for by dual-wavelength referencing.

These disadvantages of ratiometric measurements can partially be overcome by making use of the Dual Lifetime Referencing (DLR) scheme. In this scheme, the ratio of the intensities of two dyes is converted into a phase shift that depends on the differences in the decay times of the two fluorophores, namely that of the fluorescent probe (indicator; τ_{ind} ~ 5 ns) and that of an added phosphorescent reference dye (τ_{ref} ~ 6 µs), respectively[3-5]. As described in Chapter 2.2.1.2., the ratio can be determined in either the time domain or the frequency domain.

Suitable reference dyes for the DLR scheme are metal ligand complexes of ruthenium, osmium, rhenium, europium, terbium, platinum, and palladium. These metal complexes possess decay times in the microsecond or millisecond range and their luminescence usually is not affected by the analyte solution. The problem of cross-sensitivity towards oxygen quenching was solved by embedding the metal complex into nanobeads or polymers with extraordinary low oxygen permeability. In this work, the ruthenium(II)-tris-4,7-diphenyl-1,10-phenanthroline complex [(Ru(dpp)$_3$] dissolved in polyacrylnitril (PAN)-beads with diameters of 100 nm was used to convert the intensity of a carboxyfluorescein loaded PAN-polymer acting as the pH-sensitive element. Although, optical pH sensors based on HPTS as sensitive fluorophore and Ru^{2+}-PAN-beads as reference dye have been already published[6] and are now commercially available, this chapter introduces the new prototype Phase Detection Device PDD 505 from Presens Precision Company. Although, an imaging pH sensor based on fluorescein using the t-DLR scheme, has been published[7], this chapter presents a device that allows frequency domain DLR spectroscopy with fluorescein sensors and enables the use of fluorescein as short-lived fluorophores in DLR-pH-membranes. In this chapter, novel amino-modified polymers, based on polyacrylamide, were loaded with carboxyfluorescein and embedded in charge-free hydrogel, together with

phosphorent reference particle. The resulting sensors were characterized and checked on their cross-sensitivity towards IS by means of the new phase detection device PDD 505.

6.2. Material and Methods

6.2.1. Chemicals

N-(3-Dimethylaminopropyl)-N'-ethyl-carbodiimide-hydrochloride (EDC, product no. 03449) and 5(6)-carboxyfluorescein (product no. 21877) were purchased from Fluka (Buchs, Switzerland; www.fluka.com). The amino-modified polymers AA-Q-N-1, AA-Q-N-2, and GA-Q-N-1 and the Ru^{2+}(dpp)-PAN-beads PD-8 (reference beads) were a gift from Optosense (Landshut, Germany; www.optosense.de). The polymer Hydromed D4 (formerly known as Hydrogel D4) was received from Cardiotech Inc. (Woburn, MA, USA; www.cardiotech-inc.com) by request. The polyester support (product no. LS 1465585, polyethyleneterephthalat ("PET" or "Mylar") was obtained from Goodfellow (Cambridge, UK; www.goodfellow.com). Ethanol, sodium hydroxide and hydrochloric acid were also of analytical grade. Aqueous solutions were prepared from doubly distilled water.

6.2.2. Apparatus

Excitation and Emission spectra were recorded with an Aminco-Bowman Series 2 luminescence spectrometer from SLM (Rochester, NY, USA; www.thermo.com) as described in chapter 4.2.2. If not stated otherwise, measurements of time traces were performed at excitation and emission wavelengths of 500 and 530 nm, respectively. DLR measurements were performed with a phase detection device PDD 505 from Presens Precision GmbH (Regensburg, Germany; www.presens.de). The device uses a 505 nm LED for excitation and collects light at 570 nm by an optical long-pass filter. Light is modulated at 45 kHz. Figure 6.1. gives an overview on the electronic and optical components of the phase detection device.
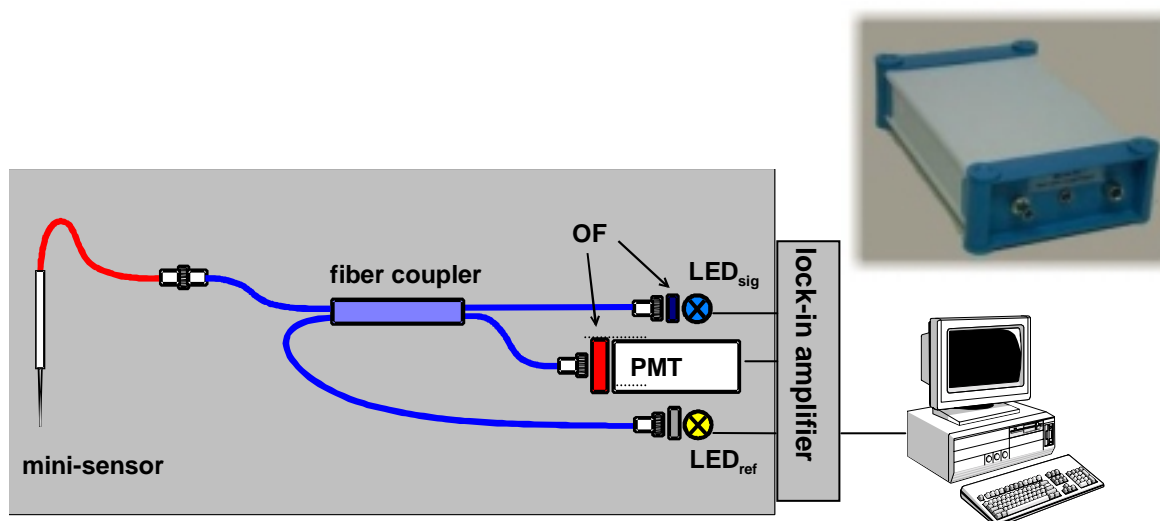
Fig. 6.1. Set-up of phase detection PDD 505 (OF = optical filter, LED_{sig} = 505 nm (blue-green)).

Insert: Picture of PDD 505.

6.2.3. Buffer preparation

Phosphate buffers of varying ionic strength in the range from 25 mM to 500 mM were prepared as described in chapter 4.2.9.

6.2.4. Determination of the Content of Amino Groups via Titration

The contents of amino groups were determined for all polymers via the following procedure:

1. 500 mg of the polymer were suspended in 20 mL of 0.001 mol / L NaOH (pH 11) for 15 minutes.
2. the polymer was removed via filtration and resuspended in deionized water (pH 7.0) for 15 minutes.
3. the polymer was removed via filtration and steps 1 and 2 were repeated two times.
4. the wet polymer was suspended in 20 mL of 0.01 HCl for 30 minutes
5. HCl solution was removed carefully via decantation and filtration and transferred quantitatively in a flask.
6. the polymer was suspended in deionized water for 30 minutes.
7. the liquid was removed and added to the HCl solution.
8. step 7 was repeated twice.
9. the concentration of the HCl solution was determined by a titration using 0.01 NaOH. pH was controlled by a pH meter.

10. the amino-loading was calculated by the consumption of NaOH.

6.2.5. Covalent Immobilization of the Indicator

1 g of the amino-modified polymer (AA-Q-N-1, AA-Q-N-2, or GA-Q-N-1, see Table 6.1.)) in 50 mL of water were reacted with 41 mg (110 µmol) 5(6)-Carboxyfluorescein in the presence of 23 mg (110 µmol) of EDC for 24 hours at pH 4.6. The dyed polymer was filtered off and washed thoroughly with water, 1 M HCl and 1 M NaOH solutions, rinsed with brine and finally treated with ethanol and ether until the filtrate was colorless. After drying overnight at a temperature of 60 °C, the colored polymer was sieved by means of a 100 nm particle sieve.

6.2.6. Membrane preparation

Hydrogel cocktails were prepared from 100 mg D4 hydrogel and 100 mg of the respective polymer in 1.08 g ethanol and 0.12 g water. The mixtures were vigorously stirred at room temperature overnight. In case of DLR membranes, 5 mg of PAN-based reference beads were added to the hydrogel cocktail. 100 µL of each cocktail were knife-coated onto dust-free, 125 µm polyester supports as shown in Figure 4.2. 120 µm spacers were used to set the thickness of the layer. Table 6.1. gives information about the membrane compositions.

Table 6.1. Membrane compositions

Membrane	polymer	m (dyed polymer) [mg] in 100 mg hydrogel
M_{PA1}	AA-Q-N-1	100
M_{PA2}	AA-Q-N-2	100
M_{GA1}	GA-Q-N-1	100
M_{DLR}	AA-Q-N-1/PD-8	100/5

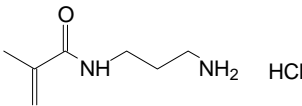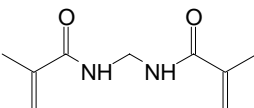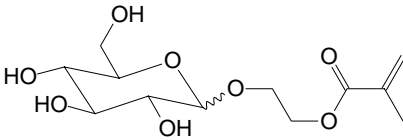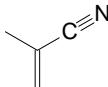## 6.3. Results and Discussion

6.3.1. Choice of materials

As discussed in chapter 4, carboxyfluorescein can be easily bound to amino groups via EDC linking. Through the covalent binding, the chromophore is not washed out and the charge of the chromophore is reduced because the charge of one carboxy group is eliminated. The reduced charge of the chromophore results in a small cross-sensitivity

towards ionic strength. Effects of IS higher than that of fluorescein are caused by charges of the matrix. Further on, the pK_a of the free dye in aqueous solution is around pH 6.4 which matches the physiological range from pH 6.5 to 7.5.

Polymers based on acrylamide (AA-Q-N-1, AA-Q-N-2) or 2-methacryloxy-ethylglucoside (GA-Q-N-1) were chosen, because they can be easily polymerized and show a high ion permeability, which is advantageous for ion or pH sensors. The aminogroups were introduced by using N-(3-Aminopropyl)acrylamid as a co-monomer. N,N'-methylene-bisacrylamid was used as cross-linker. 2-methacryloxyethylglucoside was chosen to increase the hydrophilic character of the polymer. In contrast to the celluloses described in chapter 4, the polymers contain no additional charges. The free amino groups are mainly covalently linked to carboxyfluorescein and thus "inactive". Therefore, the matrix of the sensor, consisting of the polymers and the D4 hydrogel contribute only a marginal effect to the cross-sensitivity towards IS. Therefore, the main effect is caused by the ionic pH indicator and reference additives. Table 6.2. shows the components of each polymer.

Table 6.2. Monomers and composition of amino-containing polymers.

Monomer	Structure	mass of monomer [g]		
		AA-Q-N-1	AA-Q-N-2	GA-Q-N-1
N-(3-Aminopropyl) acrylamide		0.300	0.500	0.300
N,N'-methylene-bisacrylamide		25	25	25
2-Methacryloxyethyl glucoside		---	---	25
acrylnitril		25	25	---
theor. amino content [mM/kg]		33	55	33
determined amino content [mM/kg]*		30	48	46

* via titration as previously described

It is obvious that the polymerization works reliable for the polymers with acrylnitrile as comonomer, while theoretically calculated and practically determined amount of amino groups differ significantly for the glycosidyl-modified polymer.

For application of DLR in fluorescence sensing, a reference luminophore has to be added to the sensor system. It is expected to meet the following criteria: (a) a decay time in the microsecond range, (b) spectral properties including decay time, fluorescence quantum yield and spectral shape that are not affected by the analyte and any other substances in the sample and (c) spectral match with the indicator dye.

The ruthenium complexes are particularly well established due to their high quantum yields and decay times in the lower microsecond range[8, 9]. However, their luminescence is often quenched by molecular oxygen[10] and oxidative or reductive compounds[8]. Therefore, the dyes have to be encapsulated in a material which shields it from oxygen or other potential interferents so to warrant a constant background signal. Ru(dpp) trimethylsilylpropansulfonate (Scheme 6.1.) was used as the reference luminophore due to its quantum yield of > 0.3, insolubility in water, and luminescence decay time of approximately 6 µs[9]. Ru(dpp) was dissolved in PAN beads since PAN is oxygen-impermeable.
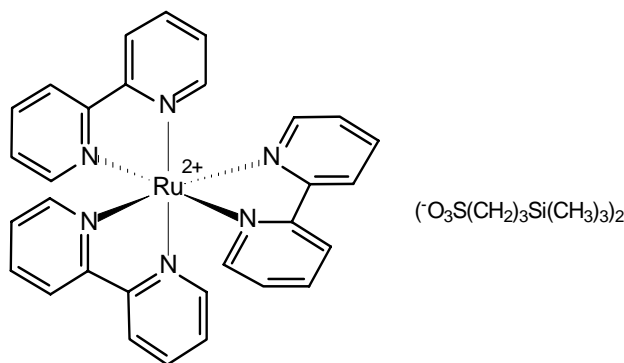
Scheme 6.1. Structure of oxygen-sensitive Ru(II)(dpp) complex (TMSPS salt)

Although a variety of fluorescent pH indicators are known[11, 13], only a few meet the following criteria that are required for the application in DLR sensors: (a) an excitation maximum beyond 450 nm to allow the use of blue LEDs as a light source that matches that of the reference luminophore, (b) a large Stokes shift, (c) high photostability, (d) fluorescence quantum yields higher than 0.5, and (e) commercial availability. HPTS was found to be the ideal indicator fulfilling all these requirements. It is commercially available and can be covalently bound to amino-modified substrates. Phase Detection devices for the

use of HPTS are already in use and commercially available. HPTS is very suitable for the DLR scheme, because its excitation maximum is at 468 nm and therefore it has a bigger overlap with the excitation spectra of the Ru^{2+}-complex than fluoresceins, which results in a stronger emission of Ru^{2+}-complex, when both dyes are excited at 470 nm. Based on the results previously described in chapter 3, HPTS is less suitable as pH indicator when special attention is given to the minimization of the cross-sensitivity towards IS. Carboxyfluorescein and fluorescein are less affected by changes in IS due to the smaller charge of the chromophore system, but these dyes can not be excited beyond 450 nm.

Using a blue-green LED (λ_{exc} = 505 nm), the intensity information of fluorescein can be converted to a phase shift information by addition of phosphorescent Ru(dpp)$_3$/PAN particles. The spectral properties of the indicator couple are shown in Figure 6.2. Both, the pH-sensitive dye carboxyfluorescein and the reference dye Ru(dpp)$_3$ can be excited by the blue-green LED while their emission spectra are quite different. However, using an appropriate long-pass filter, both signals can be detected with a single photodetector. On a change of pH, the fluorescence of the indicator decreases. Consequently, the spectral overlap of the indicator dye and the reference luminophore becomes smaller, resulting in an emission that is dominated by that of the ruthenium complex.
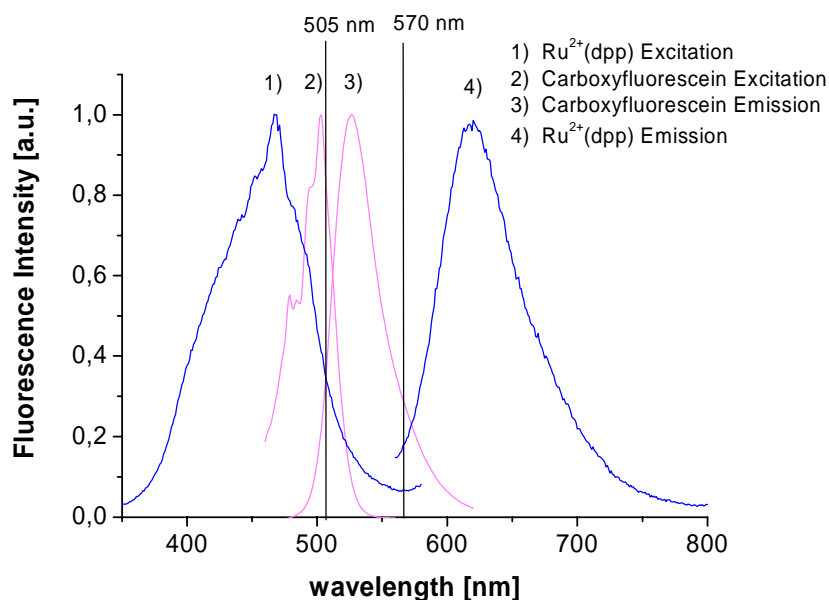
Fig. 6.2. Spectral properties of carboxyfluorescein and Ru(dpp).

6.3.2. Sensor Characteristics

Before applying the DLR scheme, all membranes were tested in a flow-through cell with respect to the response of fluorescence intensity to various pH-values ranging from 9.0 to 4.0. Ionic strength varied from 25 to 500 mM. Figure 6.3. shows the excitation and emission spectra of membrane M_{PA1} for varying pH with PBS solutions of IS = 100 mM.

Fig. 6.3. Fluorescence excitation (left; λ_{em}= 580 nm) and emission spectra (right; λ_{exc} = 480 nm) of membrane M_{PA1}.

Titration plots were determined from a series of time traces with ten seconds resolution, where fluorescence intensity depending on change of pH was measured. The response curve of membrane M_{PA1} is shown in Figure 6.4.

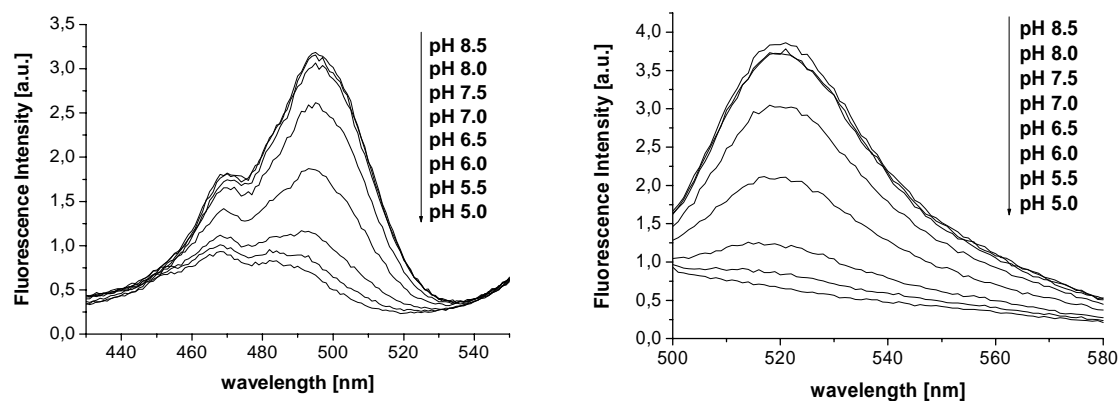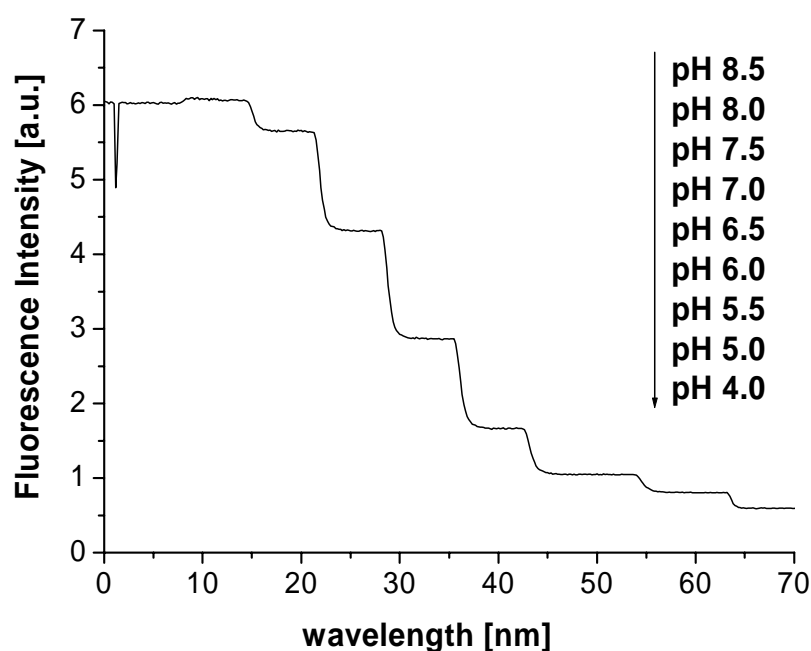**Fig. 6.4.** Time trace with respective fluorescence intensities of membrane M_{PA1} for PBS of IS = 50 mM.

4.3.2. Figures 6.5-6.6. show the calibration plots of membranes M_{PA1}, M_{PA2} and M_{GA2} (see chapter 6.2.6.) for ionic strength from 25 mM to 500 mM. In general, all signals were taken as mean of at least 100 seconds. It is obvious that the replacement of acrylnitril by 2-methacryloxyethyl has two effects on the sensor. On the one hand, the glucosidic substituent reduces the cross-sensitivity towards ionic strength. Although, the polymers AA-Q-N-2 and GA-Q-N-2 have almost the same amount of amino-groups, the pH error caused by changes in ionic strength is much lower for GA-Q-N-2. One can assume that the glucosidic substituents lowers the surface potential of the polymer. Therefore, ions in the bulk solution are less repulsed and changes in ionic strength are less notable. On the other hand, membrane M_{GA2} shows a contrary behavior when the pK_a is displayed vs. ionic strength. Therefore, it should be possible to apply the mixed-matrix compensation method (MMCM) as described in chapter 4.3.2. with the polymers AA-Q-N-1 or AA-Q-N-2 (see Table 6.2.) as negative component.
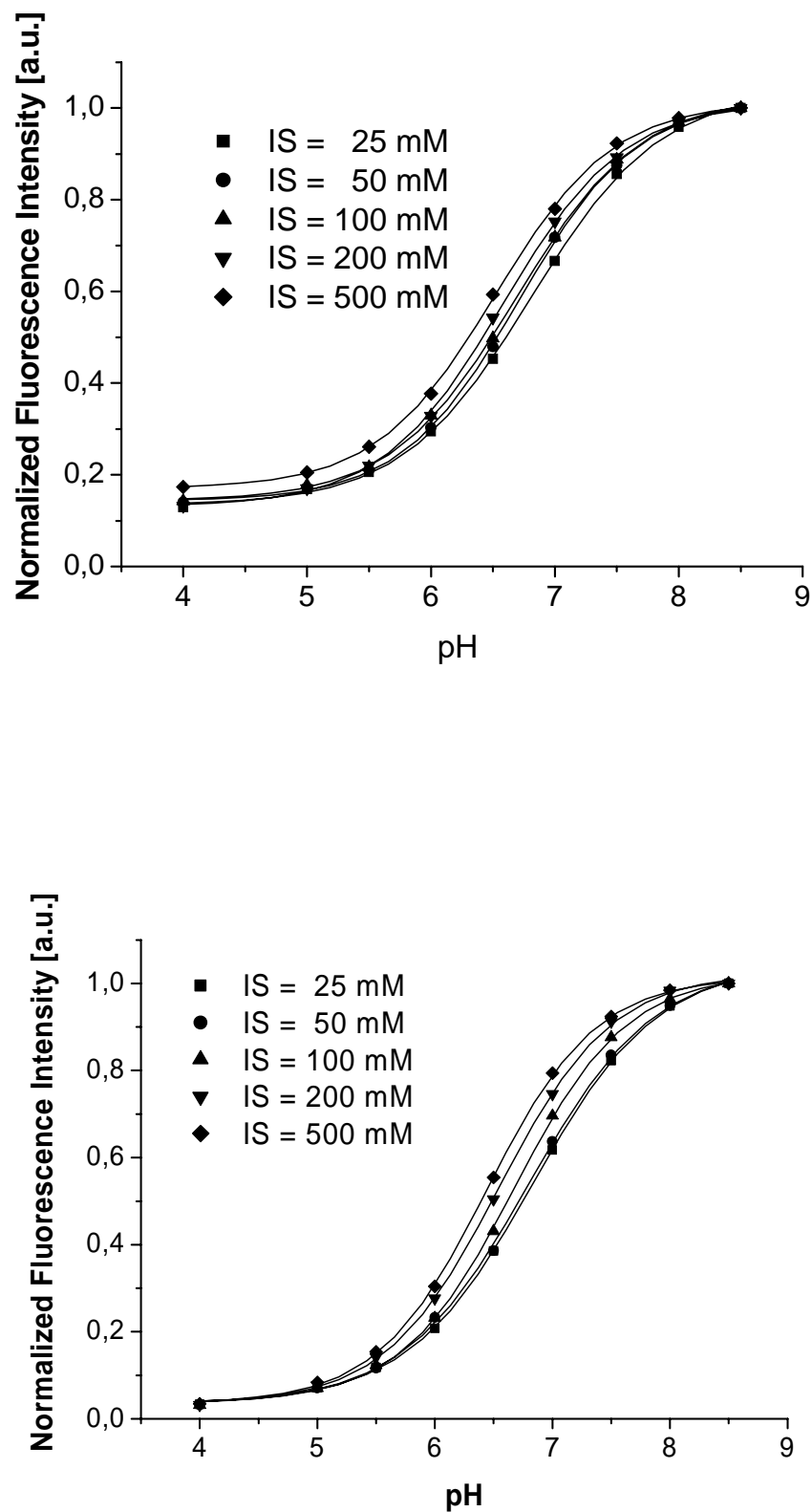
Fig. 6.5. Titration plots of membrane M_{PA1} (top) and M_{PA2} (bottom) with phosphate buffers of varying ionic strength.
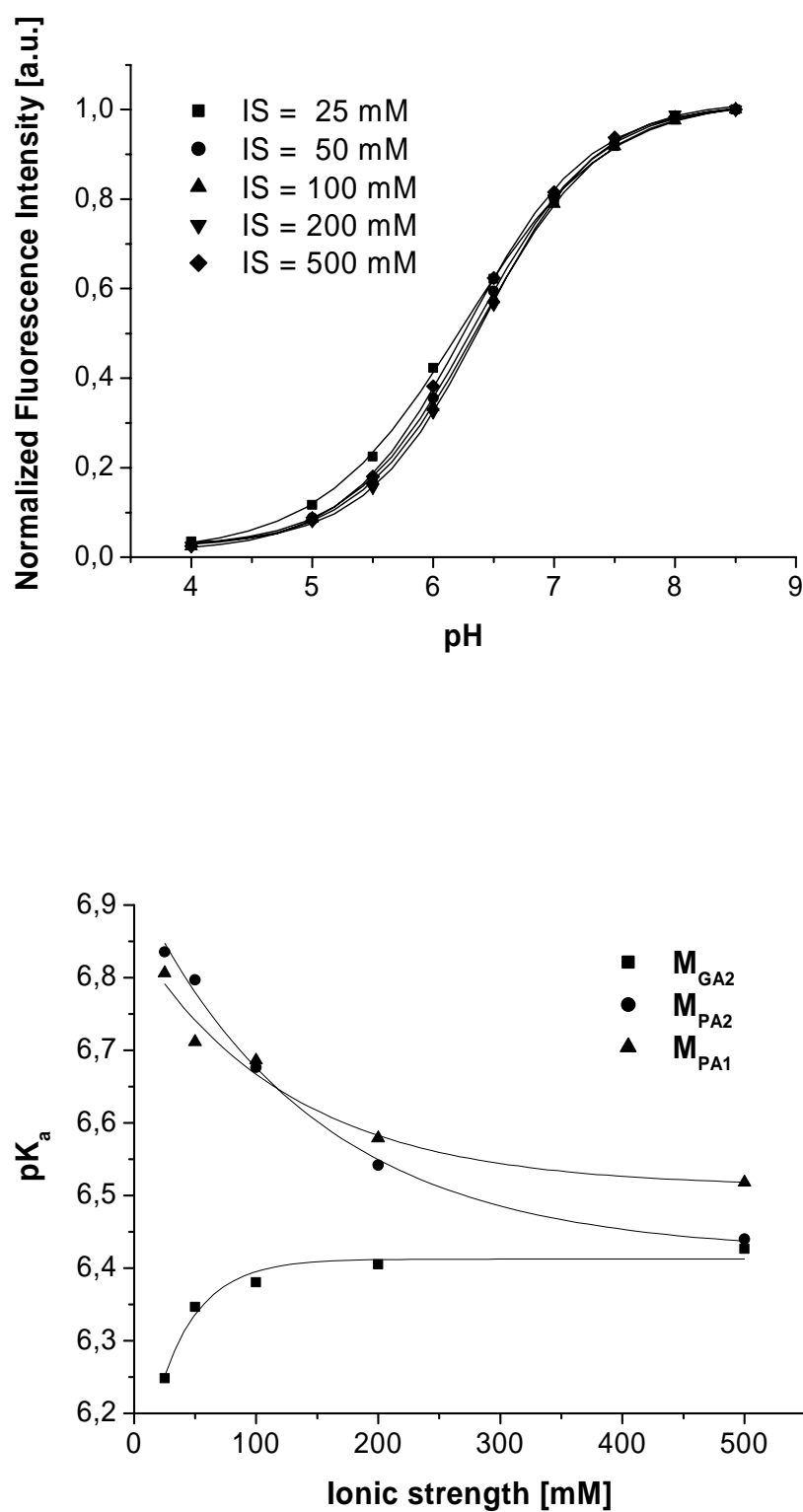
Fig. 6.6. Titration plots of membrane M_{GA1} (top) and comparison of apparent pK_a's of the three polymers with increasing ionic strength.

6.3.3. DLR-referenced pH-membrane

In contrast to membrane M_{PA1}, membrane M_{DLR} contains inert phosphorent reference beads with an emission maximum at 620 nm. The cocktail was prepared as described in chapter 6.2.6. Additionally, 5 mg of reference beads were added. The amount of reference beads were obtained from a series of membranes containing 5, 10, and 15 mg reference beads, wherein the "5 mg-membrane" showed the highest signal change between pH 4.0 ($\Phi = 54,9°$) and pH 8.5 ($\Phi = 43,6°$), while the other membranes showed phase shifts of less than 8°. Figure 6.7. shows the time-trace of M_{DLR}, recorded with the phase detection device PDD, wherein the sensor membrane was fixed with silicone to the tip of a 2 mm fiber and dipped into PBS solutions.
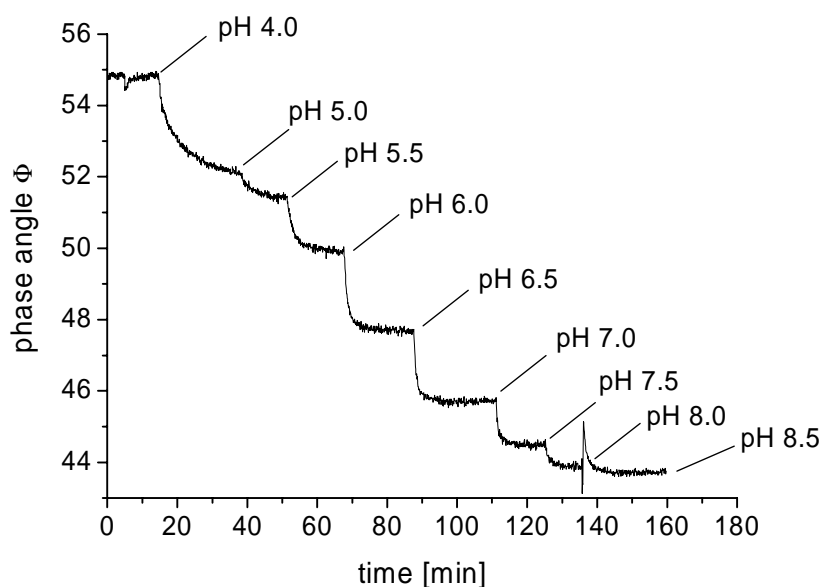
Fig. 6.7. Time trace of membrane M_{DLR} for phosphate buffers of IS = 50 mM (Operational frequency $\nu = 45$ kHz; continuous mode; $\lambda_{exc} = 505$ nm, $\lambda_{em} > 570$ nm (long-pass filter)).

In analogy to the single-intensity based measurements, the DLR-membrane was checked on the cross-sensitivity towards IS. The measured phase angle was converted to its cotangents to ease the comparison of the four different calibration curves.
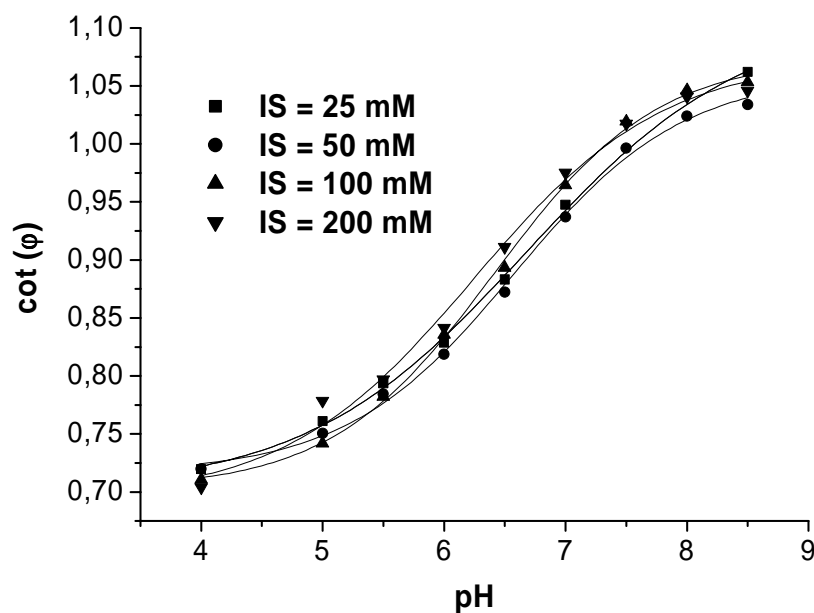
Fig. 6.8. Titration plots of membrane M_{DLR} with phosphate buffers of varying ionic strength.

Table 6.2 gives a comparison of the apparent pK_a's of the membranes M_{PA1} and M_{DLR}. It is obvious that the DLR-based membrane shows lower pKa's than the normal membrane. Additionally, the pH error caused by changes in ionic strength is higher for the DLR-based membrane. The reference particles contain free carboxyl groups in their surface according to the manufacturer's information. This circumstance explains the fact that the pK_a's are different: By addition of negatively charged particles, the total ionic strength in the system is increased and the sensor shows a lower pK_a. The higher cross-sensitivity can be explained by the fact that the surface potential is also increased. In case of negative charges, this results in a lower dissociation constant (see chapter 4).

Table 6.1. Comparison of apparent pKa's of M_{PA1} and M_{DLR} and corresponding pH error.

Ionic strength [mM]	M_{PA1}	M_{DLR}
25	6,80636	6,6739
50	6,71144	6,5764
100	6,68586	6,4128
200	6,579	6,245
$\Delta pH = (pK_{25}-pK_{200})/2$	0,11368	0,21445

6.4. Conclusion

A polyacrylamide-based polymer was loaded with carboxyfluorescein and embedded, along with Ru^{2+}-PAN-particles in a hydrogel matrix. The results of membrane M_{DLR} clearly demonstrate that the DLR scheme can be adapted to fluorescein. A 505 nm-LED can be used as light source to excite both dyes. An amount of 5% (m/m) reference particle results in a phase shift of 55° to 44° for pH 4.0 and 8.5, respectively. The fact that the referenced membrane shows a higher cross-sensitivity than the single-intensity based membrane was explained by the additional charges of the reference particles. The cross-sensitivity of the sensor membrane can be improved reducing the amount of reference particles to an optimum.

6.5. References

1.   C. A. Parker, **Photoluminescence of Solutions**, Elsevier, Amsterdam, **1968**.

2.   R. P. Haugland, **Handbook of Fluorescent Probes**. chap. 1, Eugene (Oregon), **1999**.

3.   I. Klimant, Ger. Pat. Appl DE 198.29.657, **1997**.

4.   I. Klimant, O. S: Wolfbeis, **Book of abstracts, 6th European Conference on Optical Chemical Sensors & Biosensors (Europt(r)ode)**,p. l25, **1998**.

5.   J. R. Lakowicz, F. R. Castellano, J. Dattelbaum, L. Tolosa L, G. Rao, I. Gryszynski, **Low-frequency modulation sensors using nanosecond fluorophores,** Anal. Chem., **1998**, 70, 5115-5121.

6.   I. Klimant, C. Huber, G. Liebsch, G. Neurauter, A. Stangelmayer, O. S. Wolfbeis, **Dual Lifetime Referencing (DLR) a New Scheme for Converting Fluorescence Lifetime into a Frequency-Domain or Time-Domain Information**, in New Trends in Fluorescence Spectroscopy, chapter 13, Springer-Verlag, Berlin, **2001**,

7.   G. Liebsch, I. Klimant, C. Krause, O. S. Wolfbeis, **Fluorescent Imaging of pH with Optical Sensors Using Time Domain Dual Lifetime Referencing**, Anal. Chem., **2001**, 73(17), 4354-4363.

8.   A. Juris, V. Balzani, F. Barigelletti, S. Campagna, P. Belser, A. von Zelewsky, **Ruthenium(II) polypyridine complexes: photophysics, photochemistry, electrochemistry, and chemiluminescence,** Coord Chem. Rev., **1988**, 84, 85-277.

9.   C. T. Lin, W. Boettcher, M. Chou, C. Creutz, N. Sutin, **Mechanism of the quenching of the emission of substituted polypyridineruthenium(II) complexes by iron(III), chromium(III), and europium(III) ions,** J. Am. Chem. Soc., **1976**, 98, 6536-6544.

10.   I. Klimant, O. S. Wolfbeis, **Oxygen-Sensitive Luminescent Materials Based on Silicone-Soluble Ruthenium Diimine Complexes,** Anal. Chem., **1995**, 67, 3160-3166.

11.   A. S. Verkman, M. C. Sellers, A. C. Chao, T. Leung, R. Ketcham, **Synthesis and characterization of improved chloride-sensitive fluorescent indicators for biological applications**, Anal. Biochem., **1989**, 178, 355-361.

12.   J. Biwersi, B. Tulk, A. S. Verkman, **Long-wavelength chloride-sensitive fluorescent indicators,** Anal. Biochem., **1994**, 219, 139-143.

13.   C. Huber, T. Werner, K. Fähnrich, C. Krause, **Synthesis and characterization of new chloride-sensitive indicator dyes based on dynamic fluorescence quenching**, J. Photochem. & Photobiol.,**1999**, 128, 111-120.

Chapter 7

Abbreviations, Acronyms and Symbols

Φ	Phase shift or phase angle of the modulated light
QY	Quantum yield
λ_{em}	Position of the emission maximum
λ_{exc}	Position of the excitation maximum
μM	µmol per liter
a_{H+}	activity of hydrogen ions
AETA	(2-aminoethyl)trimethylammonium chloride hydrochloride
BCECF	2', 7'-bis(carboxyethyl)-5(or 6)-carboxyfluorescein
BSA	Bovine serum albumine
c_{H+}	concentration of hydrogen ions
CHF	2'-chloro-7'-hexylfluorescein
CHFOE	2'-chloro-7'-hexylfluorescein octadecylester
CNF	5(or 6)-carboxynaphtofluorescein
D4	Hydrogel based on polyurethane
DCF	2', 7'-dichlorofluorescein
DCFOE	2', 7'-dichlorofluorescein octadecylester
DHF	2', 7'-dihexylfluorescein
DHFOE	2', 7'-dihexylfluorescein octadecylester
DLR	Dual Lifetime Referencing
EDC	N-(3-Dimethylaminopropyl)-N'-ethyl-carbodiimide-hydrochloride
F	Fluorescence intensity
FAM	5(or 6)-carboxyfluorescein
HTS	High throughput screening
HPTS	1-Hydroxypyrene-3,6,8-trisulfonate trisodium salt
IS	Ionic strength
LED	Light emitting diode
MCF	2'-Chlorofluorescein
MCFOE	2'-Chlorofluorescein octadecylester
mM	mMol per Liter

MES	2-(N-Morpholino)ethanesulfonic acid
MOPS	3-(N-Morpholino)propanesulfonic acid
MPLC	Medium pressure liquid chromatography
MTP	Micro-titer plate
n. d.	Not determined
nm	Nanometer
nM	Nanomol per liter
ns	Nanosecond
Ψ	Surface potential
PAN	Poly(acrylonitrile)
PD-8	Reference beads (particles) containing Ru(dpp)
PMT	Photomultiplier tube
PVC	Poly(vinyl chloride)
Ru(dpp)	Ruthenium(II)-tris-4,7-diphenyl-1,10-phenanthroline
R. S. D	Relative standard deviation
SNAFL	Semi-naphthofluorescein
SNARF	Semi-naphthorhodafluorescein
surf	Surface
τ	Fluorescence decay time
TRIS	Tris(hydroxymethyl)aminomethane
VIS	Visible
UV	Ultraviolet

Chapter 8

Summary

The thesis describes the development, characterization and application of fluorescence-based, optical pH sensors. Special attention is given to the dependence of the sensor signal and changes of ionic strength in the analyte solution. Based on three different methods for minimization of this dependence, various sensor membranes are presented in detail. Further, a new concept to reference fluorescence intensity signals is introduced and applied to an optical pH sensor.

Chapter 1 emphasizes the necessity of precise pH control and measurements by means of examples. An overview of possible fields of pH sensors is given in general. In particular, three different formats of optical pH sensors are presented. Furthermore, the cross-sensitivity of the calibration curve of optical sensors towards ionic strength is mentioned.

At the beginning of chapter 2, a short, review on the development of the term "pH" is given, followed by the explanation of the principle of optical pH sensors. The effect of ionic strength on the signal of optical pH sensor is explained by means of the law of Debye and Hückel and the definition of activity coefficients. A paragraph about the state of the art in optical pH sensor technology is followed by the second half of chapter 2, concerning the phenomena luminescence. Beside from basics, also methods for referencing and measurement techniques are explained.

Chapter 3 describes the application and spectral properties of commercially available, pH-sensitive fluorescent dyes. HPTS, carboxyfluorescein and fluorescein were checked on their cross-sensitivity towards IS in the range from 25 to 500 mM. According to the theory of Debye and Hückel, the two-fold negative charged indicator fluorescein is less affected by IS than HPTS which carries four negative charges. A novel, partially positive charged indicator shows a contrary change of the dissociation constant. In an equimolar mixture with carboxyfluorescein, the effect of IS was distinctly reduced.

In chapter 4, two methods are presented based on the principle described previously for the compensation of the effect of IS. The pH-indicator carboxyfluorescein was immobilized on partially amino-modified carboxycellulose. For the first method, the remaining carboxy groups were converted to positively charged groups. Again, mixing

positively and negatively charged celluloses made an improvement of the cross-sensitivity towards IS in the range from 25 mM to 500 mM possible.

For the second method, the negatively charged cellulose strand was partially loaded with negative charges. Six differently charged sensors were checked on their cross-sensitivity towards IS. One sensor shows a minimal cross-sensitivity towards IS and it shows the smallest zeta-potential, meaning a low charge density and a successful compensation of negative and positive charges.

Chapter 5 deals with the third method for minimization the cross-sensitivity towards IS. Novel, fluorescein-based, lipophilic pH-indicators were embedded in an ion-permeable, charge-free polymer. The indicators were made lipophilic by esterification of the carboxy group with a C_{18} alkyl chain. This ester-modification reduces the number of charges to one and zero for basic and acid form, respectively. As a result of the charge reduction, the effect of IS is reduced to minimum and becomes negligible in the range from 25 to 500 mM. The fluorescent dyes differ in their substituents at 2'- and 7'-position of the xanthene structure. This variation of substituents results in dissociation constants between 5.5 and 8.5. Sensor properties like photo stability, temperature dependence and fluorescent lifetime were analyzed and discussed in detail. Finally, two applications using these sensor membranes were demonstrated.

The chapter 6 deals with new amino-modified polymers. The polymers were embedded in hydrogel together with pH-inert reference particles. The fluorescence intensity of the sensors is converted into a phase shift by means of a novel referencing method (Dual Lifetime Referencing) using luminophores with different fluorescent decay times.

Chapter 9

Zusammenfassung

Diese Arbeit beschreibt die Entwicklung, Charakterisierung und Anwendung auf Fluoreszenzfarbstoffen basierender, optischer pH-Sensoren. Als Schwerpunkt wird die Abhängigkeit des Sensorsignals von der Ionenstärke der Analytlösung behandelt. Basierend auf drei unterschiedlichen Methoden zur Minimisierung des Effektes der Ionenstärke, werden verschiedene Sensormembranen detailliert vorgestellt. Ferner wird eine neuartige Methode zur Referenzierung des Fluoreszenz-Intensitätssignales vorgestellt und auf pH-Sensoren angewendet.

Im ersten Kapitel wird die Notwendigkeit einer genauen Erfassung des pH Wertes anhand verschiedener Beispiele verdeutlicht. Ein Überblick über Einsatzbereiche von pH-Sensoren im Allgemeinen wird gegeben. Speziell werden drei unterschiedliche Ausführungen für optische Sensoren vorgestellt. Weiterhin wird die Problematik optischer pH-Sensoren und der Abhängigkeit des Messsignals von der Ionenstärke kurz erläutert.

Im zweiten Kapitel wird zu Beginn ein historischer Überblick über die Entwicklung des pH-Wertes gegeben. Weiterhin wird das Prinzip der optischen pH-Wert-Messung erläutert und anhand der Gesetze von Debye und Hückel und der Definition von Aktivitätskoeffizienten wird der Einfluss der Ionenstärke auf das Signal, bzw. Dissoziationskonstante optischer pH-Indikatoren (bzw. Sensoren) geschildert. Nach einem kurzen Überblick über den Stand der Technik optischer pH Sensoren wird in der zweiten Hälfte des Kapitels das Phänomen Lumineszenz behandelt. Neben den Grundlagen werden auch Mess- und Referenzierungsmethoden erläutert.

Im dritten Kapitel werden Anwendungen und spektrale Eigenschaften kommerziell erhältlicher, pH-sensitiver Fluoreszenzfarbstoffe beschrieben. Die Farbstoffe HPTS, Carboxyfluorescein und Fluorescein wurden im Bereich von IS = 25 mM bis 500 mM auf ihre IS-Querempfindlichkeit hin untersucht. Der Theorie von Debye und Hückel folgend, zeigt der zweifach negative geladene Farbstoff Fluorescein eine weitaus geringere Abhängigkeit als das vierfach, negativ geladene HPTS. Ein neuartiger, partiell positiv geladener Farbstoff zeigt eine konträre Veränderung der Dissoziationskonstante als die vorher untersuchten Farbstoffe. In einer äquimolaren Mischung mit Carboxyfluorescein konnte der Einfluss der Ionenstärke deutlich vermindert werden.

Im vierten Kapitel werden zwei, auf dem oben genannten Prinzip, basierende Methoden zur Kompensation des Einflusses der Ionenstärke auf das Messsignal erarbeitet: Der Farbstoff Carboxyfluorescein wird auf teilweise amino-modifizierter Carboxycellulose immobilisiert. In der ersten Methode werden nachträglich die restlichen Carboxylgruppen dieser gefärbten Cellulose zu positiv geladenen Gruppen umgewandelt. Wiederum kann durch Mischung von positiv und negativ geladenen Cellulosen eine Verbesserung der IS-Querempfindlichkeit im Bereich von IS = 25 mM bis 500 mM im Vergleich zu den Ausgangssensoren erreicht werden.

In der zweiten Methode wird die gefärbte, negativ geladene Cellulose schrittweise mit positiven Gruppen beladen. Sechs unterschiedlich geladene Sensoren werden auf ihre IS-Querempfindlichkeit hin untersucht. Ein Sensor zeigt eine minimale Querempfindlichkeit gegenüber der IS. Dieser Sensor zeigt bei Untersuchungen des Zeta-Potentials den kleinsten Wert und somit die kleinste Ladungsdichte, d.h. eine erfolgreiche Kompensation negativer und positiver Ladung.

Im fünften Kapitel wird die dritte Methode zur Minimiserung des IS-Einflusses vorgestellt. Neuartige, auf Fluorescein basierende, lipophile pH-Indikatoren werden in ein ionenpermeables, ladungsneutrales Polymer eingebettet. Die hohe Lipophilie wird erreicht durch Veresterung der Carboxylgruppe in 2-Position mit einer C_{18}-Kette. Durch die Veresterung wird die Zahl der Ladungen am Chromophor auf –1, bzw. 0 im basischen, bzw. sauren Milieu reduziert. Durch die Ladungsreduzierung erniedrigt sich der Einfluss der IS auf ein Minimum und wird vernachlässigbar im Bereich von 25 mM bis 500. Durch Variation der Substituenten in 2'- und 7'-Position am Xanthengerüst des Farbstoffes kann die Dissoziationskonstante von etwa 5.5 bis 8.5 variiert werden. Sensoreigenschaften wie Photostabilität, Temperaturabhängigkeit, Fluoreszenzabklingzeit wurden ausführlich untersucht und im Vergleich zu einem käuflichen Fluoresceinderivat diskutiert. Zwei Anwendungen der Sensormembranen werden am Ende des Kapitels mit der Messung des pH Wertes von „synthetischem" Blutplasma und der Messung der Enzymaktivität von Urease demonstriert.

Im sechsten Kapitel werden neue, amino-modifizierte Polymere mit Carboxyfluorescein beladen. Diese Polymere wurden mit pH-inerten Referenzpartikeln in ein ladungsneutrales Hydrogel eingebettet. Mit Hilfe eines neuartigen Referenzierungsverfahrens (Dual Lifetime Referencing) wird die Fluoreszenzintensität der Sensormembranen über die unterschiedlichen Abklingzeiten der beiden Luminophore in eine Verschiebung der Phasenwinkels konvertiert.

Chapter 10

Curriculum Vitae

PERSONAL DATA

Surname	Weidgans
First Name(s)	Bernhard Markus
Date of birth	Jan. 15th 1976
Place of birth	Passau (Bavaria)
Nationality	German

EDUCATION

09/1982 – 07/1985	Primary School, Schalding/Passau
09/1985 – 09/1986	Primary School, Heining/Passau
09/1986 – 06/1995	Gymnasium, Passau
06/1995	Degree: Abitur

MILITARY SERVICE

07/1995 – 10/1995	Basic Training in Schwalmstadt/Hesse

STUDIES

11/1995 – 03/2000	Chemistry (Diploma) at the University of Regensburg
03/2000	Exam: Diploma
04/2000-01/2001	Diploma Work at the Institute of Analytical Chemistry, Chemo- and Biosensors (Prof. Wolfbeis) at the University of Regensburg (Title: Diode Laser Compatible Fluorescent Markers for Bioanalytical Applications)
01/2001	Degree: Diplom-Chemiker (univ.)
06/2001-05/2004	PhD Work at the Institute of Analytical Chemistry, Chemo- and Biosensors (Prof. Wolfbeis) at the University of Regensburg

EXTRACURRICULAR ACTIVITIES

03/2000-05/2001	freelance work for Presens Precision GmbH
06/1998	Seminar at the Karl-Winnacker-Institute/DECHEMA, Frankfurt/Main
10/2001-05/2004	Participation at the DFG Graduate College *Sensory Photoreceptors in Natural and Artificial Systems*

LECTURER AT THE

09/2002	3rd *Advanced Study Course on Optical Chemical Sensors*, Wroclaw, PL
10/2002	1st Wacker Symposium for Process Analytics, Burghausen/Bavaria
11/2002	15th International Scientific Conference Mittweida, Mittweida/Saxony

Chapter 11

Publications

Diploma Thesis

"**Diode Laser Compatible Fluorescent Markers for Bioanalytical Applications**."
Institute of Analytical Chemistry, Chemo- and Biosensors, University of Regensburg
(2001).

Poster Presentations

10/2001	Innovative Biosystemtechnik, Waldheim/Saxony
04/2002	6th Europt(r)ode, Manchester, UK
02/2003	2nd Conference for Ion Analytics (CIA), Berlin
08/2003	8th Conference on Methods and Applications of Fluorescence Spectroscopy, Imaging and Probes, Prague, Czech Republic
04/2004	7th Europt(r)ode, Madrid, Spain

Publications

1. B. Weidgans, T. Werner, O.S. Wolfbeis, M. Berthold, R. Müller, H. Kaden, **Optische Chemosensoren für die pH-Messung,** Scientific reports, J. Univ. of Appl. Sci. Mittweida 10 (2002), 10-17.

2. B. Wetzl, M. Gruber, B. Oswald, A. Duerkop, B. Weidgans, M. Probst, O.S. Wolfbeis, **Set of fluorochromophores in the wavelength range from 450 to 700 nm and suitable for labeling proteins and amino-modified DNA,** Journal of Chromatography, B: (2003), 793(1), 83-92

3. B. Weidgans, C. Krause, I. Klimant, O.S. Wolfbeis, **Fluorescent pH sensors with Negligible Sensitivity to Ionic Strength,** Analyst (2004), 129, 645-650.

4. B. Weidgans, C. Krause, I. Klimant, **Minimizing the Effect of Ionic Strength in an Optical pH Sensor for Physiological pH's**, Analytica Chimica Acta, subm. 2004.

5. O. S. Wolfbeis, B. M. Weidgans, **Fiber Optic Chemical Sensors and Biosensors – A View back,** in **"Optical Chemical Sensors",** F. Baldini & J. Homola (eds.), NATO Adv. Study Series, **2004**, Kluwer (Doordrecht), in press.

6. C. Schröder, B. Weidgans, I. Klimant, **Novel Carboxyfluorescein Derivatives for the Application as pH indicators in Marine Environment**, Analyst, in prep.